

An Investigation of the Effects of Pitch-Roll (De)Coupling on Helicopter Handling Qualities

C. L. Blanken, H.-J. Pausder, and C. J. Ockier

May 1995



National Aeronautics and
Space Administration



US Army
Aviation and Troop Command

An Investigation of the Effects of Pitch-Roll (De)Coupling on Helicopter Handling Qualities

C. L. Blanken, Aeroflightdynamics Directorate, U.S. Army Aviation and Troop Command, Ames Research Center, Moffett Field, California

H.-J. Pausder and C. J. Ockier, Deutsche Forschungsanstalt für Luft- und Raumfahrt, Forschungsbereich Flugmechanik/Flugführung, Institut für Flugmechanik, Abteilung Flugmechanik der Drehflügelflugzeuge, Lilienthalplatz 7, D-38108 Braunschweig

May 1995



National Aeronautics and
Space Administration

Ames Research Center
Moffett Field, CA 94035-1000



US Army
Aviation and Troop Command

Aeroflightdynamics Directorate
Moffett Field, CA 94035-1000

Contents

	Page
List of Tables	v
List of Figures	vii
Symbols	xi
Summary	1
1. Introduction	1
2. Review of the Existing Data	2
3. Motivation	3
4. Airborne and Ground-Based Simulators	4
4.1. The Airborne Simulator ATTheS	4
4.2. The Ground-Based Flight Simulator	4
5. Definition of the Simulation Models	4
5.1. The Baseline Model	4
5.2. The Cross-Coupling Model	5
6. Description of the Tests	6
6.1. Description of the Slalom-Tracking Task	6
6.2. The Flight Tests	7
6.3. The Ground-Based Simulator Tests	7
7. Discussion of the Results	7
7.1. The Baseline Configuration	7
7.2. Control Coupling	8
7.3. Rate Coupling	9
7.4. Combined Control-Rate Coupling	10
7.5. The Effect of the Pitch-due-to-Roll over Roll-due-to-Pitch Coupling Ratio	10
7.6. The Effect of Reduced On-Axis Damping	11
7.7. Washed-Out Coupling	12
7.8. Configurations with Modified Frequency Domain Characteristics	13
8. Analysis of the Results	14
8.1. Pilot Control Strategy	14
8.2. Evaluation of the ADS-33C Time Domain Criterion	15
8.3. Frequency Domain Analysis	16
8.4. Definition of a New Pitch-Roll Coupling Criterion	18
9. Conclusions	20
Appendix A: The 1992 Flight Test Data Base	21
Appendix B: The Ground-Based Simulator Test Data Base	25
Appendix C: The 1993 Flight Test Data Base	31
Appendix D: Pilot Questionnaire	35

References 39

Tables 40

Figures 55

List of Tables

Table	Title	Page
1.1	ADS-33C maximum values for roll-due-to-pitch and pitch-due-to-roll coupling	40
7.1	Handling qualities ratings and principal pilot comments for control coupling configurations	41
7.2	Handling qualities ratings and characteristic pilot comments for control coupling configurations with different direction of coupling (1993 flight test results only)	42
7.3	Handling qualities ratings and principal pilot comments for rate coupling configurations	43
7.4	Handling qualities ratings and characteristic pilot comments for rate coupling configurations from the ground-based simulation—ADS-33C slalom task	44
7.5	Handling qualities ratings and pilot comments for combined control and rate coupling configurations (all data from 1992 flight tests)	45
7.6	Handling qualities ratings and pilot comments for control coupling configurations with different pitch-due-to-roll over roll-due-to-pitch ratio (all data from the 1993 flight tests)	46
7.7	Handling qualities ratings and pilot comments for rate coupling configurations with different pitch-due-to-roll over roll-due-to-pitch ratios	47
7.8	Handling qualities ratings and characteristic pilot comments for rate coupling configurations with reduced on-axis bandwidth ($L_p = 5.0$ rad/sec and $M_q = 2.5$ rad/sec) (data only for pilot C in fixed-base simulator)	49
7.9	Handling qualities ratings and characteristic pilot comments for control coupling configurations with reduced on-axis damping ($L_p = 5.0$ rad/sec and $M_q = 2.5$ rad/sec) (data only for pilot C in fixed-base simulator)	50
7.10	Handling qualities ratings and characteristic pilot comments for rate coupling configurations with reduced roll axis bandwidth ($L_p = 5.0$ rad/sec and $M_q = 2.5$ rad/sec) (data only for pilot C in fixed-base simulator)	50
7.11	Handling qualities ratings and characteristic pilot comments for washed-out coupling configurations with $L_{\delta_x}/M_{\delta_y} = -1.8$ (pilots C and E only)	51
7.12	Handling qualities ratings and characteristic pilot comments for washed-out coupling configurations with $L_{\delta_x}/M_{\delta_y} = -1.8$ (pilot D only)	52
7.13	Handling qualities ratings and characteristic pilot comments for washed-out coupling configurations with $L_{\delta_x}/M_{\delta_y} = -1.0$ (1993 flight test data)	53
7.14	Handling qualities ratings and characteristic pilot comments for rate coupling configurations with modified frequency domain characteristics ($L_{p,c} = M_{q,c}$ and $M_{\delta_y} = L_{\delta_x}$) (1993 flight test data)	54
7.15	Handling qualities ratings and characteristic pilot comments for washed-out coupling configurations with modified frequency domain characteristics ($L_{p,c} = M_{q,c}$ and $M_{\delta_y} = L_{\delta_x}$) (1993 flight test data)	54
8.1	Frequency domain pitch-roll coupling parameters for the BO 105 at 80 knots (2 flights) and an attack helicopter at 60 knots	54

List of Figures

Figure	Title	Page
2.1	Pilot ratings from fixed base simulation in a combination dolphin/slalom task vs. L_q/L_p (from ref. 11)	55
2.2	Pilot ratings vs. θ_{pk}/ϕ for an “easy” and a “difficult” slalom (from ref. 9)	56
2.3	Results of the pitch-due-to-roll coupling criterion for a conventionally controlled BO 105 (from ref. 13)	57
2.4	Results of the roll-due-to-pitch coupling criterion for a conventionally controlled BO 105 (from ref. 13)	57
2.5	Typical time history of the response of a roll step input to the left with a conventionally controlled BO 105	58
4.1	The DLR in-flight simulator ATTheS	59
4.2	Response of ATTheS with a decoupled command model (baseline model) to a lateral control step input	59
5.1	Rate command configurations evaluated during the bandwidth-time delay study (from ref. 14)	60
5.2	Cross-coupling models of pitch and roll axis	61
5.3	Roll and pitch rate responses to a lateral step input for different types of coupling: (1) control coupling, (2) rate coupling, (3) washed-out coupling, and (4) combined control and rate coupling ..	62
5.4	Bode plot of the roll and pitch rate responses to a lateral cyclic input, p/δ_y and q/δ_y , for three different types of coupling: (1) control coupling, (2) rate coupling, and (3) washed-out coupling	62
5.5	Bode plot of the pitch rate to roll rate response (lateral cyclic input), $q/p \delta_y$, for three different types of coupling: (1) control coupling, (2) rate coupling, and (3) washed-out coupling	63
6.1	The slalom-tracking course used for the VMS ground-based and ATTheS in-flight simulations	63
6.2	Typical task performance through the slalom-tracking course (ATTheS baseline configuration, no inter-axis coupling, and Level 1 handling qualities)	64
6.3	Power spectrum of the lateral control inputs for the slalom of figure 6.2	64
7.1	Representative control input positions for control coupling configurations (all data from the 1992 flight tests)	65
7.2	Power spectrum of the control inputs for typical control coupling configurations (all data from the 1992 flight tests)	66
7.3	Comparison of the 1992 and 1993 flight test control inputs and power spectra of the control coupling configuration with $M_{\delta_y} = -0.0429 \text{ rad}\cdot\text{sec}^{-1}\cdot\text{percent}^{-1}$	67
7.4	Comparison of the control coupling configurations with conventional and unconventional direction of coupling (both results from the 1993 flight tests)	68
7.5	Comparison of the HQRs with the ADS-33C coupling parameters for control coupling configurations	69
7.6	Representative control input positions for rate coupling configurations (data from 1992 and 1993 flight tests)	70
7.7	Representative power spectra of the control inputs for rate coupling configurations (data from 1992 and 1993 flight tests)	71

7.8	Comparison of the HQRs with the ADS-33C coupling parameter for two different slalom tasks with rate coupling configurations	72
7.9	Modified ADS-33C slalom course (evaluated on the ground-based simulator only)	72
7.10	Representative control input positions for combined control-rate coupling configurations (data from 1992 flight tests)	73
7.11	Representative power spectra of the control inputs for combined control-rate coupling configurations (data from 1992 flight tests)	74
7.12	Comparison of the HQRs with the ADS-33C coupling parameters for combined control and rate coupling configurations	75
7.13	Ratio of off-to-on axis derivatives for several helicopters vs. airspeed (data from ref. 20).....	75
7.14	Definition of the off-to-on axis coupling ratio, C , for two examples.....	76
7.15	Control input positions for two rate coupling configurations with different amounts of off-to-on axis coupling ratios, C (data from 1993 flight tests).....	77
7.16	Power spectrum of the control inputs for typical rate coupling configurations with different amounts of off-to-on axis coupling ratios, C (data from 1993 flight tests).....	78
7.17	Comparison of the HQRs with the ADS-33C coupling parameters for cases with different off-to-on axis coupling ratios, C (data from fixed-base simulator)	79
7.18	Comparison of the HQRs with the ADS-33C coupling parameter for cases with different off-to-on axis coupling ratios, C (data from 1993 flight tests).....	79
7.19	Comparison of the pilot HQRs with the ADS-33C coupling parameters for rate coupling configurations with different on-axis damping (fixed-base simulator data)	80
7.20	Comparison of the pilot HQRs with the ADS-33C coupling parameters for control coupling configurations with different on-axis damping (fixed-base simulator data)	80
7.21	Control input positions for typical washed-out coupling configurations. All data for $M_{\delta_x}/L_{\delta_y} = -1.0$ and $M_{q,c} = -4.0 \text{ sec}^{-1}$, except for (a) which has $M_{\delta_x}/L_{\delta_y} = -1.8$ (data from 1993 flight tests)	81
7.22	Power spectrum of the control inputs for typical washed-out coupling configurations. All data for $M_{\delta_x}/L_{\delta_y} = -1.0$ and $M_{q,c} = -4.0 \text{ sec}^{-1}$, except for (a) which has $M_{\delta_x}/L_{\delta_y} = -1.8$ (data from 1993 flight tests)	82
7.23	Comparison of the task performance of pilots C and D for a washed-out coupling configuration (data from 1993 flight tests)	83
7.24	Pilot ratings vs. M_{δ_y} for the washed-out coupling configurations with $M_{q,c} = -4.0 \text{ sec}^{-1}$	84
7.25	Comparison of the HQRs with the ADS-33C coupling parameters for washed-out coupling configurations	84
7.26	Control input positions and power spectra for the washed-out coupling configuration with $L_{p,c} = M_{q,c}$ (data from 1993 flight tests)	85
7.27	Comparison of the HQRs with the ADS-33C coupling parameters for control coupling and washed-out coupling configurations with modified frequency characteristics	86
8.1	Typical figure eight cyclic control path for a control coupling configuration	87
8.2	Simplified model of the pilot as a two-axis single loop feedback system	87
8.3	Lateral and longitudinal power spectra for selected control coupling configurations (notice differences in scale between lateral and longitudinal spectra; data from the 1992 flight tests)	88

8.4	Lateral and longitudinal power spectra for selected rate coupling configurations (notice differences in scale between lateral and longitudinal spectra; data from flight tests)	89
8.5	Simplified model of the pilot using a feedforward control strategy	90
8.6	Typical cyclic control crossplot for diagonalized inputs	90
8.7	Four-second ADS-33C time domain coupling parameters vs. individual pilot ratings for the control, rate, and combined coupling cases with an L_q/M_p and/or $L_{\delta_x}/M_{\delta_y}$ ratio close to that of the BO 105	91
8.8	Two-sided representation of the ADS-33C time domain coupling parameters for all control, rate, and combined coupling cases. Individual pilot ratings and the ADS-33C level boundaries are shown	92
8.9	Two-sided representation of the ADS-33C time domain coupling parameters for all control, rate, and combined coupling cases. Averaged HQRs and suggested level boundaries are shown	93
8.10	Magnitude of q/p at the pitch bandwidth frequency vs. individual pilot ratings for the control, rate, and combined coupling cases with an L_q/M_p and/or $L_{\delta_x}/M_{\delta_y}$ ratio close to that of the BO 105	94
8.11	Magnitude (in decibels) of q/p at the pitch bandwidth frequency vs. individual pilot ratings for the control, rate, and combined coupling cases of figure 8.10	94
8.12	Magnitude of q/p at the pitch neutral stability frequency vs. individual pilot ratings for the control, rate, and combined coupling cases with an L_q/M_p and/or $L_{\delta_x}/M_{\delta_y}$ ratio close to that of the BO 105	95
8.13	Magnitude (in decibels) of q/p at the pitch neutral stability frequency vs. individual pilot ratings for the control, rate, and combined coupling cases of figure 8.12	95
8.14	Magnitude of q/p at the pitch bandwidth frequency vs. individual pilot ratings for the washed-out coupling cases and some selected rate coupling cases (flight data only)	96
8.15	Magnitude of q/p at the pitch neutral stability frequency vs. individual pilot ratings for the washed-out coupling cases and some selected rate coupling cases (flight data only)	96
8.16	Magnitude of q/p at the pitch bandwidth frequency vs. individual pilot ratings for the modified frequency cases and some selected rate coupling cases	97
8.17	Magnitude of q/p at the pitch neutral stability frequency vs. individual pilot ratings for the modified frequency cases and some selected rate coupling cases	97
8.18	Magnitude of q/p at the pitch bandwidth frequency vs. individual pilot ratings for the reduced on-axis bandwidth frequency cases and some selected rate coupling cases	98
8.19	Magnitude of q/p at the pitch neutral stability frequency vs. individual pilot ratings for the reduced on-axis bandwidth frequency cases and some selected rate coupling cases	98
8.20	Two-sided representation of the pitch bandwidth frequency criterion for all control, rate, and combined coupling cases. Individual pilot ratings and suggested level boundaries are shown	99
8.21	Two-sided representation of the pitch neutral stability frequency criterion for all control, rate, and combined coupling cases. Individual pilot ratings and suggested level boundaries are shown	100
8.22	Two-sided representation of the pitch bandwidth frequency criterion for all washed-out coupling cases and some selected rate coupling cases. Individual pilot ratings and suggested level boundaries are shown	101

8.23	Two-sided representation of the pitch neutral stability frequency criterion for all washed-out coupling cases and some selected rate coupling cases. Individual pilot ratings and suggested level boundaries are shown	102
8.24	Two-sided representation of the pitch bandwidth frequency criterion for all modified frequency coupling cases and some selected rate coupling cases. Individual pilot ratings and suggested level boundaries are shown	103
8.25	Two-sided representation of the pitch neutral stability frequency criterion for all modified frequency coupling cases and some selected rate coupling cases. Individual pilot ratings and suggested level boundaries are shown	104
8.26	Two-sided representation of the pitch bandwidth frequency criterion for all reduced on-axis bandwidth coupling cases and some selected rate coupling cases. Individual pilot ratings and suggested level boundaries are shown	105
8.27	Two-sided representation of the pitch neutral stability frequency criterion for all reduced on-axis bandwidth coupling cases and some selected rate coupling cases. Individual pilot ratings and suggested level boundaries are shown	106
8.28	Amplitude of the frequency response of p/δ_y , q/δ_y , and q/p for two data sets obtained from two separate flight tests with the BO 105 S-123 (80 knots).....	107
8.29	Amplitude of the frequency response of q/δ_x , p/δ_x , and p/q for two data sets obtained from two separate flight tests with the BO 105 S-123 (80 knots).....	108
8.30	Bode plot of q/p (solid line) and p/q (dashed line) of an attack helicopter at 60 knots	109
8.31	Individual pilot HQRs of all control, rate, and combined coupling cases in the frequency domain format using an averaged coupling parameter	110
8.32	Individual pilot HQRs of all washed-out coupling cases and some selected rate coupling cases in the frequency domain format using an averaged coupling parameter	111
8.33	Suggested level boundaries of the pitch-roll coupling criterion using an averaged coupling parameter. Data points shown are for the BO 105 at 80 knots and an attack helicopter at 60 knots	112

Symbols

C	coupling coefficient (defined in sec. 7.5)	M_q	pitch damping (pitching moment due to pitch rate)
L	moment about the longitudinal axis (rolling moment)	$M_{q,c}$	pitch damping seen by the coupling contributions
L_p	roll damping (rolling moment due to roll rate)	M_{δ_x}	pitch sensitivity (pitching moment due to longitudinal stick input)
$L_{p,c}$	roll damping seen by the coupling contributions	M_{δ_y}	control coupling term (pitching moment due to lateral stick input)
L_q	rate coupling term (rolling moment due to pitch rate)	p	roll rate
L_{δ_x}	control coupling term (rolling moment due to longitudinal stick input)	q	pitch rate
L_{δ_y}	roll sensitivity (rolling moment due to lateral stick input)	δ_x	longitudinal control input (positive backward)
M	moment about the lateral axis (pitching moment)	δ_y	lateral control input (positive to the right)
M_p	rate coupling term (pitching moment due to roll rate)	θ	pitch angle
		ϕ	bank angle
		$\omega_{BW\theta}$	pitch-axis bandwidth frequency
		$\omega_{180\theta}$	pitch-axis neutral stability frequency

An Investigation of the Effects of Pitch-Roll (De)Coupling on Helicopter Handling Qualities

C. L. BLANKEN, H.-J. PAUSDER,* AND C. J. OCKIER*

U.S. Army Aeroflightdynamics Directorate (USAATCOM), Ames Research Center

Summary

An extensive investigation of the effects of pitch-roll coupling on helicopter handling qualities was performed by the U.S. Army and Deutsche Forschungsanstalt für Luft- und Raumfahrt (DLR), using a NASA ground-based and a DLR in-flight simulator. Over 90 different coupling configurations were evaluated using a high gain roll-axis tracking task. The results show that although the current ADS-33C coupling criterion discriminates against those types of coupling typical of conventionally controlled helicopters, it not always suited for the prediction of handling qualities of helicopters with modern control systems. Based on the observation that high frequency inputs during tracking are used to alleviate coupling, a frequency domain pitch-roll coupling criterion that uses the average coupling ratio between the bandwidth and neutral stability frequency is formulated. This criterion provides a more comprehensive coverage with respect to the different types of coupling, shows excellent consistency, and has the additional benefit that compliance testing data are obtained from the bandwidth/phase delay tests, so that no additional flight testing is needed.

1. Introduction

To achieve adequate mission effectiveness, the helicopter of the future will have to operate at night and in bad weather in a low level environment and will have to perform a broader spectrum of tasks than ever before. This can only be achieved with helicopters that are very agile yet easy to control. However, typical high agility helicopters, such as the BO 105, exhibit severe inter-axis coupling. This coupling is inherent to the stiff rotor systems and large hinge offset needed for high maneuverability. Strongly coupled helicopters require complicated multi-axis control inputs for even the simplest tasks, which leads to increased workload for the pilot and degraded handling qualities. Active control technology can provide an answer to this problem by effectively

decoupling the helicopter control inputs. However, whether flight control systems can and should be designed to eliminate all coupling at all times is questionable—cost and technological considerations may determine otherwise; and, when the flight control system or a component fails, the pilot should not be left with an uncontrollable aircraft.

Therefore, minimum requirements for helicopter handling qualities have been defined by the U.S. Army, an effort that culminated in the drafting of Aeronautical Design Standard 33 (the latest version of which is known as ADS-33C (ref. 1)). ADS-33 is essentially a mission oriented specification, with criteria depending on selected mission task elements, helicopter response types, failure probabilities, and attention states. In order to accommodate night and poor weather operations, the handling qualities requirements are made dependent on the available visual cues. ADS-33 comprises both quantitative and qualitative criteria. Compliance of the quantitative criteria is computed directly from the aircraft response to prescribed inputs; they constitute a design guide which, if not satisfied, will most likely result in degraded flying qualities. Compliance of the qualitative criteria is determined for specific flight test maneuvers from pilot ratings on the Cooper–Harper handling qualities scale (ref. 2); they constitute a comprehensive evaluation of the overall helicopter flying qualities for selected stylized mission tasks.

The ADS-33C criteria for inter-axis coupling are defined in the time domain. The pitch-roll cross-coupling criterion in forward flight, which forms the subject of this report, applies only to the more aggressive mission task elements, i.e., ground attack, slalom, pull-up/push-over, assault landing, and air combat. The requirement is defined in terms of the ratio of peak off-axis response to desired on-axis response, i.e., θ_{pk}/ϕ for pitch-due-to-roll and ϕ_{pk}/θ for roll-due-to-pitch coupling. The peak off-axis response must be measured within 4 seconds following an abrupt longitudinal or lateral cyclic step input; the desired on-axis response must be measured exactly 4 seconds following the input. The coupling limits, as specified in table 1.1, are the same for pitch-due-to-roll and roll-due-to-pitch. ADS-33C further

*Deutsche Forschungsanstalt für Luft- und Raumfahrt, Forschungsbereich Flugmechanik/Flugführung, Institut für Flugmechanik, Abteilung Flugmechanik der Drehflügelflugzeuge, Lilienthalplatz 7, D-38108 Braunschweig.

specifies that this requirement “shall hold for control input magnitudes up to and including those required to perform the specified mission task elements.” ADS-33C requirements in hover are identical to those in forward flight.

The U.S. Army Aeroflightdynamics Directorate (AFDD) and Deutsche Forschungsanstalt für Luft- und Raumfahrt (DLR) Institute of Flight Mechanics, under the U.S./German Memorandum of Understanding (MoU), have recently completed a comprehensive study of pitch-roll cross-coupling handling qualities for a slalom-tracking task in forward flight. During this study, complementary use was made of the German in-flight simulator ATTHes (Advanced Technology Testing Helicopter System) and the U.S. ground-based simulation facilities at NASA Ames Research Center. The objectives of this work were (1) to expand the cross-coupling data base so that it would include coupling of all types, and (2) to review the existing ADS-33C cross-coupling criterion and suggest improvements if necessary.

The report briefly reviews the existing data base, provides some background in pitch-roll cross-coupling dynamics, describes the task and facilities used for the evaluations, discusses the results, presents analysis, and, finally, makes a suggestion for a modified pitch-roll cross-coupling handling qualities criterion.

Handling qualities testing is the work of many. The authors gratefully acknowledge the test pilots, Steve Cheyne (DRA), Walter Druck (WTD-61), Fuchs (WTD-61), Kus (WTD-61), Heribert Siffl (WTD-61), Rick Simmons (NASA Ames), Tom Reynolds (U.S. Army), and Tom Wallace (U.S. Embassy); the DLR safety pilots Klaus Sanders and Manfred Rössing; the engineers Malcolm Charlton (DRA), Gerd Bouwer (DLR), Wolfgang von Grünhagen (DLR), Steve Mouritsen (DLR); the PATS technicians; the VMS operators and technicians; the ATTHes instrumentation group under Horst Meyer; the telemetry and data conversion specialists; and the many other contributors without whom this study would never have been possible.

2. Review of the Existing Data

As previously mentioned, there have been a number of investigations into helicopter pitch-roll cross coupling (refs. 3–10). The four most recent of these will be discussed in some detail as they have formed the primary sources for establishing pitch-roll cross-coupling criteria in ADS-33 and therefore are particularly relevant to the current investigation.

In reference 7 (see also ref. 11), a large variation in rotor system dynamic design parameters was investigated while performing nap-of-the-Earth (NOE) flight tasks on a fixed-base simulator. One range of rotor design parameters included the effects of pitch-roll cross coupling, i.e., pitching moment due to roll rate, M_p , and rolling moment due to pitch rate, L_q . Two pilots flew three courses: a longitudinal (or hurdles) course, a lateral-directional (or slalom) course, and a course consisting of a combination of these two. The pilots were instructed to fly as fast as possible and as low or close to the obstacles as possible. Published results were presented for the combination task and indicate that the handling qualities ratings (HQRs) given by the two pilots differed markedly (fig. 2.1). One pilot gave mostly HQRs of 3, 4, and 5, while the other pilot, who flew the course approximately 10 knots faster and commented on adverse pitch-due-to-collective coupling, gave mostly 5s, 6s, and 7s. The results appear inconclusive, but underline the dependency or influence of the task performance parameters.

In reference 8, a helicopter in-flight simulation was conducted to investigate the effects of variations in roll damping, roll control sensitivity, and pitch-roll inter-axis coupling on rate coupling during low-altitude maneuvering. The experiment utilized the NASA Ames UH-1H VSTOLAND variable stability and control helicopter. Configurations evaluated included low to moderate on-axis damping ($M_q = -2 \text{ sec}^{-1}$, $L_p = -2 \text{ to } -8 \text{ sec}^{-1}$, and $N_r = -1.2 \text{ and } -3.5 \text{ sec}^{-1}$) and three levels of pitch-roll cross coupling. The cross coupling was described in terms of the ratios of L_q/L_p and M_p/M_q which were set equal to each other at 0, 0.25, and 0.50. The evaluation task was a series of s-turns around markers 1000 feet apart along the sides of a 200 foot wide runway. The pilots were instructed to maintain a reference altitude (about 100 feet) and speed (60 knots). The results of this investigation were also somewhat inconclusive. It is speculated that there were some problems in the configuration models as the UH-1H manual mode (basic UH-1H with stabilizer-bar-on) was given the best ratings (HQR = 3) by all the pilots. Also, the evaluation task may have lacked the aggressiveness and precision to differentiate the coupling configurations. Autospectrum of the lateral cyclic control from flying the task indicates the dominant frequency band was relatively low, i.e., less than 1.5 rad/sec. There were some very small secondary peaks around 5 rad/sec when the coupling was increased from zero.

The reference 9 pitch-roll coupling investigation focused on hover and low-speed tasks. It was conducted on the NASA Ames Vertical Motion Simulator (VMS) with the principal objective of determining the influence of varying task demands on cross-coupling effects. Two tasks, a 100 foot sidestep and a 30 knot slalom, were each

performed with two different levels of aggressiveness. An “easy” slalom consisted of flying around 40 foot diameter cylinders placed 400 feet apart. For the “difficult” slalom, the cylinder diameters were enlarged to 340 feet. The easy and difficult slaloms showed the task influences on the HQRs for all the configurations evaluated; i.e., the difficult slalom was consistently rated 1 to 1.5 ratings worse than the easy slalom. Configurations included control and rate coupling with two different on-axis responses representative of a hingeless rotor and an articulated rotor. The configurations and HQRs were compared with recommended control and rate coupling limits from previous investigations (refs. 3 and 7) and with the current ADS-33 pitch-roll cross-coupling limits (fig. 2.2). The results of these comparisons were mixed; that is, for some of the configuration and task combinations these recommended limits correlated well but for others they did not. In general, none of the recommended cross-coupling limits were perfectly consistent measures for reliably correlating the degree of coupling with pilot opinion rating.

Reference 10 (see also ref. 12) was an in-flight extension of the reference 9 investigation and therefore included the same general type of coupling configurations and tasks although the on-axis responses were constrained to relatively low bandwidths by the in-flight simulator. The study was conducted at NASA Ames using the NASA-Army CH-47B variable-stability helicopter. The in-flight experiment supported the data from VMS that the on-axis damping characteristics determine the impact of coupling and in the roll axis increased roll damping causes increased sensitivity to the angular rate coupling metric $|L_q/L_p|$. The control coupling results and recommendations were strongly dependent on the demands of the task. For the sidestep task, the results suggested that a maximum of approximately 30 degrees of control coupling could be allowed for adequate handling qualities.

An evaluation of the BO 105 (ref. 13) with the ADS-33C criteria uncovered some problems with the existing cross-coupling criterion. The pitch-due-to-roll criterion measurements showed a strong difference between lateral step inputs to the left and to the right. The BO 105 was predicted to have good Level 2 pitch-due-to-roll handling qualities (fig. 2.3) and very poor Level 3 roll-due-to-pitch handling qualities (fig. 2.4). This difference in handling qualities could not be substantiated by the pilots. Figure 2.5 shows a typical time history of a step roll input to the left. As can be seen, the helicopter responds with a

negative roll rate (roll to the left) and a positive pitch rate (nose up). The fact that Euler angles are used in combination with a large bank angle and the fact that yaw rate is not kept constant seem to cause the pitch angle to peak after about 2.5 seconds while the bank angle continues its buildup.

3. Motivation

As is evident from the review of the existing data, the results from these pitch-roll cross-coupling studies do not provide the necessary data base to establish definitive handling qualities criteria for pitch-roll coupling. The data are sparse and filled with inconsistencies; tasks were often not adequately defined nor constrained; effects other than roll-pitch coupling were allowed to affect the ratings; and the frequency dependent nature of coupling was mostly ignored. Therefore, the ADS-33 cross-coupling requirements were only a first cut at establishing coupling limits. These limits were made somewhat generous to minimize unnecessary complexity. However, even such loose criteria are beneficial because they force the designer to consider cross coupling and the tester to evaluate and quantify coupling. Nonetheless, as mission tasks become more demanding, and rotor designs tend toward greater stiffness for maximum agility, the need for precise criteria is apparent and underlines the emphasis for the current study. The modern flight control systems, that will be the backbone of many future helicopters, provide the decoupling potential needed for the application of such specific coupling criteria.

During an earlier cooperative research effort under the U.S./German MoU, the effects of bandwidth and phase delay on helicopter roll-axis handling qualities were investigated (ref. 14). The study, which was performed jointly on the VMS ground-based and the ATTHes in-flight simulators, evaluated fully decoupled rate and attitude command systems with different bandwidths and phase delays for a slalom-tracking task. The result was a consistent and reliable data base which covered Level 1 to Level 3 handling qualities.

By building on these earlier achievements, the pitch-roll coupling study conducted and described herein seeks to expand this data base. A Level 1 rate command configuration from reference 14 was selected as the baseline configuration for the cross-coupling study and the same slalom-tracking task was used. For practical reasons, the study of the effect of pitch-roll cross coupling was limited to rate command systems with known Level 1 on-axis (decoupled) handling qualities.

4. Airborne and Ground-Based Simulators

4.1 The Airborne Simulator ATTheS

The piloted in-flight simulation was conducted on the DLR's in-flight simulator ATTheS (fig. 4.1). ATTheS is a modified BO 105 helicopter equipped with a full authority nonredundant fly-by-wire (FBW) control system for the main rotor and fly-by-light (FBL) system for the tail rotor. The aircraft is operated by a crew consisting of an evaluation pilot and a safety pilot. The safety pilot's position is equipped with the standard mechanical link to the rotor controls, whereas the evaluation pilot's controls are linked to the rotor via a control computer, the FBW/L system, and power actuators. The FBW/L actuator inputs, which are commanded by the evaluation pilot via the control computer, are mechanically fed back to the safety pilot's controls, which can overrule the FBW/L actuator inputs at any time should the need occur. In simulation mode, the flight envelope of ATTheS is restricted to not lower than 50 feet above the ground in hover and 100 feet in forward flight.

The control system of ATTheS is based on an explicit model following control system (MFCS) design (W. von Grünhagen, G. Bouwer, et al., A High Bandwidth Control System for a Helicopter In-Flight Simulator; to be published in the International Journal of Control). It provides high quality simulation fidelity up to a frequency of about 10 rad/sec in the roll axis (ref. 15). For the pitch-roll coupling study, a control computer cycle time of 40 msec was realized. To smoothen the actuator output, the FBW/L actuator inputs were refreshed with a 16 msec subcycle. The equivalent time delay for the overall system due to high-order rotor effects, actuators dynamics, computational time, and pilot input shaping was 100 to 110 msec in the roll axis and 150 to 160 msec in the pitch axis, related to first-order rate command responses. Figure 4.2 shows the response of ATTheS with a decoupled command model to a lateral control step input. As can be seen, almost full decoupling of the roll and pitch motions can be achieved. This high level of decoupling made it possible to accurately implement complex coupling types, even when only small coupling amplitudes were required. For the coupling tests, up to 20 coupling configurations were programmed into the ATTheS control computer and could be changed in-flight by the evaluation pilot.

4.2 The Ground-Based Flight Simulator

The piloted ground-based simulation was conducted on a NASA Ames fixed-base simulator. The cockpit had a single pilot seat mounted in the center of the cab and

three image presentation "windows" to provide outside imagery. The visual imagery was generated using an Evans and Sutherland CT-5A Computer Image Generator (CIG). The CIG data base was carefully tailored to contain adequate macro-texture (i.e., large objects and lines on the ground) for the determination of the rotorcraft position and heading with reasonable precision. The equivalent time delay for the overall system (stick-to-visual) due to computational and visual system delays was 98.4 msec. A seat shaker provided vibration cueing to the pilot, with frequency and amplitude programmed as functions of airspeed, collective position, and lateral acceleration. Aural cueing was provided to the pilot by a WaveTech sound generator and cab-mounted speakers. Airspeed and rotor thrust were used to model aural fluctuations. Standard helicopter instruments and controllers were installed in the cockpit.

Mathematical models of the following items were programmed in the simulation host computer: (1) trim capability, (2) stability command and augmentation system (SCAS), (3) dynamics of the helicopter, and (4) ground effects. The SCAS was a stability-derivative model with known dynamics and no coupling (ref. 16), and the character of its response was easily manipulated by changing the stability derivatives. The flight control architecture and hence the implementation of the cross coupling was the same as in the in-flight simulator.

5. Definition of the Simulation Models

The simulation model used in the study consists of two parts: (1) an uncoupled baseline model with known Level 1 handling qualities and (2) a pitch-roll cross-coupling model. The definition of separate models allows changes in the cross-coupling response without altering the remaining helicopter dynamics.

5.1 The Baseline Model

The baseline model is a decoupled first-order rate command model in pitch and roll. This model is identical to the rate command model used for the bandwidth and time delay study (ref. 14). The selected baseline configuration was consistently evaluated as Level 1 with an average HQR of 2.5 (fig. 5.1, ref. 14). A rate of climb response and sideslip command were defined for the vertical and directional axes. For the baseline model, the responses to the pilot's inputs were fully decoupled, except for the terms governing turn coordination and roll attitude thrust compensation (pseudoaltitude hold). The on-axis roll and pitch responses are given by the following transfer functions:

$$\frac{p}{\delta_y} = \frac{L\delta_y}{s - L_p} \quad \text{and} \quad \frac{q}{\delta_x} = \frac{M\delta_y}{s - M_q} \quad (4.1)$$

Where L_p is roll damping, M_q is pitch damping, and $L\delta_y$ and $M\delta_x$ are the roll and pitch control sensitivities. No additional time delays were used. Damping and roll sensitivity for the baseline configuration are given by:

$$\begin{aligned} L_p &= -8.0 \text{ sec}^{-1} \\ M_q &= -4.0 \text{ sec}^{-1} \\ L\delta_y &= 0.143 \text{ rad/sec}^2 \% \\ M\delta_x &= 0.052 \text{ rad/sec}^2 \% \end{aligned} \quad (4.2)$$

Full stick travel in the BO 105 is 220 mm (8.66 inches) in lateral and 310 mm (12.20 inches) in longitudinal direction. For the in-flight simulator, the roll axis bandwidth and phase delay (as defined in ref. 1) of the baseline configuration was 3.44 rad/sec and 77 msec, respectively. Pitch axis bandwidth and phase delay for the baseline configuration was 2.00 rad/sec and 114 msec. The ground-based simulator had a slightly higher bandwidth and lower phase delay (roll axis 3.64 rad/sec and 69 msec, pitch axis: 2.43 rad/sec and 71 msec). It should be noted that some configurations in the ground-based simulator had reduced on-axis damping and control sensitivities (discussed in sec. 7.6).

5.2 The Cross-Coupling Model

The two main sources of pitch-roll cross coupling can be seen from the following simplified equations of motion:

$$\begin{aligned} \dot{p} &= L_p p + L_q q + L\delta_y \delta_y + L\delta_x \delta_x \\ \dot{q} &= M_p p + M_q q + M\delta_y \delta_y + M\delta_x \delta_x \end{aligned} \quad (4.3)$$

These equations describe the dominant aircraft motions (ref. 17) for lateral and longitudinal cyclic inputs and show the on-axis terms damping (L_p and M_q) and control sensitivity ($L\delta_y$ and $M\delta_x$), and the off-axis terms representing rate coupling (L_q and M_p) and control coupling ($L\delta_x$ and $M\delta_y$). From this, the pitch and roll response follow:

$$\begin{aligned} p &= \frac{\left[L\delta_x \left(s - M_q + L_q \frac{M\delta_x}{L\delta_x} \right) \delta_x \right. \\ &\quad \left. + L\delta_y \left(s - M_q + L_q \frac{M\delta_y}{L\delta_y} \right) \delta_y \right]}{(s - L_p)(s - M_q) - L_q M_p} \\ q &= \frac{\left[M\delta_x \left(s - L_p + M_p \frac{L\delta_x}{M\delta_x} \right) \delta_x \right. \\ &\quad \left. + M\delta_y \left(s - L_p + M_p \frac{L\delta_y}{M\delta_y} \right) \delta_y \right]}{(s - L_p)(s - M_q) - L_q M_p} \end{aligned} \quad (4.4)$$

Typical for this model is an oscillatory coupling effect that occurs when an input causes an off-axis response (as a result of coupling) which in turn causes an on-axis response (as a result of coupling in the other axis), etc. This effect can be eliminated by assuming that the terms ($L_q M_p$), ($L_q M\delta_y$), and ($M_p L\delta_x$) are small compared to the other terms in equation (4.4), which is not an unreasonable assumption for moderately coupled systems. Roll and pitch response now reduce to:

$$\begin{aligned} p &= \frac{L\delta_y}{s - L_p} \delta_y + \left[\frac{L\delta_x}{s - L_p} + \frac{L_q M\delta_x}{(s - L_p)(s - M_q)} \right] \delta_x \\ q &= \frac{M\delta_x}{s - M_q} \delta_x + \left[\frac{M\delta_y}{s - M_q} + \frac{M_p L\delta_y}{(s - L_p)(s - M_q)} \right] \delta_y \end{aligned} \quad (4.5)$$

As can be seen from the equations, the on-axis response is a first-order response that is not influenced by the off-axis response. The parameters $M\delta_y$ and $L\delta_x$ define an off-axis control coupling response induced by the pilot control inputs. The parameters M_p and L_q define an off-axis rate coupling response induced by the on-axis pitch and roll rates.

One of the objectives of this study is to investigate the cross-coupling behavior of helicopters with feedback control systems. In such an augmented helicopter, any off-axis rates that result from control or rate coupling will be reduced to zero by the feedback system. This results in a washed-out response characteristic in the off-axis and can be realized by setting:

$$L_q M \delta_x = M_q L \delta_x \quad \text{and} \quad M_p L \delta_y = L_p M \delta_y \quad (4.6)$$

To be able to independently vary the washed-out coupling dynamics, the damping in the off-axis loop is allowed to be different from the on-axis damping. This leads to the final cross-coupling model shown in figure 5.2. For this model, roll and pitch response are given by:

$$\begin{aligned} p &= \frac{L \delta_y}{s - L_p} \delta_y + \left[\frac{L \delta_x}{s - L_{p,c}} + \frac{L_q M \delta_x}{(s - L_{p,c})(s - M_q)} \right] \delta_x \\ q &= \frac{M \delta_x}{s - M_q} \delta_x + \left[\frac{M \delta_y}{s - M_{q,c}} + \frac{M_p L \delta_y}{(s - L_p)(s - M_{q,c})} \right] \delta_y \end{aligned} \quad (4.7)$$

The ratio of the off-axis response to the on-axis response is given by:

$$\begin{aligned} \left. \frac{q}{p} \right|_{\delta_y} &= \frac{s - L_p}{s - M_{q,c}} \cdot \frac{M \delta_y}{L \delta_y} + \frac{M_p}{s - M_{q,c}} \\ \left. \frac{p}{q} \right|_{\delta_x} &= \frac{s - M_q}{s - L_{p,c}} \cdot \frac{L \delta_x}{M \delta_x} + \frac{L_q}{s - L_{p,c}} \end{aligned} \quad (4.8)$$

The initial values ($t = 0$) of the coupling response ratio are given by:

$$\left. \frac{q}{p} \right|_{\delta_y} = \frac{M \delta_y}{L \delta_y} \quad \text{and} \quad \left. \frac{p}{q} \right|_{\delta_x} = \frac{L \delta_x}{M \delta_x} \quad (4.9)$$

And, the final values ($t = \infty$) of the coupling response ratio are given by:

$$\left. \frac{q}{p} \right|_{\delta_y} = \frac{M \delta_y L_p}{M_{q,c} L \delta_y} - \frac{M_p}{M_{q,c}} \quad \text{and} \quad \left. \frac{p}{q} \right|_{\delta_x} = \frac{L \delta_x M_q}{L_{p,c} M \delta_x} - \frac{L_q}{L_{p,c}} \quad (4.10)$$

Figure 5.3 shows the on- and off-axis response to a lateral step input for four different types of cross coupling: control coupling, rate coupling, washed-out coupling, and combined control and rate coupling. Figure 5.4 shows a frequency response of the roll (on-axis) and pitch (off-axis) rate to a lateral cyclic step input. Figure 5.5 shows the frequency response of the pitch-due-to-roll rate. Initially, the ratio of pitch-due-to-roll to roll-due-to-pitch coupling was chosen to be close to the standard BO 105 helicopter. Subsequently, this ratio was varied to study its effect on the handling qualities for the roll task. A detailed description of all the configurations is contained in Appendices A, B, and C.

6. Description of the Tests

The initial test was conducted in June 1992 using the ATTHes in-flight simulator. This was followed by a ground-based simulation in February 1993 and another in-flight simulation in June 1993. This section describes the task used to perform the evaluations and then the conduct of both the in-flight and the ground-based simulations.

6.1 Description of the Slalom-Tracking Task

The objective of this study was to investigate the effect of pitch-roll coupling on a precision (high gain) roll axis task. To make complementary use of the ground-based and in-flight simulators, it was vital to develop a small amplitude precision tracking task that could be implemented on both simulators while considering the constraints of each. For the ground-based simulator these constraints included a limited field of view and poor visual resolution; for the flight tests these included a 100 foot minimum altitude. In addition, it was desired to keep the complexity of the task cueing to a reasonable level to minimize the building of exotic and expensive task cues. A slalom task with precise tracking phases through a set of ground marked gates, initially developed for a U.S. Army/DLR bandwidth/phase delay study (ref. 14), was found suitable. The slalom course layout (fig. 6.1) included transition and precision tracking phases. The transition phases were intended to be a lower frequency disturbance with the emphasis of the task being the higher frequency acquisition and tracking phases just prior to and through the gates. The slalom-tracking course layout was developed using an inverse modeling technique (ref. 18) that considered the aircraft response, speed, bank angle, and the time to travel between the gates. The gates were 3 meters wide and 90 or 150 meters long. The primary task was defined as the tracking through the ground marked gates, with the maintaining of height and speed (± 10 feet and ± 5 knots for desired performance) as secondary tasks. Ground speed and altitude were 60 knots and 100 feet. From comparison of the flight test results with ground-based evaluations (ref. 14), it was found that the HQRs obtained in the ground-based simulator at 30 foot altitude best match the flight test results at 100 feet. Therefore, the “desired” and “adequate” altitude cues in the ground-based simulator were lowered so that the reference altitude was 30 feet. To ensure that the slalom task was a high frequency, high gain task where the pilot acts as a feedback system, the pilots were explicitly briefed to concentrate on the tracking phases of the slalom course. The lateral displacement between the gates was to be considered a

disturbance and the start of a new acquisition and tracking phase.

Figure 6.2 shows a typical task performance for a flight test with no inter-axis coupling and baseline (Level 1) handling qualities. As can be seen, execution of the tracking task for nearly all the gates is excellent (clear tracking phases can be distinguished), with satisfactory performance on the secondary tasks of maintaining height and speed. Figure 6.3 shows the power spectrum of the lateral control input. Four task phases can be distinguished: (1) gate sequence (lateral displacement of gates), (2) gate transition (slalom between the gates), (3) gate acquisition, and (4) tracking within the gate. The large amplitude inputs used in the transition between the gates are clearly separated from the higher frequency small amplitude inputs used for gate acquisition and tracking through the gates. From this it can be concluded that the frequency spectrum of the task is fully contained in the band from about 1 rad/sec to about 7 rad/sec.

6.2 The Flight Tests

Two flight test campaigns were conducted at the German Forces Flight Test Center (WTD 61) in Manching. The facilities in Manching consisted of a large grass area (where the 1.5 km long slalom course was built), data acquisition equipment, a telemetry monitoring station, and a precision position tracking system (PATs). During each campaign about 30 in-flight simulation hours were logged over a two and a half week period. The first flight test campaign took place in June 1992. Four experienced test pilots participated in the tests: one NASA Ames, one DRA Bedford, and two German Forces (WTD 61) pilots. The second flight test campaign took place in July 1993. Five experienced test pilots participated: one NASA Ames, one DRA Bedford, one U.S. Army, and two German Forces (WTD 61) pilots. The NASA Ames and DRA Bedford pilots were the same in both flight test campaigns. DLR pilots functioned as ATThES safety pilots.

Prior to performing evaluations, each pilot flew the course with the uncoupled baseline configuration to become familiar with the task cues and performance standards. In addition, each pilot's first flight of the day was with this baseline configuration to ensure consistent task performance throughout the test. For each coupling configuration to be evaluated, the test pilots were given adequate time for familiarization with the configuration (typically two practice runs) before they performed two evaluation runs. This was to ensure the pilot ratings and comments were not biased by the unfamiliarity of the pilot with the configuration and the task. For each configuration, the pilot completed a questionnaire

(Appendix D) and summarized his evaluation in a HQR using the Cooper–Harper scale.¹ Questions were related to task performance, pilot workload, and system response characteristics (on and off axis). The following signals were recorded during the evaluation runs: (1) position of the helicopter relative to the ground course, (2) pilot control inputs, (3) heading, attitudes, and angular rates, (4) accelerations, (5) airspeed, and (6) MFCS internal signals like commands to the actuators, actuator positions, etc. The position of the helicopter relative to the ground course and selected on-board parameters were available during the tests on a quick-look system.

6.3 The Ground-Based Simulator Tests

The ground-based simulation was conducted at NASA Ames Research Center using an Interchangeable Cab (ICAB) for the Vertical Motion Simulator (VMS) in a fixed-base mode. Over 80 evaluations were conducted during a two-week period in February 1993, with a NASA Ames and a U.S. Army experimental test pilot. The NASA pilot also participated in both in-flight simulation tests. The visual scene was one that had been used for the bandwidth and phase delay study (ref. 14) and was flown at an altitude of 30 feet. For the ground-based simulation, the same gate-tracking information as implemented for in-flight simulation was available, i.e., helicopter position relative to the tracking gates and a task performance metric that compared the helicopter track to an idealized ground track. This was used to assess pilot training and task performance. The pilots flew each configuration numerous times before flying it at least twice for evaluation. For each evaluation, the pilots answered a questionnaire and summarized their evaluation in a Cooper–Harper HQR.

To anchor the results from the ground-based simulation relative to the flight test results, a range of control, rate, and washed-out coupling configurations evaluated in flight were reevaluated on the ground-based simulator. This was done prior to expanding the variation of system configurations.

7. Discussion of the Results

7.1 The Baseline Configuration

During the bandwidth and phase delay study (ref. 14), the baseline configuration was evaluated with an average HQR of 2.5. Although it was not the objective of this

¹Half rating points were used with the exception of the Level boundary ratings (HQR 3.5 and HQR 6.5). In this report, ratings that were said to be “borderline,” “high 6,” “low 4,” etc., were supplemented with a “+” or “–” sign.

study to reevaluate this configuration, all pilots did fly the baseline configuration and rated it. The first line in table 7.1 ($M_{\delta_y} = 0$) shows the HQRs that were obtained. Ratings vary between 2 and 4, with an average HQR of 2.8. Most pilots evaluated the baseline configuration during their first evaluation flight and several of them commented that unfamiliarity with task and system, or fatigue from the journey to the test site affected their rating. Therefore, the actual HQR for this configuration is likely to be lower than 2.8.

Figure 7.1(a) shows the cyclic stick position time history of pilot C for a typical evaluation with the baseline configuration. Control inputs are very slightly diagonal (which might be caused by biomechanics) and contain only few excursions in the longitudinal direction. This confirms that the slalom task was essentially a single axis task that, in the absence of cross coupling, required very few pitch inputs.

7.2 Control Coupling

Control coupling is the most immediate kind of coupling. It is similar to the effect of cyclic stick input phasing and is directly proportional to the magnitude of the on-axis control input. With control coupling, the pitch and roll rates are given by:

$$q = \frac{M_{\delta_x} \delta_x + M_{\delta_y} \delta_y}{s - M_q} \quad (\text{with } M_{q,c} = M_q)$$

$$p = \frac{L_{\delta_y} \delta_y + L_{\delta_x} \delta_x}{s - L_p} \quad (\text{with } L_{p,c} = L_p)$$

For this study, the magnitude of the control coupling was varied through changes in the parameters L_{δ_x} and M_{δ_y} . Initially, the ratio of $|M_{\delta_y}/L_{\delta_x}|$ was kept constant at 0.55, which is close to the $|M_{\delta_y}/L_{\delta_x}|$ ratio of the standard BO 105. Experiments where the ratio of the on-to-off-axis response was varied are discussed in section 7.5.

A total of 24 control coupling evaluations provided HQRs that were consistent with comments and task performance. Table 7.1 shows the HQRs with the principal pilot comments listed per test campaign. There is a steady increase in average HQRs with increasing control coupling. The 1992 flight tests received slightly higher HQRs than the 1993 flight tests. This was attributed to experience gained with this type of coupling and will be addressed later. The ground-based simulation data fits the flight test data surprisingly well, considering that the simulation was fixed base and therefore lacked acceleration cueing. Pilot comments indicated that small and moderate amounts of cross coupling are perceived

primarily as an on-axis phenomenon (“notchy/jerky roll response,” “on-axis oscillations”). Higher amounts of coupling were perceived as a coupling and predictability problem (“moderate to large roll-due-to-pitch coupling,” “lack of predictability”).

Figure 7.1(b–f) shows some control position time histories for different control coupling configurations. For the baseline and the smallest coupling configurations (a–b), only a few excursions in the longitudinal axis are needed for mid- to long-term corrections to airspeed and height. With increasing amounts of coupling, the longitudinal control inputs become larger and start to follow a figure eight pattern: a pure lateral input is followed by a pure longitudinal input. This indicates the pilot uses an almost pure feedback control strategy rather than a feedforward control strategy that would contain more diagonally oriented inputs. For very large amounts of coupling, activity in the longitudinal axis starts to dominate the lateral inputs.² Figure 7.2 shows the lateral and longitudinal control input power spectra for the same configurations. As can be seen, the lateral (on-axis) control power spectrum magnitude decreases significantly with increasing coupling, indicating reduced aggression is needed to cope with the coupling. In the meantime, the magnitude of longitudinal control inputs increases with increased coupling. For the most severe coupling case, there is almost as much longitudinal as lateral control activity.²

All the above figures were obtained from 1992 flight test data. Ratings for these tests were shown to be somewhat more severe than for the 1993 flight tests. Careful comparison of identical configurations shows significant diagonal components in the 1993 control inputs (fig. 7.3 compares the configuration with $M_{\delta_y} = -0.0429 \text{ rad} \cdot \text{sec}^{-1} \cdot \text{percent}^{-1}$). Apparently, experience with coupling allowed the pilots to use more feedforward input. The use of feedforward causes smaller excursions in the pitch axis and hence makes the task easier to perform. A second difference between the 1992 and 1993 flight tests can be seen by looking at the off-axis power spectrum for high-frequency inputs. During the 1992 flight tests, longitudinal and lateral input power match closely up to a frequency of about 3.5 rad/sec. Beyond that frequency, where gate acquisition and tracking take place, longitudinal input power is significantly lower than lateral input power. During the 1993

²It should be pointed out that all diagrams are based on stick displacements in percent, and not on actual stick travel. Stick travel per percent is not equal for the lateral and longitudinal axes. Lateral stick travel, δ_y , is 2.2 mm/percent (0.0866 inches/percent); longitudinal stick travel, δ_x , is 3.1 mm/percent (0.1220 inches/percent).

tests, as a result of the diagonalized inputs, the shape of the longitudinal and lateral power spectra is the same, even for high frequencies. The use of diagonalized inputs may, at least partly, account for the different ratings given in 1992 and 1993. Other factors may have been the increased familiarity with the task and higher tolerances to coupling.

To investigate the effect learning has on the performance with coupled systems, two configurations were flown where coupling was in a different direction than usual. Pilot ratings and comments for these configurations are given in table 7.2. The first configuration, which was only very weakly coupled, received HQRs of 3 and 4-. Comments indicated that the pilots were aware of some coupling being present, though not that this coupling had changed direction. Unfortunately, no onboard data were available for these evaluations. The second configuration was very strongly coupled ($M\delta_y = 0.0429 \text{ rad}\cdot\text{sec}^{-1}\cdot\text{percent}^{-1}$). Because the coupling was backwards from all previous configurations, the pilot was struggling just to retain control of the aircraft. Figure 7.4 shows the pilot control inputs, the power spectrum, and the ϕ - θ plot for this configuration in comparison with the “normal” configuration with $M\delta_y = -0.0429 \text{ rad}\cdot\text{sec}^{-1}\cdot\text{percent}^{-1}$. As can be seen, no systematic inputs were made to alleviate the effects of coupling. Also, the power spectrum shows significantly less longitudinal than lateral inputs. This failure to remove the effects of coupling is clearly reflected in the ϕ - θ plot, and is corroborated by the pilot’s comment that coupling “got worse [when he tried] to reduce the amount of off-axis response.” This indicates that feedforward control is indeed a function of training and is not a natural response to the control problem.

Comparison of the given HQRs with the ADS-33C pitch-roll coupling parameters shows a clearly increasing pilot rating with increasing $\theta_{pk}/\phi_{t=4s}$ (fig. 7.5). Again, the differences between the 1992 and the 1993 flight tests and the ground-based simulator tests are obvious. Additional control coupling configurations with different pitch-due-to-roll to roll-due-to-pitch coupling ratios were evaluated. These will be discussed in section 7.5.

7.3 Rate Coupling

Off-axis rate coupling (or gyroscopic coupling) is proportional to the magnitude of the on-axis angular rate. Therefore, it can be seen as an indirect coupling with respect to the pilot’s inputs. For pure rate coupling, the pitch and roll rate are given by:

$$q = \frac{M\delta_x \delta_x + M_p p}{s - M_q} \quad (\text{with } M_{q,c} = M_q)$$

$$p = \frac{L\delta_y \delta_y + L_q q}{s - L_p} \quad (\text{with } L_{p,c} = L_p)$$

The magnitude of the rate coupling (roll-due-to-pitch and pitch-due-to-roll) was varied through changes in the parameters L_q and M_p . The ratio of $|M_p/L_q|$ was kept constant at 0.166, which is near the ratio of the standard BO 105 helicopter. Configurations with different $|M_p/L_q|$ ratios will be discussed in section 7.5.

Table 7.3 shows a list of pilot HQRs with selected comments for the evaluated rate coupling configurations. There is a more or less steady increase in HQRs with increased rate coupling. As with control coupling, small to moderate amounts of rate coupling were perceived mainly as a degradation of the on-axis performance (“jerky roll response”). Higher amounts of coupling rendered the response “unpredictable” and required “lots of compensation” by the pilot.

Figure 7.6 shows control position time histories for different rate coupling configurations. The same figure eight pattern as for control coupling is visible. Control inputs for the highest rate coupling configuration, $M_p = -2.5 \text{ rad/sec}$, seem somewhat more erratic. This configuration, however, was said to have a very unpredictable response, which might have caused the somewhat irregular control inputs. With the rate coupling configurations, much less diagonalized inputs were used than with control coupling. The use of diagonalized inputs with rate coupling tends to introduce additional dynamics, which could be objectionable. Analysis of the power spectra (fig. 7.7) shows the same trend as for control coupling: reduced lateral input power for more severe coupling configurations and increased longitudinal inputs with increased coupling.

Figure 7.8 shows a comparison of the pilot ratings against the ADS-33C coupling parameters. Some differences between the 1992 flight tests and the 1993 flight and ground-based simulator tests are obvious, especially at lower amounts of coupling. Again, the ground-based simulator data seem to correlate well with the flight test data. Some additional rate control configurations are discussed in section 7.5.

To investigate the influence or interaction between task demands and pitch-roll cross coupling, during the ground-based simulation a slightly modified ADS-33C slalom task was flown with several rate coupling configurations. This modified slalom task (fig. 7.9), consists of a series of s-turns initiated and completed in level unaccelerated

flight at 65 knots lined up with the centerline of the test course. The turns are performed around markers placed 50 feet off the centerline and 500 feet apart. The maximum distance from the centerline should not exceed 100 feet. The maneuver was to be accomplished at a reference altitude below 100 feet. Desired performance was to maintain an airspeed of at least 60 knots throughout the course. For adequate performance, an airspeed of least 40 knots was to be maintained. This modified slalom task differs from the ADS-33C slalom in that for the ADS-33C slalom there are no markers placed 50 feet off the centerline and 500 feet apart, i.e., the ADS-33C slalom task is to rapidly displace the aircraft 50 feet laterally from the centerline and immediately reverse direction to displace the aircraft 50 feet on the opposite side of the centerline. The modified slalom is similar to tasks used in previous coupling studies (ref. 8).

Table 7.4 shows a list of the pilot HQRs with characteristic comments for the evaluated rate coupling configurations while flying the modified slalom task on the ground-based simulator. There is a gradual degradation in the HQRs as the rate coupling increases with the main pilot compensation associated with maintaining airspeed.

Figure 7.8 shows a comparison of the pilot ratings against the ADS-33C coupling parameter. Shown are pilot ratings from the ground-based simulation and flight tests for the slalom-tracking task along with the ground-based simulation results from the modified slalom task. Several important observations can be made. For the slalom-tracking task, the ground-based simulator HQRs seem to correlate well with the flight test data. For the modified slalom task, the degradation in HQRs with increased rate coupling is not nearly as severe as it is from the slalom-tracking task. Specifically, in terms of $\theta_{pk}/\phi_{t=4s}$, the degradation into Level 2 occurs around 0.1 for the slalom-tracking task and around 0.35 for the modified slalom task. It is also interesting to note that when the HQRs for the modified slalom are solidly into Level 2, the HQRs for the slalom-tracking task are crossing over into Level 3.

This limited investigation into the effects of pitch-roll cross coupling for two different tasks highlights the fact that acceptable coupling is task dependent. The slalom-tracking task is a small amplitude precision tracking task, whereas the modified slalom task is a larger amplitude less precise task for which the effects of increased coupling do not appear to be as degrading. These results and observations imply that it will be necessary to define and demark which criteria and standards should apply to which mission task element groups.

7.4 Combined Control-Rate Coupling

So far, we have considered only pure rate or pure control coupling configurations. Most conventional helicopters exhibit a combination of both control and rate coupling. For combined control and rate coupling, the pitch and roll rates are defined by:

$$q = \frac{M_{\delta_x} \delta_x + M_{\delta_y} \delta_y + M_p p}{s - M_q} \quad (\text{with } M_{q,c} = M_q)$$

$$p = \frac{L_{\delta_y} \delta_y + L_{\delta_x} \delta_x + L_q q}{s - L_p} \quad (\text{with } L_{p,c} = L_p)$$

Variations of the amount of coupling are achieved through changes in the parameters L_{δ_x} , M_{δ_y} , L_q , and M_p . For all the considered configurations, the ratio of $|M_{\delta_y}/L_{\delta_x}|$ was kept constant at 0.55 and the ratio of $|M_p/L_q|$ was kept constant at 0.166 (similar to the BO 105). Some configurations with extreme amounts of coupling were included.

Configurations with combined control and rate coupling were only evaluated as part of the 1992 flight tests. HQRs and the principal pilot comments are given in table 7.5. The ratings show a steady increase with increasing coupling, with the exception of the rating given for the most severe coupling case. Comments for those severe coupling cases indicated some controllability problems (one pilot was unable to complete the task without losing control of the aircraft and subsequently gave an HQR of 10). Figure 7.10 shows the pilot stick inputs for selected configurations. The figure eight pattern is clearly discernible, up to the highest coupling levels. For these configurations, the amplitude of the longitudinal inputs is larger than the lateral inputs. For the most severe coupling case (fig. 7.10(f)), a slightly diagonalized control strategy can be seen, which may explain the lower HQR for this configuration. The same conclusions follow from the input power spectra (fig. 7.11).

Figure 7.12 shows the pilot HQRs versus the ADS-33C criterion for combined control and rate coupling cases. Transition from Level 1 to Level 2 can be found at about 15 percent coupling. The Level 2–3 boundary is not as well defined, with several data points lying exactly on the boundary. For high amounts of coupling, there is strong scatter in the data. Nevertheless, all configurations with $\theta_{pk}/\phi_{t=4s}$ over 50 percent were rated Level 3 or above.

7.5 The Effect of the Pitch-due-to-Roll over Roll-due-to-Pitch Coupling Ratio

The slalom-tracking task discussed in this report is basically a single axis roll task. When no coupling is

present, the pilot needs only very few longitudinal inputs to complete the course. With the introduction of pitch-due-to-roll coupling, longitudinal inputs with increasing magnitude are needed to maintain height and speed. In the presence of roll-due-to-pitch coupling, these longitudinal inputs will, in turn, produce a roll response. This may be perceived as an oscillatory motion.

To initially gain some insight into how the ratio of off-to-on axis coupling varies in helicopters as a function of airspeed, coupling derivative data was collected from reference 19 and the ratio of $(M_p/M_q)/(L_q/L_p)$ plotted. Figure 7.13 shows the coupling ratios for the BO 105C, the OH-6A, the UH-1H, and the CH-53D versus airspeed from hover to 120 knots. For all aircraft except the BO 105C, the off-to-on axis coupling ratio decreases with speed. All coupling configurations discussed so far in this report used a coupling ratio similar to that of the BO 105: $|M_{\delta_y}/L_{\delta_x}| = 0.55$ and $|M_p/L_q| = 0.166$. In order to evaluate the effects of the roll-due-to-pitch coupling on the evaluation of the roll axis task, configurations with different off-to-on axis coupling ratios were tested. A pitch-due-to-roll over roll-due-to-pitch coupling coefficient, C , was defined as follows:

$$C = \frac{\frac{|q_{\max}|}{|p_{\max}|} \delta_y}{\frac{|p_{\max}|}{|q_{\max}|} \delta_x}$$

Definition of p_{\max} and q_{\max} is shown graphically for two coupling types in figure 7.14.

Configurations with different off-to-on axis ratios ($C = \infty, 1.0, 0.55$, and 0.33) were tested in the fixed-base simulator and during the 1993 flight tests. Pilot HQRs and principal comments are given in table 7.6 for control coupling configurations and in table 7.7 for rate coupling configurations. Results for the rate coupling configurations indicate a distinct trend toward improved ratings with decreased roll-due-to-pitch coupling (increased C). This trend is quite pronounced for cases with quite severe cross coupling. For moderate to light cross-coupling configurations, the differences are negligible. Results of the control coupling configurations seem to indicate an opposite trend, although differences in HQRs are very small for the moderate cross-coupling cases, and the ratings for the strong cross coupling were influenced by the fact that both pilots had configuration A9 (see Appendix C) as their first coupling evaluation of the test campaign. Comparison of only the pilot comments shows no trends for the low and moderately coupled cases. For the more severe cases, the pilots complained of a “jerky” and “oscillatory” on-axis response that seemed to become

more pronounced with increased roll-due-to-pitch coupling (decreased C).

Figure 7.15 shows the control input crossplots for two rate coupling configurations with different amounts of roll-due-to-pitch coupling. No significant differences in control strategy can be discerned for the case where $M_p = -0.5$ rad/sec (left column). For the more severe coupling case, $M_p = -2.0$ rad/sec (right column), a slight increase in pitch input amplitude can be seen with increasing roll-due-to-pitch coupling. Comparison of the power spectra (fig. 7.16) shows an increase in roll input frequency with an increase in pitch input amplitude for the more severely coupled case. The power spectra show no definitive trends for the moderately coupled case.

Figure 7.17 shows a comparison of the ADS-33C coupling parameters with HQRs from pilot C in the fixed-base simulator. As the coupling ratio, C , increases from 0.33 to ∞ , the Level 2–3 transition seems to shift from about 45 percent to about 60 percent. The Level 1–2 transition, however, does not seem affected by the coupling ratio. Figure 7.18 compares the ADS-33C coupling parameters with rate coupling results from the 1993 flight tests. Although the spread in data is somewhat larger, the trends found from the fixed-base simulator tests were confirmed. Because of the limited number of reliable data, the control coupling results were not plotted.

7.6 The Effect of Reduced On-Axis Damping

All coupling configurations discussed so far had the on-axis characteristics of the baseline model, i.e., on-axis damping $L_p = -8.0 \text{ sec}^{-1}$ and $M_q = -4.0 \text{ sec}^{-1}$, roll axis bandwidth and phase delay of 3.44 rad/sec and 77 msec , and pitch axis bandwidth and phase delay of 2.00 rad/sec and 114 msec .³ For the slalom-tracking task, a reduction of the helicopter bandwidth causes a degradation of task performance and pilot HQRs (ref. 14). To investigate the cumulative effects of cross coupling and bandwidth, two sets of configurations with different bandwidth characteristics were tested in the fixed-base simulator. The first set of configurations had reduced on-axis damping in both axes; i.e., the L_p/M_q ratio (or coupling coefficient C) was the same as for the baseline configurations. On-axis damping for this configuration was $L_p = -5.0 \text{ sec}^{-1}$ and $M_q = -2.5 \text{ sec}^{-1}$. Bandwidth and phase delay were 2.80 rad/sec and 71 msec for the roll axis and 1.76 rad/sec and 72 msec for the pitch axis. From interpolation of the results from the bandwidth-phase delay study (ref. 14),

³Values for the fixed-base simulator experiments differ slightly: roll axis bandwidth and phase delay are 3.64 rad/sec and 69 msec ; pitch axis bandwidth and phase delay are 2.43 rad/sec and 71 msec .

marginal Level 1 handling qualities (HQR = 3) were expected for this configuration. The second set of reduced damping configurations only had its roll axis damping changed ($L_p = -6.0 \text{ sec}^{-1}$); the pitch axis damping was the same as for the baseline configuration ($M_q = -4.0 \text{ sec}^{-1}$). It was suspected that the reduction of the roll but not the pitch axis bandwidth might have some consequences on the perception of coupling. For these cases, roll axis bandwidth and phase delay were 3.12 rad/sec and 70 msec. The control derivatives for both configurations were proportioned based upon the relationships developed during the bandwidth-time delay study. Direct and coupled on-axis damping were kept identical for all reduced on-axis damping configurations ($L_p = L_{p,c}$ and $M_q = M_{q,c}$).

Results of the configurations with reduced on-axis damping in both axes are given in table 7.8 for rate coupling and in table 7.9 for control coupling cases. Results for the configurations with reduced roll axis damping only are given in table 7.10 for control coupling cases. All cases were evaluated in the fixed-based simulator with a single pilot participating. The uncoupled cases were both evaluated with HQR = 3. Comments mentioned increased sluggishness, lower precision, and increased planning that was required prior to entering the gate. For all other configurations, a steady degradation in pilot rating with increased coupling can be seen. Pilot comments were compatible with the fixed-base simulator comments for the higher bandwidth configurations (tables 7.1 and 7.3). Analysis of crossplots and power spectra did not show significant differences between the high and low bandwidth configurations.

Figures 7.19 and 7.20 show the pilot HQRs versus the ADS-33C coupling parameters for the rate and control coupling cases. In both cases, the symmetrically reduced bandwidth configurations ($L_p = -5.0 \text{ sec}^{-1}$ and $M_q = -2.5 \text{ sec}^{-1}$) seem to degrade into Level 2 with lesser amounts of coupling than the two other cases ($L_p = -8.0 \text{ sec}^{-1}$ and $M_q = -4.0 \text{ sec}^{-1}$, and $L_p = -6.0 \text{ sec}^{-1}$ and $M_q = -4.0 \text{ sec}^{-1}$). Through the moderate amounts of coupling (Level 2), the three configurations were rated almost identical. At higher coupling levels, there is a typical spread in data points. The differences in ratings could be due to the fact that (for the lower damping case) there is less margin between the task bandwidth and the aircraft bandwidth and therefore a smaller capacity for coupling before the pilot has to start adding lead compensation. As coupling starts dominating the ratings, this difference would tend to disappear.

7.7 Washed-Out Coupling

Future helicopters will have stiff hingeless or bearingless rotors with a full authority control system to alleviate the resulting cross coupling. Traditional feedback control systems do not eliminate coupling, but reduce coupling as soon as it occurs. This leads to a coupling that is “washed out” with time. When the current ADS-33C cross-coupling requirements were drafted, this type of coupling was not considered. Under the current requirement, even very high levels of washed-out coupling would still be predicted with Level 1 handling qualities, which seems unrealistic. Therefore, several washed-out coupling configurations were tested. For washed-out coupling, the roll and pitch rate are given by the following equations (using $M_q L_{\delta_y} = L_p M_{\delta_x}$ and $M_{\delta_x} = M_q L_{\delta_x}$):

$$p = \frac{L_{\delta_y}}{s - L_p} \delta_y + \frac{L_{\delta_x} s}{(s - M_q)(s - L_{p,c})} \delta_x$$

$$q = \frac{M_{\delta_x}}{s - M_q} \delta_x + \frac{M_{\delta_y} s}{(s - L_p)(s - M_{q,c})} \delta_y$$

The parameters L_{δ_x} and M_{δ_y} were varied to change the amplitude of the washed-out coupling. The off-axis damping parameters $L_{p,c}$ and $M_{q,c}$ were varied to change the amplitude and rapidity of the washing out. Configurations with two different ratios of $M_{\delta_x}/L_{\delta_y}$ were flight tested: $M_{\delta_x}/L_{\delta_y} = -1.8$ and $M_{\delta_x}/L_{\delta_y} = -1.0$.

Table 7.11 shows the HQRs for the case where $M_{\delta_x}/L_{\delta_y} = -1.8$, for pilots C and E with the principal comments of pilot C. As can be seen, the results from the two different flight test series correlate well. The results from the fixed-base simulation, however, do not correlate with the flight test results at all. This is also evident from the pilot comments. The discrepancies were blamed on the lack of acceleration cues in the fixed-base simulator. During flight tests, “unnatural accelerations” were mentioned as a reason for the degradation of handling qualities. In the absence of these acceleration cues the validity of the HQRs becomes questionable. Therefore, fixed-base simulator results are ignored from the discussion of the washed-out coupling results. From the comments of pilot C, it can be seen that washed-out coupling manifests itself mainly as a multi-axis oscillatory response.

Table 7.12 lists the HQRs and principal comments of pilot D for the configurations with $M_{\delta_x}/L_{\delta_y} = -1.8$. Comparison with the HQRs of pilot C (table 7.11) shows that pilot D generally was more tolerant of washed-out coupling. All HQRs, with the exception of the most severe coupling case, are either 3 or 4. Pilot ratings and

comments for the configurations with $M\delta_x/L\delta_y = -1.0$ can be found in table 7.13. Again, the ratings of pilot C are significantly degraded compared to those of pilot D. This is also reflected in the comments; although both pilots seem to experience a jerky/notchy response, pilot C seems to object more to this response than pilot D.

The difference in HQRs between both pilots is reflected by a difference in control strategy. Figure 7.21 shows the control crossplots for selected washed-out coupling configurations with $M\delta_x/L\delta_y = -1.0$ and $M_{q,c} = -4.0 \text{ sec}^{-1}$ (except for one configuration for which $M\delta_x/L\delta_y = -1.8$). The control inputs of pilot D (left column) contain relatively few longitudinal excursions. With increasing coupling, a moderate figure eight shape can be seen. The control inputs of pilot C (right column) contain significant longitudinal inputs that seem to follow an irregular pattern. The same follows from analysis of the power spectra (fig. 7.22). For the most severe coupling case, pilot C has a significant amount of longitudinal inputs which seem to follow the spectral peaks of the lateral inputs. Pilot D has only minimal longitudinal activity. Comparison of the task performance (fig. 7.23) for this case shows that pilot D performs slightly better than pilot C, who seems to have more trouble getting a clear tracking phase. This leads to the conclusion that each pilot used a different control strategy. Pilot D mainly used lateral control inputs and only used longitudinal inputs to correct for the integral part of the washed-out coupling, not for the transient rate part. He just “rode the coupling.” Pilot C used a lot of longitudinal inputs to try and eliminate the transient coupling effects. This renders the helicopter more difficult to control, something which is reflected in the poorer task performance and higher HQRs of pilot C.

Figure 7.24 shows the pilot HQRs versus $M\delta_y$ for the case where $M_{q,c}$ equals -4.0 sec^{-1} . The difference between both pilots is obvious. Figure 7.24 shows no significant effects of $M\delta_x/L\delta_y$ on HQRs. The same follows from comparison of tables 7.11 and 7.12 with table 7.13 and from comparison of the control crossplots and power spectra. Where the effect of coupling amplitude (parameters $L\delta_x$ and $M\delta_y$) on handling qualities is quite pronounced, the effect of wash-out speed (parameters $L_{p,c}$ and $M_{q,c}$) is far less obvious. From the available data, a trend toward degraded ratings with a slower washout of the coupling can be seen. Significant differences in control strategy or power spectra, however, were not observed.

Because of the way in which the ADS-33C criterion is formulated, levels of $\theta_{pk}/\phi_{t=4s}$ for washed-out coupling are very low compared to control or rate coupling cases. In fact, even the most severe washed-out coupling cases

still had less than 5 percent coupling according to the ADS-33C definition. Figure 7.25 shows pilot ratings versus $\theta_{pk}/\phi_{t=4s}$. As can be seen, the results do not correlate with the control or rate coupling cases of figures 7.5 and 7.6. Because washed-out coupling is more a short-term phenomenon, the frequency domain may provide a more suitable method for analysis.

7.8 Configurations with Modified Frequency Domain Characteristics

In order to gain a better understanding of the coupling phenomenon in the frequency domain, some rate and washed-out coupling configurations with modified values of $L_{p,c}$ and $M_{q,c}$ (coupled on-axis damping) were flight tested. Most coupling configurations so far used $L_{p,c} = -8 \text{ sec}^{-1}$ and $M_{q,c} = -4 \text{ sec}^{-1}$. This means that the corner frequencies of the cross-coupled motions were well above the highest input frequencies. By reducing $L_{p,c}$ and $M_{q,c}$, these corner frequencies are lowered and high frequency inputs will be effectively uncoupled. In the meantime, the on-axis characteristics of the helicopter remain unchanged, i.e., $L_p = -8 \text{ sec}^{-1}$ and $M_q = -4 \text{ sec}^{-1}$.

Four rate coupling configurations with severely reduced $L_{p,c}$ and $M_{q,c}$ were tested. For these modified rate coupling configurations, the pitch and roll rate are given by:

$$\begin{aligned} q &= \frac{M\delta_x}{s - M_q} \delta_x + \frac{M_p}{s - M_{q,c}} p \\ &= \frac{M\delta_x}{s - M_q} \delta_x + \frac{M_p}{(s - L_p)(s - M_{q,c})} \delta_y \\ p &= \frac{L\delta_y}{s - L_p} \delta_y + \frac{L_q}{s - L_{p,c}} p \\ &= \frac{L\delta_y}{s - L_p} \delta_y + \frac{L_q}{(s - M_q)(s - L_{p,c})} \delta_x \end{aligned}$$

The off-axis damping coefficients were identical, $L_{p,c} = M_{q,c}$. The ratio $|M_p/L_q|$ was kept constant at 1.0, so that the coupling coefficient $C = 1.0$.

Table 7.14 shows the results of the four rate coupling cases. The HQR for the configuration with $M_p = -0.25 \text{ sec}^{-1}$ and $M_{q,c} = -1.0 \text{ sec}^{-1}$ seems somewhat overly degraded. Unfortunately, onboard or ground tracking measurement data are not available to provide an explanation. Comments mentioned a jerky response and slow and unusual coupling as the main contributors to the HQRs. Measurement data were

available only for two configurations, which makes comparison difficult.

Two washed-out configurations with severely reduced $L_{p,c}$ and $M_{q,c}$ were tested. For these modified washed-out coupling configurations, the pitch and roll rates are given by:

$$q = \frac{M\delta_x}{s - M_q} \delta_x + \frac{sM\delta_y}{(s - L_p)(s - M_{q,c})} \delta_y$$

$$p = \frac{L\delta_y}{s - L_p} \delta_y + \frac{sL\delta_x}{(s - M_q)(s - L_{p,c})} \delta_x$$

The off-axis damping coefficients were identical, $L_{p,c} = M_{q,c}$. Coupling coefficient, C , was about 0.45.

Results show that both coupling cases are very similar (table 7.15). Comments mentioned a “jerky response” and nonsymmetry of the coupling sensitivities and damping. Control crossplots and power spectra for this configuration are given in figure 7.26. As can be seen, the configuration with $M_{p,c} = -2.0 \text{ sec}^{-1}$ has somewhat larger amplitude longitudinal inputs than the configuration with $M_{p,c} = -0.5 \text{ sec}^{-1}$. This can be seen both from the crossplots and the power spectra.

In figure 7.27, all modified frequency cases are compared to the ADS-33 coupling parameters. The figure shows a rather large spread in the control coupling data points. The results for the washed-out coupling do not correlate well with the ADS-33C criterion, as expected.

8. Analysis of the Results

8.1 Pilot Control Strategy

To gain a better understanding of how pitch-roll coupling affects handling qualities, it is necessary to study pilot control strategy. Analysis of the uncoupled baseline configuration (sec. 7.1) confirmed that the slalom-tracking task is essentially a roll axis task. When no coupling is present, only a minimum of longitudinal inputs are needed to maintain height and speed. Four task phases were identified from the lateral input spectrum: (1) sequencing of the gates at about 1 rad/sec, (2) transition between the gates at about 2 rad/sec, (3) acquisition of the gates near 3.5 rad/sec, and (4) the tracking of the gates up to about 7 rad/sec. Lateral control power shows a significant reduction above 4 rad/sec and is almost nonexistent above 7 rad/sec. It is striking that these frequencies are close to the roll-axis bandwidth and neutral stability frequencies of 3.4 and 7.45 rad/sec.

In the presence of control/rate coupling, the pilot used a control strategy that resembled a figure eight pattern (fig. 8.1). Such a figure eight pattern is indicative of the feedback control strategy (ref. 20) shown in figure 8.2. This is further confirmed by the control input pattern of the washed-out coupling cases. Because coupling is washed out, the control inputs no longer follow the same figure eight pattern; rather, they seem to wash out with time. While acting as a feedback system, the pilot primarily controls the roll axis—where his primary task is—and uses his spare capacity to eliminate the effects of pitch coupling that show up as pitch attitude, altitude, or velocity errors.⁴ As coupling increases, more attention is channeled toward controlling the pitch axis. Since the slalom-tracking task is a demanding task which leaves the pilot with only limited spare capacity to control the secondary axes, there exists a “saturation level” beyond which the pilot will have to reduce his aggressiveness in roll to cope with the pitch-axis demands. This reduction of roll-axis aggressiveness results in reduced performance and is reflected by Cooper–Harper ratings of 5 or more.

Figures 8.3 and 8.4 show the lateral and longitudinal power spectra for some selected control and rate coupling cases. The lateral input power spectra (left column) show that input power is reduced when the saturation level—characterized by HQRs of 5 or more—is reached. The longitudinal power spectra (right column, different scale) show a steady increase of input power with increased coupling. Apart from this increase in input power, there is also an obvious shift toward higher frequencies. For mild coupling cases, most longitudinal input activity is centered around the pitch bandwidth frequency of 2 rad/sec. For more severe coupling cases, longitudinal input activity shifts to about 3 to 4 rad/sec. For some of the most severe coupling cases, input activity above the pitch-axis neutral stability frequency, $\omega_{180\theta}$, was observed. Analysis of these cases showed some mild pitch oscillations which seemed pilot induced.

In the previous chapter, it was discussed how diagonalized inputs were sometimes used for the elimination of coupling. Those diagonalized inputs are characterized by the feedforward control strategy shown in figure 8.5. Since the diagonalization seems to occur mainly with lateral inputs (see fig. 8.6), only pitch-due-to-roll feedforward element was modeled. Most diagonalized inputs were used during the 1993 flight tests

⁴This model, known as a two-axis single loop feedback model, is a simplification of the true pilot model. Any pilot who is aware that the aircraft is coupled will anticipate that coupling. The magnitude of his input, however, will generally be a function of the resulting pitch response, not of the anticipated pitch response.

for the elimination of control coupling. All pilots who used diagonalized inputs had flown quite a few coupled configurations before. The effect of using diagonalized inputs is similar to using control input phasing and hence is very efficient in reducing the effects of control and rate coupling. Because of the feedforward loop, input frequencies higher than the neutral stability frequency can be used without the risk of instabilities (pilot-induced oscillations (PIOs)). When the pilot used diagonalized inputs, the helicopter was given better HQRs than when a regular feedback control strategy was used. The use of feedforward seems to be the result of a rationalization of the coupling problem, and not the product of normal adaptation. During the 1993 flight test campaign, two control coupling configurations that the same cross-coupling magnitude but a different coupling sign were tested. When the cross coupling was in the direction the pilot had become used to, he gave an HQR of 5. When the sign of the coupling was changed, his HQR deteriorated to 9. It is doubtful that a feedforward strategy can be easily adapted to different tasks, especially multi-axis tasks. Therefore, it seems inappropriate to let those cases that were affected by a feedforward control strategy play a significant role in the determination of Level boundaries.

A final aspect of pilot control strategy is the differences between pilots in responding to washed-out coupling. In the discussion of washed-out coupling (sec. 7.7), it was pointed out that the two evaluating pilots—pilot C and pilot D—used a different control strategy, and that such differences could not be found with the control and rate coupling cases. For the washed-out coupling cases, on-axis aggressiveness of both pilots was found to be more or less comparable (see, e.g., fig. 7.20 or 7.21). The off-axis inputs, however, revealed significant differences. Pilot C seemed much more aggressive in trying to reduce coupling; his inputs were larger, less regular, and contained more high-frequency components. Pilot D seemed to just compensate for the integral part of the washed-out coupling (the change in attitude that results from the washed-out rate). Pilot D did notice a “ratcheting response” and “strange accelerations,” but did not seem to make an effort to eliminate the coupling that caused these complaints. Despite these differences in control strategy, the differences in task performance were only minimal. In fact, pilot D who just “rode the coupling” had a slightly better task performance than pilot C who seemed to “fight the coupling.” The underlying difference in control strategy must be sought in the cues used for the elimination of coupling. Pilot C probably picked up on the rate and acceleration cues to control against the coupling. Pilot D waited for the rate response to wash out and reacted only to the angular part of the coupling. Despite these differences, the results from pilots will be

considered in the following discussion of pitch-roll coupling criteria.

8.2 Evaluation of the ADS-33C Time Domain Criterion

The pitch-roll cross-coupling criterion as defined in ADS-33C (ref. 1) places a requirement on the mid- to long-term behavior of the helicopter attitude following a step input. For the slalom-tracking task, the pilot uses compensatory longitudinal inputs up to a frequency of about 4.5 rad/sec. This would indicate that short-term effects play a role in the perception of coupling and that cues other than attitude might be relevant to the coupling discussion (e.g., angular rates). As pointed out by Ockier (ref. 21), the use of a step input and Euler angles for the definition of the ADS-33C coupling parameters also causes the coupling parameter to be dependent on the sign and, to a lesser effect, the amplitude of the input.

In the previous chapter, a comparison of the pilot HQRs with the ADS-33C pitch-due-to-roll coupling parameter, $|\theta_{pk}/\phi_{t=4s}|$, was given for most configurations.⁵ Consistency between the ADS-33C criterion and the pilot ratings was shown for the control, rate, and combined control-rate coupling cases. For washed-out coupling, the ADS-33C criterion does not show this inconsistency. Figure 8.7 shows the ADS-33C criterion versus the individual pilot HQRs for control, rate, and combined control-rate coupling. Only the cases with the on-axis to off-axis coupling ratio similar to that of the BO 105 (tables 7.1, 7.3, and 7.4) were included in the figure. The figure shows an obvious trend toward deteriorated handling qualities with increased coupling, although this trend is a bit overshadowed by the large data spread. Level separations are at about 0.1 for the Level 1–2 boundary and at about 0.6 for the Level 2–3 boundary. Closer examination shows that the coupling configurations from the 1992 flight tests received a more severe rating than those from the fixed-base simulator or 1993 flight tests. This was attributed to the pilot’s adaption to those types of coupling (e.g., by using diagonalized inputs). The lack of acceleration cues in the fixed-base simulator may have caused some discrepancies in that area, especially at small amounts of coupling. Figure 8.7 also reveals minor differences between the control, rate, and combined control-rate coupling configurations. In general, rate and combined coupling were rated somewhat more severely than the pure control coupling cases. This

⁵For all cases, the values of θ_{pk} and $\phi_{t=4s}$ were calculated from model parameters using the small angle assumption. Excellent correlation of these parameters with flight test parameters was verified for a large number of cases.

difference is particularly pronounced for the 1993 flight tests, and can be explained by the use of diagonalized inputs which were used more (successfully) with control coupling cases. It should be pointed out, once again, that differences in dynamic behavior between control and rate coupling are not really discernible at frequencies below about 4 rad/sec, which is the highest pitch-axis input frequency.

In considering the differences between rate and control coupling, there is another aspect that should not be disregarded: the effect of the pitch-due-to-roll over roll-due-to-pitch coupling ratio. For equal amounts of pitch-due-to-roll coupling, the rate coupling cases in figure 8.7 have much larger levels of roll-due-to-pitch coupling than the control coupling cases. Figure 8.8 shows a two-sided diagram of the ADS-33C roll-due-to-pitch and pitch-due-to-roll coupling parameters for all control, rate, and combined coupling configurations. The individual pilot ratings are shown as labels to the data points. As pointed out, the effect of the roll-due-to-pitch to pitch-due-to-roll coupling ratio is most noticeable at high coupling levels. This accounts for some of the data spread in figure 8.7, as is confirmed in figure 8.8. It can also be seen that, for the roll-axis task under consideration, significantly more $|\phi_{pk}/\theta_{t=4s}|$ than $|\theta_{pk}/\phi_{t=4s}|$ is tolerated. For the control, rate, and combined coupling configurations investigated, Level separation boundaries are shown in figure 8.9 along with the averaged data from figure 8.8. It should be pointed out that the drawing of Level boundaries is complicated by the spread in data. This poses a problem at the Level 1–2 boundary. It is clear, however, that for this roll tracking task, the Level 1–2 boundary must be significantly lower than the ADS-33C values. Since the roll task used for the evaluations required little or no pitch maneuvering, no hard recommendations for the roll-due-to-pitch boundaries can be made.

For washed-out coupling configurations, the ADS-33C criterion does not present a useful method of evaluation. Even the most severe washed-out coupling configuration (HQRs 7 and 6) have a $\theta_{pk}/\phi_{t=4s}$ of less than 4 percent, which falls well within any limits for Level 1 handling qualities (see fig. 7.24).

8.3 Frequency Domain Analysis

As evident from the feedback control strategy, coupling is seen by the pilot essentially as a poorly predictable disturbance that needs to be eliminated. Each control axis is considered a separate compensatory system. Therefore, the ability of the pilot to eliminate coupling will depend largely on the system capabilities of that compensatory axis; i.e., to compensate for pitch-due-to-roll coupling, the pitch axis response characteristic will be deciding. It

was discussed how pitch-due-to-roll coupling is eliminated using longitudinal inputs with a frequency roughly between the pitch bandwidth (45 degree phase or 6 dB gain margin) and neutral stability (zero phase margin) frequency. When demand on the pilot is relatively low (i.e., coupling is moderate or the task is not very demanding), pitch-axis inputs with a frequency around the bandwidth frequency are used. When the demand on the pilot increases (e.g., due to increased coupling), the frequency in the compensatory axis increases to roughly the neutral stability frequency. Input frequencies beyond the neutral stability frequency are not useful—at least not as long as the pilot works as a pure gain feedback system—because of stability problems. Because of the importance of the bandwidth and neutral stability frequencies, the relative coupling amplitudes at those frequencies will be used as a basis for discussion of pitch-roll coupling in the frequency domain.

Figure 8.10 shows the magnitude of the body-axis pitch rate to roll rate, q/p at the pitch-axis bandwidth frequency, $\omega_{BW\theta}$, versus the HQRs for control, rate, and combined control-rate coupling cases. Only the cases with the original on-axis to off-axis coupling ratios ($|M_{\delta_y}/L_{\delta_x}| = 0.55$ and $|M_p/L_q| = 0.166$) were included. Figure 8.10 is very similar to the time domain representation in figure 8.7. The values of q/p at the bandwidth frequency are only slightly lower than the (almost) steady state coupling values of figure 8.7. Also, the differences between control and rate coupling at the bandwidth frequency are only minimal (see also fig. 5.5). Figure 8.11 shows the data from figure 8.10, using a logarithmic scale. Logarithmic scales will be used in the subsequent discussions because of their higher relevance to the frequency domain. The Level boundaries in figures 8.10 and 8.11 can be drawn somewhere around $q/p = 0.1$ (–20 dB) and $q/p = 0.45$ (–7 dB), respectively. Figure 8.12 shows the same data versus the magnitude of q/p at the pitch-axis neutral stability frequency, $\omega_{180\theta}$. The same plot is shown using a decibel scale in figure 8.13. It can be seen that the magnitude of q/p is slightly lower than at the pitch bandwidth frequency. This decrease in magnitude is more pronounced for rate coupling than for control coupling data points. This seems to enhance the effect that rate coupling was evaluated more severely than control coupling. Level 1–2 and 2–3 boundaries can be found somewhere around $q/p = 0.08$ (–22 dB) and $q/p = 0.35$ (–9 dB).

Because of its focus on mid- to long-term coupling, the ADS-33C time domain criterion proved incapable of modeling the short-term nature of washed-out coupling. By considering the coupling ratio at the bandwidth and neutral stability frequencies, the frequency domain representations presented above focus exclusively on the

short-term coupling behavior. Therefore, a much better correlation of washed-out coupling with the rate-control coupling data is expected.

Figure 8.14 shows the individual pilot HQRs versus the magnitude of q/p at the bandwidth frequency for the washed-out coupling configurations. Immediately obvious is the fact that the washed-out coupling data correlate fairly well with the rate coupling data (to keep the figure uncluttered, the control and combined data are not shown). Closer inspection reveals significant differences between the two evaluating pilots (pilots C and D). Compared to pilot C, the ratings of pilot D are significantly lower. For pilot D, the transition between Levels 1 and 2 takes place at $q/p \approx -20$ dB. No Level 3 data points are available for pilot D, but the Level 2–3 boundary necessarily lies above $q/p = -7$ dB, which is the highest Level 2 data point. These boundaries correlate quite well with the boundaries determined for the rate and control coupling cases (-20 dB and -7 dB). As could be expected, the data for pilot C do not correlate as well. At $q/p = -20$ dB, pilot C has clearly exceeded the Level 1 boundary, and Level 3 is reached before q/p exceeds -10 dB. There is also a substantial spread in the data points of pilot C. During the discussion of control strategy, it was observed how the compensatory inputs of pilot C contained significantly higher frequencies than the inputs of pilot D. Therefore, better correlation for pilot C can be expected at the pitch-axis neutral stability frequency.

Figure 8.15 shows the individual pilot ratings of the washed-out coupling cases versus q/p at the neutral stability frequency. Again, there is a fairly good correlation of the washed-out coupling data with the rate coupling data. Now, the HQRs of pilot C correlate better with the rate coupling cases than the HQRs of pilot D—as could be expected. Also significant is the fact that the spread in the data of pilot C is considerably smaller than at the bandwidth frequency. This is the result of shifts within the washed-out coupling data base (data points with different $L_{p,c}$ and $M_{q,c}$ off-axis camping values shift significantly with respect to each other as frequencies are increased). Using the neutral stability, the Level 2–3 transition takes place around $q/p = -8$ dB, which is not inconsistent with the control-rate coupling value of around -9 dB. There are no Level 1 washed-out data points for pilot C. Comments from pilot C for the two data points that lie below -23 dB indicate that the coupling mainly manifested itself as a “jerky” on-axis response. For one of those data points, the jerky response was only found “mildly objectionable.” Based on this, placing the Level 1–2 boundary at about -23 dB seems acceptable.

The data points with modified coupled damping (tables 7.13 and 7.14) represent an odd configuration where the damping of the cross-coupled motion is effectively reduced. This results in an effective decoupling of the high frequency inputs (see sec. 7.8). Data for these configurations are shown in the frequency format in figures 8.16 and 8.17. The data point with HQR = 6 and $q/p = -25$ dB in the bandwidth format and $q/p = -32$ dB in the neutral stability frequency format seems to have been significantly overrated (see discussion in sec. 7.8). This data point will therefore be ignored. The other data points follow the same trends as the control, rate, and washed-out coupling data. This confirms the validity of the frequency domain criterion, even for these unusual types of coupling. Careful analysis of the modified frequency data shows that correlation is somewhat better with the bandwidth frequency than with the neutral stability frequency. The lack of in-flight data for these configurations makes it very difficult to address the cause of this. Also, the fact that the test conditions for some of these configurations were suboptimal (only one test and one evaluation run) may have influenced the ratings.

The effects of reduced on-axis bandwidth have been investigated only in the fixed-base simulator; therefore, a comparison with in-flight data must be made with caution (see sec. 7.6). Figures 8.18 and 8.19 show the reduced on-axis bandwidth data points in the frequency domain. It should be noted that because of the reduced on-axis bandwidth and neutral stability frequencies, the frequency at which q/p was evaluated was lower than in the previous cases. In general, there is a good correlation between these data and the data with the original on-axis bandwidth. At lower amounts of coupling, HQRs are only very slightly higher than those of the other coupling configurations (probably as a result of the poorer baseline handling qualities). At higher frequencies, the differences are even less pronounced. The HQRs for the rate coupling configurations were somewhat worse than for the control coupling configurations. Although diagonalized inputs are suspected as the cause for this, confirmation for this could not be obtained. At the neutral stability frequency, the picture is similar; i.e., the rate coupling configurations cross over into Level 3 at even lower coupling values. For the cases where only the roll-axis damping (but not the pitch-axis damping) was reduced, correlation is significantly poorer. It is suspected that the magnitude of q/p at the roll bandwidth and neutral stability frequency might have an effect on these data points.

In order to include the effects of roll-due-to-pitch coupling, the parameter p/q , determined at the roll-axis bandwidth and neutral stability frequency, will be used as a second parameter in the frequency domain figures. Figure 8.20 shows the magnitude of q/p versus p/q at the

bandwidth frequency for all control-rate coupling cases. Individual pilot HQRs are plotted alongside the data points. From the data, a clear trend toward decreasing q/p limits with increased roll-due-to-pitch coupling (p/q) can be noted. Based on this observation, tentative Level boundaries were drawn. These boundaries suggest that the effects of the roll-due-to-pitch coupling are negligible for p/q less than -15 dB. Above this limit, the effects of roll-due-to-pitch coupling become increasingly more important. It should be emphasized that no limits for p/q are suggested in the figure; the use of a roll-axis piloting task allows the imposition pitch-due-to-roll limits only, not of roll-due-to-pitch limits—hence the dashed lines. The use of both q/p and p/q in one diagram clearly allows for better data correlation. Some of the discussed differences between rate and control coupling data can now clearly be identified as the result of roll-due-to-pitch coupling. Figure 8.21 shows the same data at the neutral stability frequency. This figure is very similar to figure 8.20. Because the same data points have lower coupling values at the neutral stability frequency than at the bandwidth frequency, the boundary curves were shifted slightly to the left. For the correlation of the control-rate data, there seem to be no significant differences between the bandwidth and neutral stability frequency formats.

Figures 8.22 and 8.23 show the washed-out coupling data at the bandwidth and neutral stability frequencies. As expected, correlation of the HQRs from pilot C is excellent with the neutral stability frequency format and correlation of the HQRs from pilot D is excellent with the bandwidth frequency format. The data, which were taken at two different ratios of the coupling coefficient C , seem to confirm the detrimental effect of roll-due-to-pitch on the HQRs.

Figures 8.24 and 8.25 show the modified frequency data points in the bandwidth and neutral stability format. Data correlation is excellent at the bandwidth frequency. At the neutral stability frequency, correlation is not as good, though still acceptable. The better correlation of the data at the bandwidth frequency may be due to the fact that the pilots had only a very limited time to familiarize themselves with the configuration. This may have led the pilots to reduce their input frequencies (as seems to follow from fig. 7.25).

Figures 8.26 and 8.27 show the pilot HQRs for the configurations with reduced on-axis bandwidth. For these configurations, the Level boundaries seem to be slightly too high. This suggests that the effects of increased coupling and reduced on-axis bandwidth are cumulative. Again, correlation is somewhat better at the bandwidth frequency. It should be pointed out that the reduced on-axis data were obtained only from the fixed-base

simulator where acceleration cues were lacking. This may have caused the pilots to be somewhat less receptive to the high-frequency effects.

8.4 Definition of a New Pitch-Roll Coupling Criterion

One of the objectives of this study was to review the existing ADS-33C pitch-roll coupling criteria and if necessary suggest improvements. In this report, the collected pitch-roll coupling data were synthesized in a 4 second time domain and two frequency domain formats. Results showed the frequency domain formats to be superior to the 4 second ADS-33C time domain format which was clearly deemed inadequate. Other time domain formats which were evaluated (e.g., p_{max}/q_{max} and $(p/q)_{max}$) were not able to represent the washed-out coupling cases with the consistency of the frequency domain format. The frequency domain formats both showed excellent consistency, with only minor differences due to pilot control strategy. Therefore, a frequency domain formulation for a pitch-roll coupling criterion seems most appropriate. Before formulating a handling qualities criterion, however, we must first establish whether and how this criterion can be verified from flight test data.

The flight test data for compliance of a frequency domain coupling criterion can be obtained from frequency sweeps, which are usually available from the bandwidth assessment. Therefore, the verification of the coupling criterion does not require additional flight testing. In general, the computation of the frequency response (Bode plot) will require the use of conditioning techniques. Conditioning allows the effects of secondary inputs (e.g., the longitudinal input in the case of a q/p frequency response) to be subtracted from the data. In doing so, it is important to verify that there exists no significant correlation between the pilot's control inputs, at least not over the frequency area of interest—as such, conditioning is no substitute for proper flight testing. Frequency response conditioning comes with most advanced flight data analysis programs such as DIVA (ref. 22) or CIPHER (ref. 23).

The frequency responses p/q and q/p can be determined either directly from the conditioned frequency responses of p/q and q/p , or they can be computed indirectly from the frequency responses of p/δ_x and q/δ_x (to obtain p/q) and of q/δ_y and p/δ_y (to obtain q/p). Although the former method requires only one computation, the latter is probably preferable for the insight it gives us into the contributions from the on-axis and off-axis response. The resulting frequency responses of p/q and q/p are almost identical, both in theory and in practice.

Figure 8.28 shows the amplitudes of the frequency response of p/δ_y , q/δ_y , and q/p for two data sets obtained during two separate flight tests with the conventionally controlled BO 105 S-123 (ref. 24). Each data set consisted of three consecutive lateral stick frequency sweeps of about 40 seconds each. To obtain the frequency responses, the data were conditioned with the longitudinal input, and windowing was used to minimize the error around the frequency range of interest. The coherence of the q/p frequency responses was higher than 0.75 over the frequency range shown. Differences between q/p , computed directly, and the frequency responses, computed from q/δ_y and p/δ_y , were only minimal. As can be seen in the figure, the frequency responses from the two different flight tests differ by not more than 2.5 dB. The frequency response of q/p decreases from about -10 dB (or 30 percent) at very low frequencies to about -26 dB (or 5 percent) at 12 rad/sec. Beyond 12 rad/sec, pitch-due-to-roll coupling increases again on account of air resonance. The value of 30 percent pitch-due-to-roll coupling at low frequencies compares well with the evaluation of the ADS-33C criterion (fig. 2.3 or ref. 21). The pitch-due-to-roll coupling coefficients at the pitch bandwidth and neutral stability frequencies can now easily be determined from the frequency response of q/p . Pitch-due-to-roll coupling at the pitch bandwidth frequency of 2.67 rad/sec (determined from the frequency response of q/δ_x ; see ref. 21) is -13.0 dB for flight one and -14.0 dB for flight two. Pitch-due-to-roll coupling at the pitch neutral stability frequency of 5.64 rad/sec is -17.7 dB for flight one and -16.3 dB for flight two.

Figure 8.29 shows the amplitudes of the frequency response of q/δ_x , p/δ_x , and p/q of the conventionally controlled BO 105 S-123 for two different data sets, each of which contained three longitudinal frequency sweeps. Coherence of the off-axis frequency response exceeded 0.6 over the frequency range of interest. Although the trends from the two flight tests are very similar, the values at certain frequencies show differences on the order of 5 dB or more. The frequency response of p/q shows a decrease from about 0 dB (100 percent coupled) at low frequencies to about -15 dB at 5 rad/sec. Beyond 5 rad/sec, there is an increase in pitch-due-to-roll coupling. This is the result of a decrease in q/δ_x on the one hand and an increase in p/δ_x (on account of rotor/body interactions) on the other hand. Roll-due-to-pitch coupling at low frequencies compares with values obtained from parameter estimation. It is, however, significantly lower than the coupling estimate with the ADS-33C criterion (fig. 2.4 or ref. 21). Roll-due-to-pitch coupling at the roll bandwidth frequency (5.83 rad/sec) is -10.9 dB for flight one and -13.2 dB for flight two. Roll-due-to-pitch coupling at the roll neutral stability

frequency (12.08 rad/sec) is 2.9 dB for flight one and 0.9 dB for flight two.

Figure 8.30 shows the bode plot of q/p and p/q of an attack helicopter at 60 knots forward flight with SCAS on. The conditioned frequency response was computed with CIPHER from frequency sweep data. In contrast with the BO 105, there seems to be little variation of the coupling ratio with frequency. The frequency response q/p shows a relatively noisy, but more or less constant, coupling ratio between the pitch bandwidth frequency (2.16 rad/sec) and the neutral stability frequency (3.11 rad/sec). At these frequencies, q/p was determined at -20.1 dB (at $\omega_{BW\theta}$) and -22.9 dB (at $\omega_{180\theta}$). The coupling ratio of p/q between the roll bandwidth frequency (2.49 rad/sec) and the neutral stability frequency (4.55 rad/sec) shows a small reduction from -7.8 dB to -12.2 dB. As can be seen, coherence of the off-axis frequency responses is quite poor, something which was primarily attributed to the phase plot. The low coherence seems inherent to aircraft with low coupling and is, as such, unavoidable. Analysis of data from the uncoupled ATTHes model, showed that, although the data look noisy and the coherence is low, the trends obtained from the frequency response are repeatable and match predictions.

When relatively noisy data are used to verify coupling at two discrete frequencies (the bandwidth and neutral stability frequency), distortions of the actual coupling behavior are unavoidable. Such problems could lead to incorrect decisions regarding the handling qualities of future helicopters and could jeopardize the acceptance of any proposed criteria. Therefore, a criterion is needed that deals effectively with noisy data, is easy to fly and evaluate, and is a good representation of pitch-roll handling qualities. Using the average coupling ratio between the bandwidth and neutral stability frequency satisfies these requirements. An average coupling ratio can be calculated from the linear average of the coupling ratio at the available discrete frequency points between the bandwidth and neutral stability frequency. The averaging process neutralizes the detrimental effect of noisy data and simplifies the criterion (one coupling parameter instead of two). Figure 8.31 shows how the HQRs for the control, rate, and combined control rate coupling cases of figures 8.20 and 8.21 change with the averaged coupling parameter. As can be seen, changes are only minor and correlation of the data is excellent. Figure 8.32 shows the HQRs for the washed-out coupling cases of figures 8.22 and 8.23. As could be expected, the average coupling parameter provides a (very acceptable) compromise between the bandwidth and neutral stability formats. It seems, therefore, well suited as a criterion format.

Figure 8.33 shows the suggested pitch-due-to-roll coupling criterion using the averaged coupling ratio. Also shown in the figure are the data points for the conventionally controlled BO 105 and an attack helicopter (see table 8.1). As could be expected, the BO 105 with its stiff rotor system has Level 2 pitch-due-to-roll coupling handling qualities, whereas the attack helicopter has borderline Level 1–2 pitch-due-to-roll handling qualities. It should be pointed out that the BO 105’s exceptionally high values of roll-due-to-pitch coupling are partly due to its unusually high bandwidth and neutral stability frequencies.

9. Conclusions

A comprehensive study into the effects of pitch-roll coupling on helicopter handling qualities was performed as a collaborative effort between U.S. Army Aeroflight-dynamics Directorate (USAATCOM) and the DLR Institute of Flight Mechanics. Complementary use was made of a U.S. ground-based flight simulator and the German ATHeS in-flight simulator. As many as 162 validated pilot ratings and comments were obtained for 90 different pitch-roll coupling configurations, ranging from conventional coupling types, such as control and rate coupling, to coupling types typical of helicopters with advanced feedback control systems. All coupling types were implemented as a modification of the uncoupled Level 1 rate command system used for a previous bandwidth-phase delay study. The handling qualities of the coupled system ranged from Levels 1 to 3. The coupling parameters were chosen so that a large range of dynamics was covered. The piloting task used for this study was a high-frequency slalom-tracking task, used previously for a study of bandwidth and phase delay.

From this report, several conclusions can be drawn:

1. The current ADS-33C pitch-roll coupling criterion is deficient in the prediction of handling qualities for a slalom-tracking task. For the conventional coupling types, control and rate coupling, the Level 1–2 boundaries of the ADS-33C criterion are too lenient (at least for a high-gain task). For coupling types with a washed-out characteristic or with short-term significantly different from the long-term coupling, the ADS-33C criterion is inadequate.
2. Evaluation of the cross-coupling handling qualities in the frequency domain provides much more consistent results than evaluations in the time domain. Especially at high frequencies, where the short-term coupling effects are dominating, the consistency is excellent. This is consistent with the observation that the pilot uses high-frequency inputs (up to the neutral stability frequency) to eliminate cross coupling.
3. Because most of the pilot’s compensatory activities take place between the bandwidth and neutral stability frequency of the compensatory axis, coupling was investigated at these two frequencies. At both frequencies, excellent consistency was obtained, with the only differences stemming from the differences in pilot control strategy. Evaluation of flight test data at these two discrete frequency points, however, may be susceptible to the noisiness of the computed frequency responses. Therefore, a pitch-due-to-roll coupling criterion that uses the average of the coupling ratio between the bandwidth and neutral stability frequency of the compensatory axis is suggested.
4. An evaluation of the pilot control strategy showed that the pilots tend to use a feedback type control strategy to eliminate coupling. Given time and a good understanding of the system, the pilot can be trained to use a more efficient control strategy which uses feedforward elements (characterized by diagonalized inputs). For the slalom-tracking task it was shown, however, that this control strategy is difficult to learn and is not certain to work if the task changes or is complicated by demands in secondary axes. Also, such a feedforward strategy is effective only with certain types of coupling.
5. The slalom-tracking task used for this study is a pure roll-axis task, hence pitch-due-to-roll coupling is the primary coupling response. Roll-due-to-pitch coupling occurs only when the pilot uses longitudinal inputs to alleviate the primary coupling. Therefore, the amount of roll-due-to-pitch coupling will indirectly affect the HQRs. It was shown that with increasing roll-due-to-pitch coupling, handling qualities degrade. This effect is strongest at higher amounts of coupling.
6. When the handling qualities of the decoupled (on-axis) system deteriorate, there will be a deterioration in the handling qualities of the coupled system. Although limited substantiating data are available, it was shown that a reduction of the decoupled handling qualities by one rating point, more or less, reduces the handling qualities of the coupled system with about one rating point, as compared to the baseline model.
7. Fixed-base and in-flight simulation can be used in a complementary and time-efficient manner. The fixed-base simulator can be used to screen out new configurations and provide additional data points. The fixed-base simulator results were compatible with the in-flight simulator results, except for those configurations where the high-frequency dynamics dominated the response.

Appendix A: The 1992 Flight Test Data Base

The 1992 flight test campaign took place at the German Forces Flight Test Center in Manching (Germany) from June 15 to July 2, 1992. During these 3 weeks of testing, a total of 28 configurations were evaluated for which 46 validated HQRs and comments were obtained. Four experienced test pilots participated in the tests: two pilots from WTD-61 in Manching, one pilot from NASA Ames (USA), and one pilot from DRA Bedford (GB).

In the following table, the 1992 flight test configurations are listed. The first column lists the configuration number. The dimensions of the variables are given by:

$$L\delta_x \text{ and } M\delta_y - \text{rad}\cdot\text{sec}^{-2} \cdot \text{percent}^{-1}$$

$$Lq, M_p, L_{q,c}, \text{ and } M_{p,c} - \text{sec}^{-1}$$

$$|\theta_{pk}/\phi_{t=4s}|, |\phi_{pk}/\theta_{t=4s}|, \text{ and } C - \text{dimensionless}$$

The on-axis characteristics of the model were unchanged for all configurations. The on-axis parameters for the 1992 flight tests are given by:

$$L\delta_y = 0.143 \text{ rad}\cdot\text{sec}^{-2} \cdot \text{percent}^{-1}$$

$$M\delta_x = 0.052 \text{ rad}\cdot\text{sec}^{-2} \cdot \text{percent}^{-1}$$

$$L_p = -8.0 \text{ sec}^{-1}$$

$$M_q = -4.0 \text{ sec}^{-1}$$

In the remarks column, the configurations which were repeated in other tests are listed. Configurations starting with “ASC” are flight test configurations, configurations starting with “VSC” are ground-based simulator configurations. The numbers following these configurations are the configurations numbers shown in the first column and listed in the tables throughout this report. In the table, the following footnote symbols are used:

¹ The pilot seems to have slightly underrated this configuration.

* No ground tracking data available.

No.	Type of coupling	L_{θ_i}	M_{θ_i}	L_{η}	M_p	$L_{p,c}$	$M_{q,c}$	$\left \frac{\theta}{\phi} \right _{ADS}$	$\left \frac{\phi}{\theta} \right _{ADS}$	C	Pilot HQR's				Notes
											A	B	C	D	
10	Baseline	.0000	.0000	0.0	0.0	-8.0	-4.0	.000	.000	-			2	2½	Cfr. ASC_A0, VSC_0
32	Control	.0065	-.0036	0.0	0.0	-8.0	-4.0	.048	.065	.80			3	3	Cfr. VSC_1
13	Control	.0130	-.0072	0.0	0.0	-8.0	-4.0	.097	.129	.80			4	5	Cfr. ASC_A1, VSC_2
14	Control	.0260	-.0143	0.0	0.0	-8.0	-4.0	.194	.258	.80			4		Cfr. VSC_3
15	Control	.0520	-.0286	0.0	0.0	-8.0	-4.0	.387	.517	.80		4¹	5		Cfr. ASC_A2, VSC_4
12	Control	.0780	-.0429	0.0	0.0	-8.0	-4.0	.581	.775	.80				8	Cfr. ASC_A3, VSC_5
36	Rate	.0000	.0000	1.5	-.25	-8.0	-4.0	.058	.181	.33			3	3.	Cfr. VSC_6
17	Rate	.0000	.0000	3.0	-.50	-8.0	-4.0	.117	.362	.33			5	5	Cfr. ASC_B0, VSC_7
18	Rate	.0000	.0000	4.5	-.75	-8.0	-4.0	.175	.544	.33			5	6	Cfr. VSC_7
19	Rate	.0000	.0000	6.0	-1.0	-8.0	-4.0	.234	.725	.33			5	4	Cfr. VSC_9
16	Rate	.0000	.0000	9.0	-1.5	-8.0	-4.0	.351	1.087	.33				5	Cfr. VSC_10
44	Combined	.0065	-.0036	1.5	-.25	-8.0	-4.0	.107	.246	.45		3	3		
11	Combined	.0130	-.0072	3.0	-.50	-8.0	-4.0	.214	.492	.45	4			4/4	
20	Combined	.0130	-.0072	4.5	-.75	-8.0	-4.0	.272	.673	.42			5	6	
21	Combined	.0260	-.0143	3.0	-.50	-8.0	-4.0	.310	.621	.52		6		7	
24	Combined	.0260	-.0143	4.5	-.75	-8.0	-4.0	.369	.802	.48			6	7	

No.	Type of coupling	L_{θ_1}	M_{θ_1}	L_q	M_p	$L_{p,c}$	$M_{q,c}$	$\left \frac{\theta}{\phi} \right _{ADS}$	$\left \frac{\phi}{\theta} \right _{ADS}$	C	Pilot HQR's				Notes
											A	B	C	D	
25	Combined	.0260	-.0143	6.0	-1.0	-8.0	-4.0	.427	.983	.45			6	7	
26	Combined	.0520	-.0286	4.5	-.75	-8.0	-4.0	.562	1.060	.55			9	8	
27	Combined	.0520	-.0286	6.0	-1.0	-8.0	-4.0	.621	1.242	.52		10	8'		
28	Combined	.0650	-.0358	6.0	-1.0	-8.0	-4.0	.718	1.371	.55			7'		
45	Washed-out	.0260	-.0143	-2.0	.80	-12.0	-6.0	.004	.011	.44			4	4	
42	Washed-out	.0260	-.0143	-2.0	.80	-8.0	-4.0	.006	.017	.40			4	3	Cfr. ASC_C1
46	Washed-out	.0520	-.0286	-4.0	1.6	-12.0	-6.0	.009	.022	.44			4		Cfr. VSC_38
40	Washed-out	.0650	-.0358	-5.0	2.0	-12.0	-6.0	.011	.028	.44				3	
43	Washed-out	.0520	-.0286	-4.0	1.6	-8.0	-4.0	.013	.033	.40			6	4	Cfr. VSC_40/52
29	Washed-out	.0650	-.0358	-5.0	2.0	-8.0	-4.0	.016	.042	.40					
23	Washed-out	.0520	-.0286	-4.0	1.6	-4.0	-2.0	.026	.067	.34			5		
48	Washed-out	.0650	-.0358	-5.0	2.0	-4.0	-2.0	.032	.083	.34			5		

Appendix B: The Ground-Based Simulator Test Data Base

The 1993 ground-based simulator campaign took place at NASA Ames (Moffett Field, California) on a fixed base simulator. During a 2 week period in February–March, 1993, a total of 64 coupling configurations were evaluated. Two experienced test pilots participated in the tests: one pilot from NASA Ames (USA) and one pilot from the U.S. Army.

In the following table, the 1993 ground-based simulator configurations are listed, including the on-axis parameters. The first column lists the configuration number. The dimensions of the variables are given by:

$L_{\delta_x}, M_{\delta_y}, L_{\delta_y},$ and $M_{\delta_x} - \text{rad} \cdot \text{sec}^{-2} \cdot \text{percent}^{-1}$

$L_q, M_p, L_{q,c}, M_{p,c}, L_p,$ and $M_q - \text{sec}^{-1}$

$|\theta_{pk}/\phi_{t=4s}|, |\phi_{pk}/\theta_{t=4s}|,$ and $C - \text{dimensionless}$

In the remarks column, the configurations which were repeated in other tests are listed. Configurations starting with “ASC” are flight test configurations, configurations starting with “VSC” are ground-based simulator configurations. The numbers following these configurations are the configurations numbers shown in the first column and listed in the tables throughout this report.

No.	Type of coupling	Off-axis						On-axis				$\left \frac{\theta}{\phi} \right _{ADS}$	$\left \frac{\phi}{\theta} \right _{ADS}$	C	Pilot HQR's		Notes
		L_{θ}	M_{θ}	L_{η}	M_{η}	$L_{p,c}$	$M_{p,c}$	L_{θ}	M_{θ}	L_p	M_q				C	E	
0	Baseline	.0000	.0000	0.0	0.0	-8.0	-4.0	.143	.052	-8.0	-4.0	.000	.000	-		2	Cfr. ASC_A0, ASC_10
1	Control	.0065	-.0036	0.0	0.0	-8.0	-4.0	.143	.052	-8.0	-4.0	.049	.065	0.81	3		Cfr. ASC_32
2	Control	.0130	-.0072	0.0	0.0	-8.0	-4.0	.143	.052	-8.0	-4.0	.097	.129	0.81	3	2½	Cfr. ASC_A1, ASC_13
3	Control	.0260	-.0143	0.0	0.0	-8.0	-4.0	.143	.052	-8.0	-4.0	.194	.258	0.80	4	3	Cfr. ASC_14
4	Control	.0520	-.0286	0.0	0.0	-8.0	-4.0	.143	.052	-8.0	-4.0	.387	.517	0.80	4½	5	Cfr. ASC_A2, ASC_15
5	Control	.0780	-.0429	0.0	0.0	-8.0	-4.0	.143	.052	-8.0	-4.0	.581	.775	0.80	7½	5	Cfr. ASC_A3, ASC_12
5a	Control	.0978	-.0536	0.0	0.0	-8.0	-4.0	.143	.052	-8.0	-4.0	.725	.972	0.80		6	
6	Rate	.0000	.0000	1.5	-.25	-8.0	-4.0	.143	.052	-8.0	-4.0	.058	.181	0.33	3		Cfr. ASC_36
7	Rate	.0000	.0000	3.0	-.50	-8.0	-4.0	.143	.052	-8.0	-4.0	.117	.362	0.33	3	4	Cfr. ASC_B0, ASC_17
8	Rate	.0000	.0000	4.5	-.75	-8.0	-4.0	.143	.052	-8.0	-4.0	.175	.544	0.33		4½	Cfr. ASC_18
9	Rate	.0000	.0000	6.0	-1.0	-8.0	-4.0	.143	.052	-8.0	-4.0	.234	.725	0.33	5		Cfr. ASC_19
10	Rate	.0000	.0000	9.0	-1.5	-8.0	-4.0	.143	.052	-8.0	-4.0	.351	1.088	0.33	4½	5	Cfr. ASC_16
11	Rate	.0000	.0000	12.0	-2.0	-8.0	-4.0	.143	.052	-8.0	-4.0	.468	1.450	0.33	7	7½	Cfr. ASC_B2
13	P-R Ratio	.0000	.0000	1.82	-.50	-8.0	-4.0	.143	.052	-8.0	-4.0	.117	.220	0.55	4		
14	P-R Ratio	.0000	.0000	3.64	-1.0	-8.0	-4.0	.143	.052	-8.0	-4.0	.234	.440	0.55	4½		
15	P-R Ratio	.0000	.0000	7.27	-2.0	-8.0	-4.0	.143	.052	-8.0	-4.0	.468	.878	0.55	4½		

No.	Type of coupling	Off-axis						On-axis				$\left \frac{\theta}{\phi} \right _{ADS}$	$\left \frac{\phi}{\theta} \right _{ADS}$	C	Pilot HQR's		Notes
		L_{θ}	M_{θ}	L_{ϕ}	M_{ϕ}	$L_{p,c}$	$M_{q,c}$	L_{θ}	M_{θ}	L_{ϕ}	M_{ϕ}				C	E	
15a	P-R Ratio	.0000	.0000	9.09	-2.5	-8.0	-4.0	.143	.052	-8.0	-4.0	.585	1.098	0.55	7		
16	P-R Ratio	.0000	.0000	1.0	-.50	-8.0	-4.0	.143	.052	-8.0	-4.0	.117	.121	1.00	3		Cfr. ASC_B4
17	P-R Ratio	.0000	.0000	2.0	-1.0	-8.0	-4.0	.143	.052	-8.0	-4.0	.234	.242	1.00	4		
18	P-R Ratio	.0000	.0000	4.0	-2.0	-8.0	-4.0	.143	.052	-8.0	-4.0	.468	.483	1.00	5		Cfr. ASC_B6
18a	P-R Ratio	.0000	.0000	6.0	-3.0	-8.0	-4.0	.143	.052	-8.0	-4.0	.702	.725	1.00	7½		
18b	P-R Ratio	.0000	.0000	5.0	-2.5	-8.0	-4.0	.143	.052	-8.0	-4.0	.585	.604	1.00	7½		Cfr. ASC_E8
19	P-R Ratio	.0000	.0000	0.0	-.50	-8.0	-4.0	.143	.052	-8.0	-4.0	.117	.000	∞	3		Cfr. ASC_B7
20	P-R Ratio	.0000	.0000	0.0	-1.0	-8.0	-4.0	.143	.052	-8.0	-4.0	.234	.000	∞	4		
21	P-R Ratio	.0000	.0000	0.0	-2.0	-8.0	-4.0	.143	.052	-8.0	-4.0	.468	.000	∞	4		Cfr. ASC_B9
21a	P-R Ratio	.0000	.0000	0.0	-2.5	-8.0	-4.0	.143	.052	-8.0	-4.0	.585	.000	∞	6		
21b	P-R Ratio	.0000	.0000	0.0	-3.0	-8.0	-4.0	.143	.052	-8.0	-4.0	.702	.000	∞	8		
22-un	Red. on-axis	.0000	.0000	0.0	0.0	-5.0	-2.5	.107	.036	-5.0	-2.5	.000	.000	-	3		
22	Red. on-axis	.0000	.0000	1.5	-2.5	-5.0	-2.5	.107	.036	-5.0	-2.5	.089	.283	0.33	4		
22a	Red. on-axis	.0000	.0000	.94	-.16	-5.0	-2.5	.107	.036	-5.0	-2.5	.057	.178	0.34	3		
24	Red. on-axis	.0000	.0000	6.0	-1.0	-5.0	-2.5	.107	.036	-5.0	-2.5	.358	1.133	0.33	6		
25	Red. on-axis	.0000	.0000	9.0	-1.5	-5.0	-2.5	.107	.036	-5.0	-2.5	.537	1.700	0.33	8		

No.	Type of coupling	Off-axis						On-axis				$\left \frac{\theta}{\phi} \right _{ADS}$	$\left \frac{\phi}{\theta} \right _{ADS}$	C	Pilot HQR's		Notes
		L_{θ_i}	M_{θ_i}	L_q	M_p	$L_{p\epsilon}$	$M_{q\epsilon}$	L_{θ_o}	M_{θ_o}	L_p	M_q				C	E	
25a	Red. on-axis	.0000	.0000	3.75	-.63	-5.0	-2.5	.107	.036	-5.0	-2.5	.225	.708	0.34	4½		
27a	Red. on-axis	.0000	.0000	7.5	-1.3	-5.0	-2.5	.107	.036	-5.0	-2.5	.465	1.417	0.35	7		
28a	Red. on-axis	.0049	-.0027	0.0	0.0	-5.0	-2.5	.107	.036	-5.0	-2.5	.048	.072	0.74	4		
30a	Red. on-axis	.0196	-.0108	0.0	0.0	-5.0	-2.5	.107	.036	-5.0	-2.5	.191	.287	0.74	4½		
31a	Red. on-axis	.0392	-.0215	0.0	0.0	-5.0	-2.5	.107	.036	-5.0	-2.5	.381	.575	0.74	5		
32a	Red. on-axis	.0588	-.0323	0.0	0.0	-5.0	-2.5	.107	.036	-5.0	-2.5	.572	.862	0.74	6		
32b	Red. on-axis	.0686	-.0376	0.0	0.0	-5.0	-2.5	.107	.036	-5.0	-2.5	.666	1.006	0.74	8		
33-un	Var. freq.	.0000	-.0000	0.0	0.0	-6.0	-4.0	.115	.052	-6.0	-4.0	.000	.000	-	3		
33	Var. freq.	.0065	-.0036	0.0	0.0	-6.0	-4.0	.115	.052	-6.0	-4.0	.046	.085	0.56	3		
35	Var. freq.	.0260	-.0143	0.0	0.0	-6.0	-4.0	.115	.052	-6.0	-4.0	.182	.341	0.56	4		
36	Var. freq.	.0520	-.0286	0.0	0.0	-6.0	-4.0	.115	.052	-6.0	-4.0	.365	.681	0.56	5		
37a	Var. freq.	.0908	-.0498	0.0	0.0	-6.0	-4.0	.115	.052	-6.0	-4.0	.635	1.190	0.56	5/7		
37b	Var. freq.	.1048	-.0575	0.0	0.0	-6.0	-4.0	.115	.052	-6.0	-4.0	.734	1.373	0.56	7		
38	Washed-out	.0520	-.0286	-4.0	1.6	-12.0	-6.0	.143	.052	-8.0	-4.0	.009	.022	0.44	4		Cfr. ASC_46
40/52	Washed-out	.0520	-.0286	-4.0	1.6	-8.0	-4.0	.143	.052	-8.0	-4.0	.013	.033	0.40	3	3	Cfr. ASC_43
44	Washed-out	.1236	-.0675	-9.5	3.8	-12.0	-6.0	.143	.052	-8.0	-4.0	.019	.053	0.43	4	2	

No.	Type of coupling	Off-axis						On-axis				$\left \frac{\theta}{\phi} \right _{ADS}$	$\left \frac{\phi}{\theta} \right _{ADS}$	C	Pilot HQR's		Notes
		L_{θ_s}	M_{θ_s}	L_q	M_p	$L_{p,c}$	$M_{n,c}$	L_{θ_s}	M_{θ_s}	L_p	M_q				C	E	
45	Washed-out	.1854	-.1017	-14.3	5.7	-12.0	-6.0	.143	.052	-8.0	-4.0	.030	.078	0.44		5½	
46	Washed-out	.2471	-.1356	-19.0	7.6	-12.0	-6.0	.143	.052	-8.0	-4.0	.040	.106	0.44	5	5½	
48	Washed-out	.3707	-.2034	-28.5	11.4	-12.0	-6.0	.143	.052	-8.0	-4.0	.060	.160	0.44	8	6+	
54	Washed-out	.1043	-.0572	-8.0	3.2	-8.0	-4.0	.143	.052	-8.0	-4.0	.026	.070	0.40	3+	¾	Clr. ASC_C3
56	Washed-out	.2085	-.1144	-16.0	6.4	-8.0	-4.0	.143	.052	-8.0	-4.0	.052	.138	0.40	6	6	
58	Washed-out	.3128	-.1716	-24.1	9.6	-8.0	-4.0	.143	.052	-8.0	-4.0	.077	.198	0.40	7	7	
63	Washed-out	.0621	-.0340	-4.8	1.9	-4.0	-2.0	.143	.052	-8.0	-4.0	.032	.077	0.34	3	2½	
66	Washed-out	.1655	-.0908	-12.7	5.1	-4.0	-2.0	.143	.052	-8.0	-4.0	.076	.219	0.34		5	
72	Washed-out	.0351	-.0192	-2.7	1.1	-2.0	-1.0	.143	.052	-8.0	-4.0	.022	.090	0.28		2	
74	Washed-out	.0702	-.0385	-5.4	2.1	-2.0	-1.0	.143	.052	-8.0	-4.0	.108	.180	0.31		4	
76	Washed-out	.1403	-.0770	-10.8	4.3	-2.0	-1.0	.143	.052	-8.0	-4.0	.141	.356	0.30		5½	
83	Washed-out	.0470	-.0258	-3.6	1.4	-1.0	-0.5	.143	.052	-8.0	-4.0	.128	.247	0.28		2	
84	Washed-out	.0627	-.0344	-4.8	1.9	-1.0	-0.5	.143	.052	-8.0	-4.0	.134	.331	0.27	4	3	
85	Washed-out	.0941	-.0516	-7.2	2.9	-1.0	-0.5	.143	.052	-8.0	-4.0	.145	.499	0.26		4	
86	Washed-out	.1254	-.0688	-9.6	3.8	-1.0	-0.5	.143	.052	-8.0	-4.0	.267	.662	0.27	4½	5	
88	Washed-out	.1881	-.1032	-14.5	5.8	-1.0	-0.5	.143	.052	-8.0	-4.0	.289	.918	0.26	7½	7½	

Appendix C: The 1993 Flight Test Data Base

The 1993 flight test campaign took place in June–July, 1993, at the German Forces Flight Test Center in Manching (Germany). Five experienced test pilots participated in the tests: one pilot from NASA Ames (USA), one pilot from DRA Bedford (GB), one pilot from the U.S. Army, and two pilots from WTD-61 in Manching. A total of 40 different coupling configurations were evaluated.

In the following table, the 1993 flight test configurations are listed. The first column lists the configuration number. The dimensions of the variables are given by:

$$L\delta_x \text{ and } M\delta_y - \text{rad}\cdot\text{sec}^{-2} \cdot \text{percent}^{-1}$$

$$L_q, M_p, L_{q,c}, \text{ and } M_{p,c} - \text{sec}^{-1}$$

$$|\theta_{pk}/\phi_{t=4s}|, |\phi_{pk}/\theta_{t=4s}|, \text{ and } C - \text{dimensionless}$$

The on-axis characteristics of the model were unchanged for all configurations (and identical to the 1992 configurations). The on-axis parameters for the 1992 flight tests are given by:

$$L\delta_y = 0.143 \text{ rad}\cdot\text{sec}^{-2} \cdot \text{percent}^{-1}$$

$$M\delta_x = 0.052 \text{ rad}\cdot\text{sec}^{-2} \cdot \text{percent}^{-1}$$

$$L_p = -8.0 \text{ sec}^{-1}$$

$$M_q = -4.0 \text{ sec}^{-1}$$

In the remarks column, the configurations which were repeated in other tests are listed. Configurations starting with “ASC” are flight test configurations, configurations starting with “VSC” are ground-based simulator configurations. The numbers following these configurations are the configurations numbers shown in the first column and listed in the tables throughout this report. In the table, the following footnote symbols are used:

- 1 Rating may be influenced by pilot fatigue.
- 2 Flown with tailwind; incorrect trim position may have influenced rating.
- 3 Only one practice run and one evaluation run; rating may change after learning phase.
- 4 Configuration may have been underrated.
- 5 Pilot indicated uncertainty over rating, “might also be a 5.”
- * Only ground tracking, but no on-board data available.
- ** Neither on-board nor ground tracking data available.

No.	Type of coupling	L_{θ_1}	M_{θ_1}	L_q	M_p	$L_{p,c}$	$M_{p,c}$	$\left \frac{\theta}{\phi} \right _{ADS}$	$\left \frac{\phi}{\theta} \right _{ADS}$	C	Pilot HQR's					Notes
											C	D	F	G	H	
A0	Baseline	.0000	.0000	.00	0.0	-8.0	-4.0	.000	.000	-	3	4	3.	3	3	Cfr. ASC_10, VSC_0
E0	(Control) ⁻¹	-.0036	-.0036	.00	0.0	-8.0	-4.0	.048	.036	1.45	3.		4.			
A7	Control	.0000	-.0072	.00	0.0	-8.0	-4.0	.097	.000	∞		4			(3)	
A4	Control	.0072	-.0072	.00	0.0	-8.0	-4.0	.097	.071	1.45	4				(3)	
A1	Control	.0130	-.0072	.00	0.0	-8.0	-4.0	.097	.129	0.80	3					Cfr. ASC_13, VSC_2
A8	Control	.0000	-.0286	.00	0.0	-8.0	-4.0	.387	.000	∞				(3)		
A2	Control	.0520	-.0286	.00	0.0	-8.0	-4.0	.387	.517	0.80					(4)	Cfr. ASC_15, VSC_4
A9	Control	.0000	-.0429	.00	0.0	-8.0	-4.0	.581	.000	∞	7 ¹	6 ¹				
A6	Control	.0429	-.0429	.00	0.0	-8.0	-4.0	.581	.426	1.45	5				(4)	
A3	Control	.0780	-.0429	.00	0.0	-8.0	-4.0	.581	.775	0.80	5	5				Cfr. ASC_12, VSC_5
E5	(Control) ⁻¹	-.0780	.0429	.00	0.0	-8.0	-4.0	.581	.775	0.80	9 ³					
E6	Rate	.0000	.0000	.50	-.25	-8.0	-4.0	.058	.060	1.00	(4.)		2.			
B7	Rate	.0000	.0000	.00	-.50	-8.0	-4.0	.117	.000	∞	5 ²	4	4 ^{1/2}			Cfr. VSC_19
B4	Rate	.0000	.0000	1.0	-.50	-8.0	-4.0	.117	.121	1.00	4	4				Cfr. VSC_16
B0	Rate	.0000	.0000	3.0	-.50	-8.0	-4.0	.117	.362	0.33	4			(4)	(2)	Cfr. ASC_17, VSC_7
B9	Rate	.0000	.0000	.00	-2.0	-8.0	-4.0	.468	.000	∞	5	4 ⁴	4 ⁵			Cfr. VSC_21
B6	Rate	.0000	.0000	4.0	-2.0	-8.0	-4.0	.468	.483	1.00	6	5				Cfr. VSC_18

No.	Type of coupling	L_{a_1}	M_{e_1}	L_q	M_p	$L_{p,c}$	$M_{p,c}$	$\left \frac{\theta}{\phi} \right _{ADS}$	$\left \frac{\phi}{\theta} \right _{ADS}$	C	Pilot HQR's					Notes
											C	D	F	G	H	
B2	Rate	.0000	.0000	12.0	-2.0	-8.0	-4.0	.468	1.45	0.33		6+				Cfr. VSC_11
E8	Rate	.0000	.0000	5.0	-2.5	-8.0	-4.0	.585	.604	1.00			6..			Cfr. VSC_18b
B3	Rate	.0000	.0000	15.0	-2.5	-8.0	-4.0	.585	1.81	0.33		7½	7			
D0	Washed-out	.0072	-.0072	-.55	.40	-8.0	-4.0	.003	.005	0.73		4..				
C0	Washed-out	.0130	-.0072	-1.0	.40	-8.0	-4.0	.003	.008	0.40		(4)	3			
D6	Washed-out	.0143	-.0143	-1.1	.80	-12.0	-6.0	.004	.006	0.80		4				
D5	Washed-out	.0072	-.0072	-.55	.40	-4.0	-2.0	.006	.009	0.62		4½				
D1	Washed-out	.0143	-.0143	-1.1	.80	-8.0	-4.0	.006	.009	0.73		5	3			
C1	Washed-out	.0260	-.0143	-2.0	.80	-8.0	-4.0	.006	.017	0.40		4½	4			Cfr. ASC_42
D2	Washed-out	.0286	-.0286	-2.2	1.6	-8.0	-4.0	.013	.018	0.73		4	3			
C2	Washed-out	.0520	-.0286	-4.0	1.6	-8.0	-4.0	.013	.033	0.40		5				
D9	Washed-out	.0858	-.0858	-6.6	4.8	-12.0	-6.0	.026	.037	0.80		6				
D3	Washed-out	.0572	-.0572	-4.4	3.2	-8.0	-4.0	.026	.037	0.73			4-			
C3	Washed-out	.1040	-.0572	-8.0	3.2	-8.0	-4.0	.026	.067	0.40		6	4			Cfr. VSC_54
D4	Washed-out	.0858	-.0858	-6.6	4.8	-8.0	-4.0	.039	.055	0.73		7	5			
C4	Washed-out	.1560	-.0858	-12.0	4.8	-8.0	-4.0	.039	.100	0.40		7	6			
D8	Washed-out	.0572	-.0572	-4.4	3.2	-4.0	-2.0	.052	.073	0.62		5..				

No.	Type of coupling	L_{δ_1}	M_{δ_1}	L_q	M_p	L_{pc}	M_{pc}	$\left \frac{\theta}{\phi} \right _{ADS}$	$\left \frac{\phi}{\theta} \right _{ADS}$	C	Pilot HQR's					Notes
											C	D	F	G	H	
F7	Mod. Freq.	.0572	-.0572	-4.4	3.2	-2.0	-2.0	.052	.147	0.46	5 ³		5..			
F9	Mod. Freq.	.0572	-.0572	-4.4	3.2	-.50	-.50	0.177	.496	0.41	4½ ³					
F1	Mod. Freq.	.0000	.0000	.13	-.13	-1.0	-1.0	.093	.092	1.00			6..			
F0	Mod. Freq.	.0000	.0000	.25	-.25	-2.0	-2.0	.109	.108	1.00	4					
F3	Mod. Freq.	.0000	.0000	.50	-.50	-1.0	-1.0	.374	.370	1.00	5					
F2	Mod. Freq.	.0000	.0000	1.0	-1.0	-2.0	-2.0	.435	.433	1.00	6..					

Appendix D: Pilot Questionnaire

After each evaluation flight, the pilot completed the following three page questionnaire. The questionnaire

printed below was taken from the 1993 flight test campaign, but differs only slightly from the questionnaire used during the 1992 flight test campaign.

Pilot Questionnaire	
“Slalom Tracking with Coupling”	
Manching Juni/Juli 1993	
Pilot:	Test No. ASC ___/___/___/
<hr style="border-top: 1px dashed black;"/>	
A. Task Performance	
<ul style="list-style-type: none">• Have you performed the task <input type="radio"/> aggressive? <input type="radio"/> moderate? <input type="radio"/> relaxed? • Tracking preciseness in gates ? <input type="radio"/> high <input type="radio"/> medium <input type="radio"/> low • Maintaining of height and speed? • Describe the cues which you have used.	
B. Pilot Workload	
<ul style="list-style-type: none">• Mental or/and physical effort to perform task? • How much spare capacity? • Any other factors that affected piloting task (e.g., pilot conditions, training, environment, cockpit...)? • Describe reasons for pilot workload.	

C. Helicopter On-axis Characteristics

- Roll response?
 - preciseness

 - sensitivity

 - damping

- Pitch response?

- Harmony of pitch and roll response?

- Speed control?

- Height control?

- Turn coordination?

- Was controller feel and sensitivity useful to obtain response?

D. Helicopter Off-axis Characteristics

- Roll —> pitch coupling?

- short term

- mid / long term

- Pitch —> roll coupling?

- short term

- mid/long term

- Heave / speed coupling?

- Yaw coupling?

E. Overall Cooper-Harper Rating? Use rating card!

1 / 2 / 3 / 4 / 5 / 6 / 7 / 8 / 9 / 10

- Describe main reasons for rating.

References

1. Handling Qualities Requirements for Military Rotorcraft. Aeronautical Design Standard ADS-33C, Aug. 1989.
2. Cooper, G. E.; and Harper, R. P., Jr.: The Use of Pilot Rating in the Evaluation of Aircraft Handling Qualities. NASA TN D-5153, Apr. 1969.
3. Garren, J. F.: Effects of Gyroscopic Cross-Coupling Between Pitch and Roll on the Handling Qualities of VTOL Aircraft. NASA TN D-812, Apr. 1961.
4. Garren, J. F.: Effects of Coupling Between Pitch and Roll Control Inputs on the Handling Qualities of VTOL Aircraft. NASA TN D-1233, Mar. 1962.
5. Houston, R. J.: An Exploratory Investigation of Factors Affecting the Handling Qualities of a Rudimentary Hingeless Rotor Helicopter. NASA TN D-3418, 1966.
6. Houston, R. J.; and Ward, J. F.: Handling Qualities and Structural Characteristics of Hingeless-Rotor Helicopter. Conference on V/STOL and STOL Aircraft, Ames Research Center, Moffett Field, Calif., NASA SP-116, Apr. 1966.
7. Talbot, P. D.; Dugan, D. C.; Chen, R. T. N.; and Gerdes, R. M.: Effects of Rotor Parameter Variations on Handling Qualities of Unaugmented Helicopters in Simulated Terrain Flight. NASA TM-81190, Aug. 1980.
8. Corliss, L. D.; and Carico, G. D.: A Flight Investigation of Roll-Control Sensitivity, Damping, and Cross Coupling in a Low-Altitude Lateral Maneuvering Task. NASA TM-84376, USAAVRADCOM TR-83-A-16, Dec. 1983.
9. Watson, D. C.; and Aiken, E. W.: An Investigation of the Effects of Pitch-Roll Cross Coupling on Helicopter Handling Qualities for Terrain Flight. AIAA Conference on Guidance, Navigation, and Control, Monterey, Calif., Aug. 1987.
10. Watson, D. C.; and Hindson, W. S.: In-Flight Simulation Investigation of Rotorcraft Pitch-Roll Cross Coupling. NASA TM-101059, Dec. 1988.
11. Chen, R. T. N.; and Talbot, P. D.: An Exploratory Investigation of the Effects of Large Variations in Rotor System Dynamics Design Parameters on Helicopter Handling Characteristics in Nap-of-the-Earth Flight. Presented at the 33rd Annual National Forum on the American Helicopter Society, Washington, D.C., May 1977.
12. Watson, D. C.; and Hindson, W. S.: In-Flight Simulation Investigation of Rotorcraft Pitch-Roll Cross Coupling. Presented at the Royal Aeronautical Society International Conference on Helicopter Handling Qualities and Control, London, Nov. 1988.
13. Ockier, C. J.: Flight Evaluation of the New Handling Qualities Criteria Using the BO 105. American Helicopter Society 49th Annual Forum, St. Louis, Mo., May 1993.
14. Pausder, H.-J.; and Blanken, C. L.: Investigation of the Effects of Bandwidth and Time Delay on Helicopter Roll-Axis Handling Qualities. Eighteenth European Rotorcraft Forum, Avignon, France, Sept. 1992. (Also, Piloting Vertical Flight Aircraft: A Conference on Flying Qualities and Human Factors, San Francisco, Calif., Jan. 1993.)
15. Pausder, H.-J.; Bouwer, G.; von Grünhagen, W.; and Holland, R.: Helicopter In-Flight Simulator ATTheS—A Multipurpose Testbed and Its Utilization. AIAA Paper 92-4173, AIAA/AHS Flight Simulation Technologies Conference, Hilton Head Island, S.C., Aug. 1992.
16. Lewis, M. S.; Mansur, M. H.; and Chen, R. T. N.: A Piloted Simulation of Helicopter Air Combat to Investigate Effects of Variations in Selected Performance and Control Response Characteristics. NASA TM-89438, Apr. 1987.
17. White, F.; and Blake, B.: Improved Method of Predicting Helicopter Control Response and Gust Sensitivity. American Helicopter Society preprint number 79-25, May 1979.
18. Whalley, M. S.: Development and Evaluation of an Inverse Solution Technique for Studying Helicopter Maneuverability and Agility. NASA TM-102889, USAAVSCOM TR 90-A-008, July 1991.
19. Heffley, R. K.; Jewell, W. F.; Lehman, J. M.; and Van Winkle, R. A.: A Compilation and Analysis of Helicopter Handling Qualities Data. NASA CR-3144, Aug. 1979.
20. Mouritsen, S. K.: Helicopter Roll-Pitch Coupling Feedback Model and Comparisons with Handling Qualities Flight Test Data. Presented at the AIAA Atmospheric Flight Mechanics Conference, Scottsdale, Ariz., Aug. 1994.

21. Ockier, C. J.: Evaluation of the ADS-33C Handling Qualities Criteria in Forward Flight Using the BO 105. DLR Institute of Flight Mechanics, IB 111-93/19, Braunschweig, Mar. 1993.
22. Wulff, G.; and Zöllner, M.: DIVA/MIMO Flight Test Data Analysis for the X31-A Demonstrator. AIAA Paper 91-2852, presented at the AIAA Atmospheric Flight Mechanics Conference, New Orleans, La., Aug. 1991.
23. Tischler, M. B.; and Cauffmann, M. G.: Frequency Response Method for Rotorcraft System Identification: Flight Applications to BO 105 Coupled Rotor/Fuselage Dynamics. J. Am. Helicopter Soc., vol. 37, no. 3, July 1992.
24. Ockier, C. J.; and von Grünhagen, W.: BO 105 Flight Test Data Base for the Evaluation of ADS-33C Criteria. DLR IB 111-93/20, Braunschweig, Mar. 1993.

Table 1.1. ADS-33C maximum values for roll-due-to-pitch and pitch-due-to-roll coupling

Parameter	Level 1	Level 2
$\left \frac{\phi_{pk}}{\theta} \right _{\delta_x}$	± 0.25	± 0.60
$\left \frac{\theta_{pk}}{\phi} \right _{\delta_y}$	± 0.25	± 0.60

Table 7.1. Handling qualities ratings and principal pilot comments for control coupling configurations

$M\delta_y$	No. ¹	Pilot HQRs						Characteristic comments ²
		B	C	D	E	F	G	
0.0000	10		2	2.5				No coupling, good on-axis response
	0				2			
	A0		3	4		3	3	(Tiredness and unfamiliarity with system and task mentioned by most pilots)
-0.0036	32		3	3				Slight coupling
	1		3					
-0.0072	13		4	5				Mild coupling, roll response notchy, on-axis oscillation during tracking
	2		3					Very predictable, no response problems, altitude control reason for HQR
	A1		3					Slight increase in workload, mildly unpleasant coupling, minimal compensation
-0.0143	14		4					Low compensation required, short term coupling only
	3		4					Predictability a little low, height control a problem, couldn't figure out strategy for coupling
-0.0286	15	4 ³	5					Moderate coupling, jerky roll response, poor control harmony
	4		4.5		5			Tendency to get into roll oscillation (possibly PIOs)
	A2							
-0.0429	12			8				Very unpredictable roll rate response, large inputs required, tendency to overcontrol
	5		7.5		5			Lack of predictability, tremendous amount of pitch oscillations, NOT tolerable workload
	A3		5	5				Considerable pilot compensation required, moderate to large roll-to-pitch coupling, relatively easy to counter and anticipate, tried diagonal inputs
-0.0536								
	5a				6			

¹Top line: ATTHes tests 1992. Middle line: Ground-based simulator. Bottom line: ATTHes tests 1993. Expanded definition of these configurations is contained in Appendices A, B, and C.

²Ground-based simulator comments are those of pilot C only.

³Analysis of task performance and pilot comments suggests that appropriate Cooper–Harper level may be worse than indicated.

Table 7.2. Handling qualities ratings and characteristic pilot comments for control coupling configurations with different direction of coupling (1993 flight test results only)

$M\delta_y$	$L\delta_x$	No. ¹	Pilot HQRs		Characteristic comments
			C	F	
0.0000	0.0000	–	2	3	No coupling, good on-axis response (best ratings shown)
–0.0036	–0.0036	E0	3	4–	Only mild uncommanded aircraft responses noted, some mid-term compensation required to maintain desired performance, coupling “sneaks up on you” (approximately 3 seconds after stick inputs)
+0.0429	–0.0780	E5	9 ²		Workload not tolerable just to retain control, severe pitch-due-to-roll coupling backward from all other configurations, wouldn't wish this on my worst enemy

¹ Expanded definition of these configurations is contained in Appendix C.

² Only one practice and one evaluation run was made, pilot was still in the learning phase.

Table 7.3. Handling qualities ratings and principal pilot comments for rate coupling configurations

M_p	No. ¹	Pilot HQRs			Characteristic comments ²
		C	D	E	
0.00	–	2	2.5	2	No coupling, good on-axis response (best ratings shown)
–0.25	36	3	3		Low coupling, does not influence rating
	6	3			Initial response nice and solid, predictability good, no noticeable objections, some altitude problems
–0.50	17	5	5		Jerky roll response, quite large coupling when aggressive
	7	3		4	Predictability good, no oscillations
	B0	4			Jerky response, increased workload, coupling not a problem
–0.75	18	5	6		Two step roll response, unpredictable
	8			4.5	
–1.00	19	5	4		Moderate coupling, sluggish on-axis response with time delay, used some lead compensation
	9	5			Lowered aggressiveness, tremendous increase in workload, used small inputs and off-axis lead
–1.5	16		5		Cross coupling was predictable but annoying, large stick movements required, some compensation used
	10	4.5		5	Reduced aggressiveness, lead compensation, low predictability on initial response, moderately objectionable
–2.0					
	11	7		7.5	Very low predictability, very objectionable pitch oscillations, NOT tolerable workload
	B2		6+		Very notchy response with unpredictable roll acceleration, lots of compensation needed
–2.5					
	B3	7.5	7		Considerable workload, complex multi-axis coupling, unpredictable response, “like riding on top of a ball”

¹Top: ATTheS tests 1992. Middle: Ground-based simulator. Bottom: ATTheS tests 1993. Expanded definition of these configurations is contained in Appendices A, B, and C.

²Ground-based simulator comments are those of pilot C only.

Table 7.4. Handling qualities ratings and characteristic pilot comments for rate coupling configurations from the ground-based simulation—ADS-33C slalom task

M_p	No. ¹	HQRs		Characteristic comments
		C	E	
0.00	–		2	
–0.75	8		2.5	Very minor coupling, can obtain desired performance—a little extra workload. Response is predictable and can be precise for this task.
–1.5	10	3	4	Even though the coupling is apparent, there is no problem performing the task. Mildly unpleasant. Coupling didn't really affect performance—fairly easy to get desired performance. Compensation in pitch (high-frequency small-amplitude inputs) to maintain airspeed.
–2.0	11	4	4.5	Coupling has the effect of making the on-axis appear a little slow, but no real problem. Airspeed control is the most difficult aspect of the task.

¹Expanded definition of these configurations is contained in Appendix B.

Table 7.5. Handling qualities ratings and pilot comments for combined control and rate coupling configurations (all data from 1992 flight tests)

M_{δ_y}	M_p	No. ¹	Pilot HQRs				Characteristic comments
			A	B	C	D	
0.0000	0	10			2	2.5	No coupling, good on-axis response (best ratings)
-0.0036	-0.25	44		3	3		Mild mid-term coupling, minimum increased workload
-0.0072	-0.50	11	4			4	Some cross coupling apparent, unnatural on-axis response
-0.0072	-0.75	20			5	6	Moderate amount of cross coupling that was fairly predictable, considerable workload to compensate for coupling
-0.0143	-0.50	21		6		7	(Very) large but controllable coupling, unpredictable response
-0.0143	-0.75	24			6	7	Huge cross coupling requiring lots of compensation, coupling mainly mid/long term, task becomes pitch-axis task, very objectionable
-0.0143	-1.0	25			6	7	Large and complex coupling requiring reduced pilot gain and extensive compensation
-0.0286	-0.75	26			9	8	Too much coupling, poor task performance, no spare capacity, got out of phase with multi-axis coupling, at times I felt not in control at all
-0.0286	-1.0	27		10	8		Coupling required full attention, aggressiveness must be reduced to keep the helicopter right side up, coupling cannot be compensated for
-0.0358	-1.0	28			7 ²		Strong multi-axis coupling, no spare capacity, maximum tolerable workload, roll due to pitch very difficult to anticipate and coordinate, low predictability

¹Expanded definition of these configurations is contained in Appendix A.

²Analysis of task performance and pilot comments suggests that configuration may have been underrated.

Table 7.6. Handling qualities ratings and pilot comments for control coupling configurations with different pitch-due-to-roll over roll-due-to-pitch ratio (all data from the 1993 flight tests)

$M\delta_y$	$L\delta_x$	C	No. ¹	HQRs		Characteristic comments
				C	D	
-0.0072	0.0000	∞	A7		4	Slightly sluggish and unpredictable response, minor long term coupling, no roll-due-to-pitch coupling, slightly ratchety response
-0.0072	0.0072	1.45	A4	4		Mild pitch-due-to-roll coupling which requires moderate compensation, no roll-due-to-pitch coupling noted
-0.0072	0.0130	0.80	A1	3		Slight increase in workload, mildly unpleasant coupling, minimal compensation required, no roll-due-to-pitch coupling problem noted
-0.0429	0.0000	∞	A9	7 ²	6 ²	Need to provide lead to counter moderate coupling, extensive compensation required (one pilot noted some roll-due-to-pitch coupling)
-0.0429	0.0429	1.45	A6	5		Moderate short-term pitch-due-to-roll coupling, light roll-due-to-pitch coupling noted, increased workload to avoid off-axis response
-0.0429	0.0780	0.80	A3	5	5	Considerable pilot compensation required, moderate to large pitch-due-to-roll coupling, moderate roll-due-to-pitch coupling, relatively easy to counter and anticipate, tried diagonal inputs

¹ Expanded definition of these configurations is contained in Appendix C.

² Pilot complained of jet lag and/or unfamiliarity with the aircraft.

Table 7.7. Handling qualities ratings and pilot comments for rate coupling configurations with different pitch-due-to-roll over roll-due-to-pitch ratios

M_p	L_q	C	No. ¹	Pilot HQRs				Characteristic comments ²
				C	D	E	F	
-0.25	0.50	1.00						
			E6				2	Configuration not difficult to master, no short-term coupling noted, long-term coupling difficult to separate from thermal activity
-0.25	1.50	0.33	6	3				Initial response nice and solid, no noticeable objections
-0.50	0.00	∞	19	3				Precision easy even when aggressive, predictable initial response, no oscillations
			B7	5 ³	4		4.5 ⁴	Moderate mid-term coupling, no roll-due-to-pitch coupling, objectionable step/jerky response
-0.50	1.0	1.00	16	3				Hardly a sense of off-axis coupling, no oscillations, mildly unpleasant
			B4	4	4			Very mild coupling, jerky roll response, roll-due-to-pitch coupling not noted as problem, moderate increase in pilot workload
-0.50	1.82	0.55	13	4-				Initial response sluggish, no overshoots/oscillations, the harder one works, the worse it gets
-0.50	3.0	0.33	7	3		4		Predictability good, no oscillations, didn't modify control strategy
			B0	4				Jerky response, increased workload, coupling not a problem, no roll-due-to-pitch coupling noted
-1.0	0.00	∞	20	4				A little disharmony, "bobbles" on roll-out, mid-term response somewhat undesirable, "if you're more aggressive it's a handful"
-1.0	2.0	1.00	17	4				Precision not good, "wallowing," better precision when not as aggressive
-1.0	3.64	0.55	14	4.5				Initial response somewhat illusive, mid-term response a nuisance, "wallowing," tried lead but eventually just closed loops on errors
-1.0	6.0	0.33	9	5				Lowered aggressiveness, predictable, problem with off-axis response, lack of control harmony, tremendous increase in workload

Table 7.7. Continued

M_p	L_q	C	No. ¹	Pilot HQRs				Characteristic comments ²
				C	D	E	F	
-2.0	0.00	∞	21	4				Seems sluggish, a lot of activity in pitch, moderate coupling
			B9	5	4		4 ⁵	Moderate pitch-due-to-roll and no roll-due-to-pitch coupling, slightly unpredictable, need to compensate for coupling
-2.0	4.0	1.00	18	5				Moderate coupling, backed-off on roll rates, predictability pretty low, lead in pitch produced problems with height control
			B6	6	5			Lead required to compensate for coupling, moderate roll-to-pitch coupling, pitch-to-roll coupling overshadowed by roll-to-pitch a little jerky, objectionable response
-2.0	7.27	0.55	15	4.5				Control harmony a problem, tried not to excite off-axis response, feels like flying pitch axis instead of roll axis
-2.0	12.0	0.33	11	7		7.5		Very low predictability, tried backing off, very objectionable pitch oscillations, tried using lead but didn't always work, not tolerable workload
			B2		6+			Very notchy response with unpredictable roll accelerations, lots of compensation needed, very little roll-due-to-pitch coupling noted but might have been covered up by pitch-due-to-roll
-2.5	0.00	∞	21a	6				Can't back off easily, low predictable initial response, poor harmony, nuisance response, mid-term has a different character, "weird"
-2.5	5.00	1.00	18b	7.5				Lateral control easier with pitch inputs, "scary" if flown with roll, precision low, backed off on aggressiveness, extremely high workload
			E8	6			6	Very objectionable roll oscillations, very high workload, had to think before making an input, "could be an olympic event"
-2.5	9.09	0.55	15a	7				Oscillations in pitch became objectionable, low predictability, with motion it would be scary, backed-off
-2.5	15.00	0.33						
			B3	7.5	7			Complex multi-axis coupling, large pitch-due-to-roll coupling, moderate roll-due-to-pitch coupling, maximum workload, response unpredictable, "like riding on top of a ball"

Table 7.7. Concluded

M_p	L_q	C	No. ¹	Pilot HQRs				Characteristic comments ²
				C	D	E	F	
-3.0	0.00	∞	21b	8				Out of phase, lots of pitch “bobble,” very low predictability of initial response, mid-term response highest workload, would be nasty with motion
-3.0	6.00	1.00	18a	7.5				Extreme compensation required, roll tracking with pitch inputs, if aggressive beyond task demands might have lost control

¹Top line: Ground-based simulator. Bottom line: ATTheS tests 1993. Expanded definition of these configurations is contained in Appendices A, B, and C.

²Ground-based simulator comments are those of pilot C only.

³Course was flown with tailwind, which might have had some adverse effect on roll oscillations and HQRs.

⁴Only one practice and one evaluation run; pilot said, “Given another run I might have been able to . . . attain desired [performance]” which would have resulted in HQR 4.

⁵Only one practice and one evaluation run; pilot said, “Needed more time to establish whether HQR was either 4 or 5.”

Table 7.8. Handling qualities ratings and characteristic pilot comments for rate coupling configurations with reduced on-axis bandwidth ($L_p = 5.0$ rad/sec and $M_q = 2.5$ rad/sec) (data only for pilot C in fixed-base simulator)

M_p	No. ¹	HQR	Characteristic comments
0.00	22un	3	Precision a little lower, seemed slow or sluggish, more planning required prior to gate
-0.16	22a	3	Could get aggressive, predictability of initial response good, no objectionable oscillations, aircraft a little loose during tracking
-0.25	22	4	Some oscillations during tight tracking, no harmony problem, “wallowing,” minor but annoying deficiencies
-0.63	25a	4.5	Initial response OK, mid- to long-term response very objectionable, precision for tracking gets better with tighter control but predictability goes down, more than annoying deficiencies
-1.00	24	6	Precision low, can be more aggressive but it doesn’t help, oscillations when tight in controls, very objectionable, extreme compensation
-1.30	27a	7	Extreme workload, low predictable initial response, primarily flying pitch, controllability not in question
-1.50	25	8	Couldn’t be aggressive, no predictability of response, mid/long term response very objectionable, major deficiencies, control in question

¹Expanded definition of these configurations is contained in Appendix B.

Table 7.9. Handling qualities ratings and characteristic pilot comments for control coupling configurations with reduced on-axis damping ($L_p = 5.0$ rad/sec and $M_q = 2.5$ rad/sec) (data only for pilot C in fixed-base simulator)

M_{δ_y}	No. ¹	HQR	Characteristic comments
0.0000	22un	3	Precision a little lower, seemed slow or sluggish, more planning required prior to gate
-0.0027	28a	4	Initial response OK, predictable, a little sluggish, mid-term response couples into pitch which couples into altitude, minor annoying oscillations in fine tracking which are hard to dampen out
-0.0108	30a	4.5	Harder to fly if more aggressive, some oscillations in mid-term response, moderate coupling which is easy to compensate for, more than annoying deficiencies
-0.0215	31a	5	Oscillations if aggressive, make small slow inputs, low predictable initial response, lots of pitch-due-to-roll, minor roll-due-to-pitch, difficult to coordinate
-0.0323	32a	6	Tremendous workload, precision extremely low, constant oscillations, flew pitch axis for roll task, control strategy—correct at low rates, mentally stay out of the loop as best as possible
-0.0376	32b	8	Control system not adequate for task, extreme workload, no precision, extremely low predictability of initial response, extremely poor harmony, may have lost control a couple of times

¹Expanded definition of these configurations is contained in Appendix B.

Table 7.10. Handling qualities ratings and characteristic pilot comments for rate coupling configurations with reduced roll axis bandwidth ($L_p = 5.0$ rad/sec and $M_q = 2.5$ rad/sec) (data only for pilot C in fixed-base simulator)

M_{δ_y}	No. ¹	HQRs	Characteristic comments
0.0000	33un	3	Predictable response, harmony good, a little bit of planning required, doesn't fall apart if more aggressive, a little sluggish, mildly unpleasant
-0.0036	33	3	Predictable initial response but seemed sluggish, no problem in mid- to long-term response, control harmony pretty good, seems like heavy aircraft, some mildly unpleasant deficiencies
-0.0143	35	4	Obvious coupling but predictable, figure out phasing lead input to eliminate coupling, no mid-term or oscillation problems
-0.0286	36	5	Performance goes down with more aggressiveness, initial response pretty predictable when backing off, oscillations when aggressive, mild coupling
-0.0498	37a	5/7	Precision low, low predictability of initial response, easier to fly task with pitch then correct with roll, persistent Dutch roll oscillations objectionable at higher aggressiveness, moderately objectionable/major deficiency, controllability not questioned
-0.0575	37b	7	No precision, unpredictable response, had to back off to maintain control, mid- and long-term response has very objectionable on and off axis oscillations, very difficult to pilot, no harmony

¹Expanded definition of these configurations is contained in Appendix B.

Table 7.11. Handling qualities ratings and characteristic pilot comments for washed-out coupling configurations with $L\delta_x/M\delta_y = -1.8$ (pilots C and E only)

$M\delta_y$	$M_{q,c}$	No. ¹	HQRs		Characteristic comments (pilot C only)
			C	E	
-0.0143	-6.0	45	4		Jerky tracking, increased workload due to coupling
-0.0286	-6.0	46	4		Jerky roll response due to cross-coupling, reduced pilot gain to avoid roll oscillation
		38		4	
-0.0072	-4.0				
-0.0143	-4.0	42	4		Jerky tracking, on-axis influence, mid-term coupling
		C1	4.5		Reduced predictability of on-axis response, jerky response, coupling appeared with large rapid inputs
-0.0286	-4.0	43	6		Poor performance, moderately objectionable multi-axis coupling
		40	3+	3	Couldn't identify any initial response problem, no oscillations, couldn't identify nuisances
		C2	5		Trying to avoid problems by reducing the input rate, very mild coupling, objectionable ratcheting in roll response, increased workload
-0.0358	-4.0				
-0.0572	-4.0				
		54	3+	3/4	Some mild coupling, no mid- to long-term problem, no oscillations, height control a problem
		C3	6		Greatly increased effort due to low predictability and moderate off-axis response, very jerky response, very objectionable
-0.0858	-4.0				
		C4	7		Very difficult multi-axis coupling, very jerky/ratcheting response, severe coupling which increases with pilot gain, "like riding a mechanical bull"
-0.0286	-2.0	23	5		Very jerky, oscillations during tight tracking, mild pitch-due-to-roll coupling
-0.0358	-2.0	48	5		Only adequate performance, increased workload due to coupling, moderately objectionable coupling

¹Top line: 1992 flight tests. Middle line: Fixed-base simulator. Bottom line: 1993 flight tests. Expanded definition of these configurations is contained in Appendices A, B, and C.

Table 7.12. Handling qualities ratings and characteristic pilot comments for washed-out coupling configurations with $L\delta_x/M\delta_y = -1.8$ (pilot D only)

$M\delta_y$	$M_{q,c}$	No. ¹	HQR	Characteristic comments
-0.0143	-6.0	45	4	Very little coupling, lack of control power determines rating
-0.0286	-6.0			
-0.0072	-4.0			
		C0	3	No coupling apparent, very very slight notchiness in roll
-0.0143	-4.0	42	3	Some slight mid-term coupling apparent
		C1	4	Slightly uneven roll response, small amount of roll-due-to-pitch coupling
-0.0286	-4.0	43	4	Very little coupling, very quick rise time and only moderately steady roll rate
		C2		
-0.0358	-4.0			
-0.0572	-4.0			
		C3	4	Quite a bit of roll-due-to-pitch coupling, strange response, notchy roll response, slightly unnatural accelerations felt during maneuvering
-0.0858	-4.0			
		C4	6	Lots of ratcheting, unpredictable roll response, lots of short term coupling, strange acceleration cues during acquisition
-0.0286	-2.0			
-0.0358	-2.0			

¹Top line: flight tests 1992. Bottom line: flight tests 1993. Expanded definition of these configurations is contained in Appendices A and C.

Table 7.13. Handling qualities ratings and characteristic pilot comments for washed-out coupling configurations with $L\delta_x/M\delta_y = -1.0$ (1993 flight test data)

$M\delta_y$	$M_{q,c}$	No. ¹	HQR ²	Characteristic comments
-0.0143	-6.0	D6	4	Small oscillations in both axes are minor deficiency, mid- to long-term coupling oscillations
-0.0858	-6.0	D9	6	Low-frequency wave in off-axis response “like riding an ocean wave,” high frequency washout of coupling was “like hitting a boat wake,” jerky and unpredictable short-term coupling, very objectionable but tolerable deficiency
-0.0072	-4.0	D0	4	Moderate increase in workload, jerky coupling response
-0.0143	-4.0	D1	5	Considerable workload to obtain desired performance, objectionable jerky on- and off-axis response, jerky short-term coupling
			3	No cross coupling apparent in any axis, nice and precise
-0.0286	-4.0	D2	4	Very mild short-term pitch-due-to-roll coupling, jerky roll response is minor annoying deficiency
			3	Nice primary response, slight amount of notchiness noted at very high aggression levels only, no coupling noted
-0.0572	-4.0	D3		
			4.5	Slight compensation necessary to overcome roll notchiness, very slight short-term coupling
-0.0858	-4.0	D4	7	Increased effort above tolerable level, very objectionable coupling with slow washout, couldn't find any control combination to null out coupling, very low roll predictability
			5	Ratcheting roll response increased with aggression, some short-term roll-due-to-pitch coupling
-0.0072	-2.0	D5	4.5	Increased workload, stepped/jerky response, mildly objectionable jerky response, marginally desired performance
-0.0572	-2.0	D8	5	Moderate pitch and mild roll oscillations which appeared to wash out in less than 1 sec., jerky off-axis response, considerable workload, the jerky washout of the cross coupling was very objectionable

¹Expanded definition of configuration is contained in Appendix C.

²Top line: Pilot C. Bottom line: Pilot D.

Table 7.14. Handling qualities ratings and characteristic pilot comments for rate coupling configurations with modified frequency domain characteristics ($L_{p,c} = M_{q,c}$ and $M_{\delta_y} = L_{\delta_x}$) (1993 flight test data)

M_p	$M_{q,c}$	No. ¹	HQRs		Characteristic comments
			C	F	
-0.125	1.0	F1		6	Tried all levels of aggression with same mediocre but passable result, pitch axis seemed more responsive than roll, weak coupling hard to pin down, confusing, objectionable deficiencies
-0.250	2.0	F0	4		Annoying jerky roll response which seemed to result from mild pitch-due-to-roll coupling, minor annoying deficiency
-0.500	1.0	F3	5		Very difficult to provide lead since the pitch response appeared to build slowly, low predictability of off-axis
-1.000	2.0	F2	6		Moderate increase in workload, unusual coupling, complex coupling that appeared to feed back to other axis that made pitch appear to “dig in,” very objectionable oscillations

¹ Expanded definition of these configurations is contained in Appendices A, B, and C.

Table 7.15. Handling qualities ratings and characteristic pilot comments for washed-out coupling configurations with modified frequency domain characteristics ($L_{p,c} = M_{q,c}$ and $M_{\delta_y} = L_{\delta_x}$) (1993 flight test data)

M_{δ_y}	$M_{q,c}$	No. ¹	HQRs		Characteristic comments
			C	F	
-0.0572	-0.50	F9	5 ²	5	Multi-axis coupling with different sensitivity and damping in each direction, confusing control inputs, objectionable oscillations, jerky response, “weird”
-0.0572	-2.00	F7	4.5 ²		Moderate roll-due-to-pitch coupling, nonsymmetric sensitivity in roll, annoying but tolerable, slightly jerky response, pitch-due-to-roll coupling canceled out in short term

¹ Expanded definition of these configurations is contained in Appendices A, B, and C.

² Rating based on only one practice and one evaluation run (pilot might still be in training phase).

Table 8.1. Frequency domain pitch-roll coupling parameters for the BO 105 at 80 knots (2 flights) and an attack helicopter at 60 knots

Helicopter	Type of coupling	Coupling ratio at ω_{BW} , dB	Coupling ratio at ω_{I80} , dB	Averaged coupling ratio, dB
BO 105 (flight 1)	Pitch-due-to-roll	-13.0	-17.7	-16.2
	Roll-due-to-pitch	-10.9	2.9	-5.5
BO 105 (flight 2)	Pitch-due-to-roll	-14.0	-16.3	-15.6
	Roll-due-to-pitch	-13.2	0.9	-6.2
Attack helicopter	Pitch-due-to-roll	-20.1	-22.9	-21.2
	Roll-due-to-pitch	-7.8	-12.2	-8.3

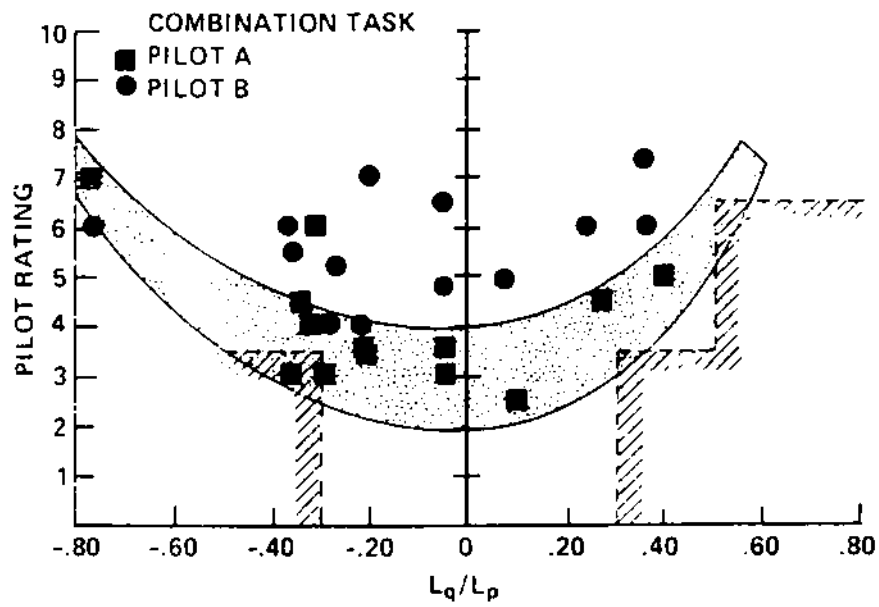
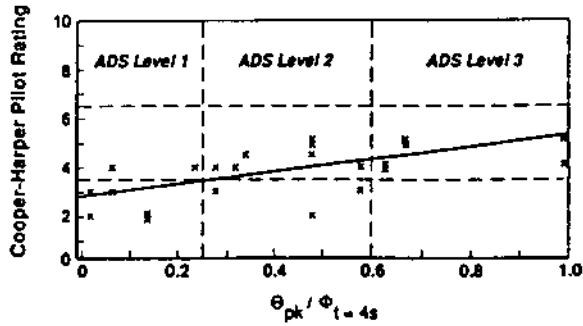
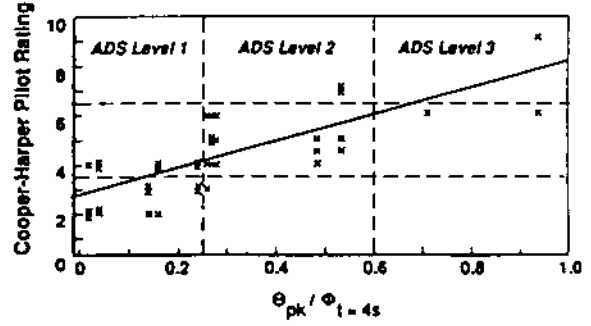


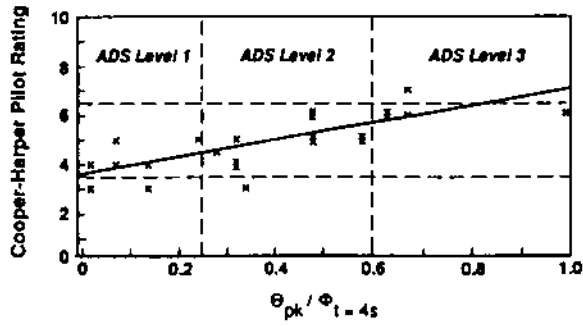
Figure 2.1. Pilot ratings from fixed base simulation in a combination dolphin/slalom task vs. L_q/L_p (from ref. 11).



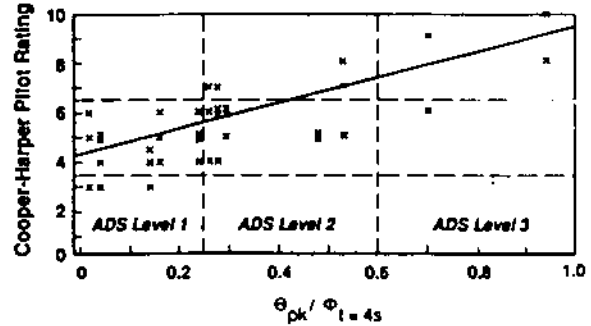
(a) Pilot ratings for the easy slalom with hingeless rotor



(b) Pilot ratings for the easy slalom with articulated rotor



(c) Pilot ratings for the difficult slalom with hingeless rotor



(d) Pilot ratings for the difficult slalom with articulated rotor

Figure 2.2. Pilot ratings vs. θ_{pk}/ϕ for an “easy” and a “difficult” slalom (from ref. 9).

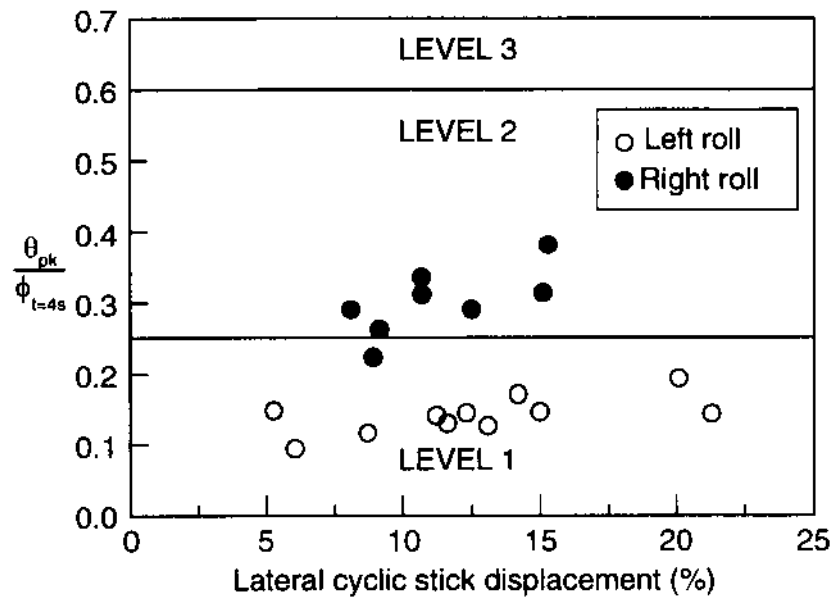


Figure 2.3. Results of the pitch-due-to-roll coupling criterion for a conventionally controlled BO 105 (from ref. 13).

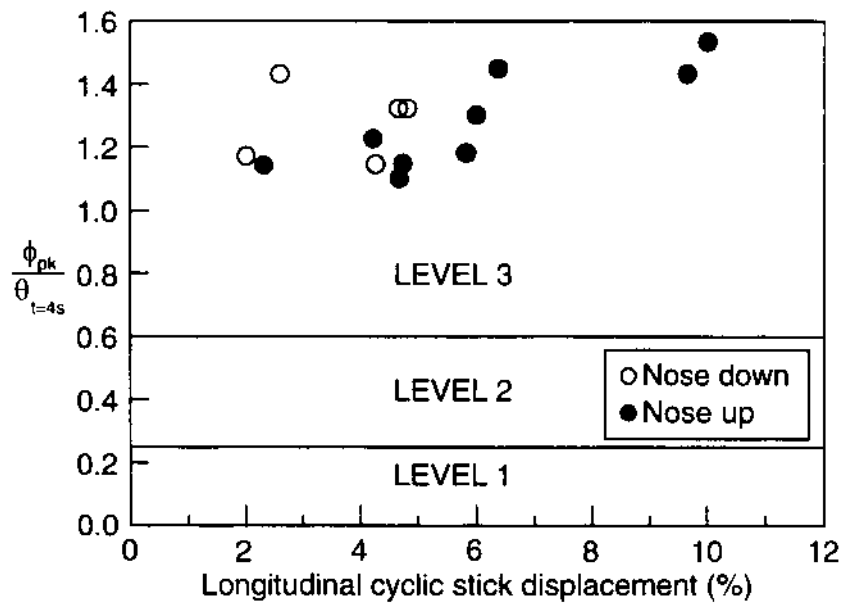


Figure 2.4. Results of the roll-due-to-pitch coupling criterion for a conventionally controlled BO 105 (from ref. 13).

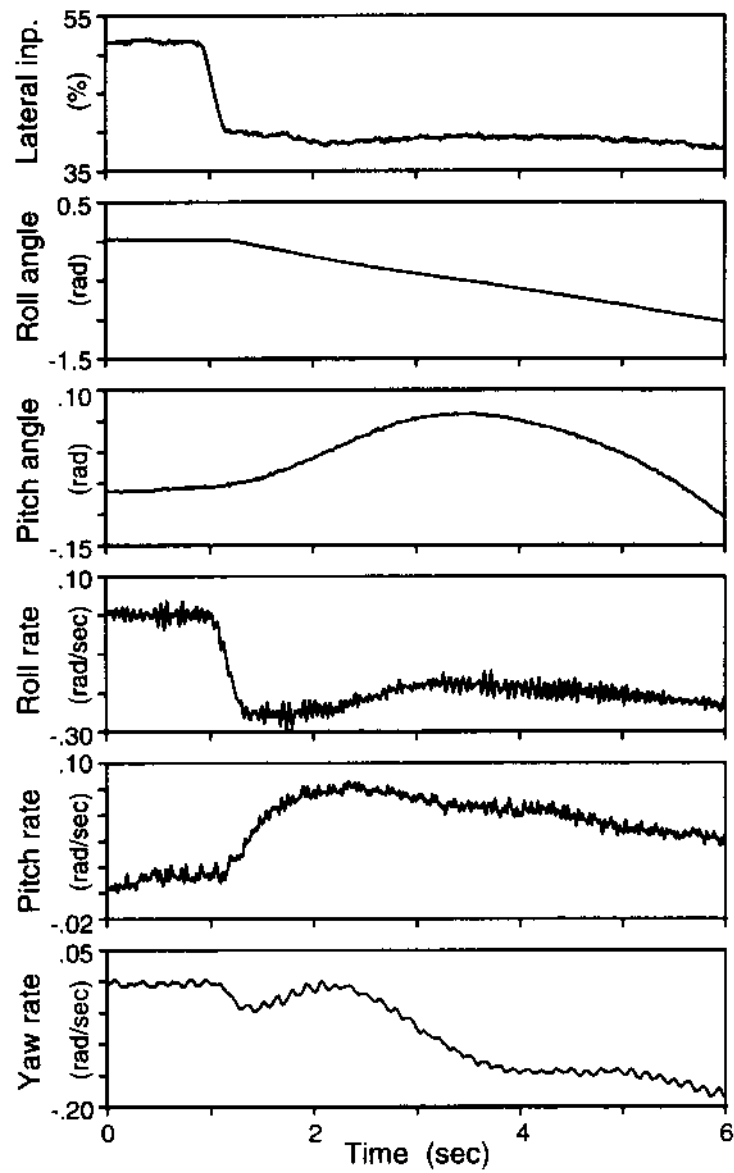


Figure 2.5. Typical time history of the response of a roll step input to the left with a conventionally controlled BO 105.



Figure 4.1. The DLR in-flight simulator ATHeS.

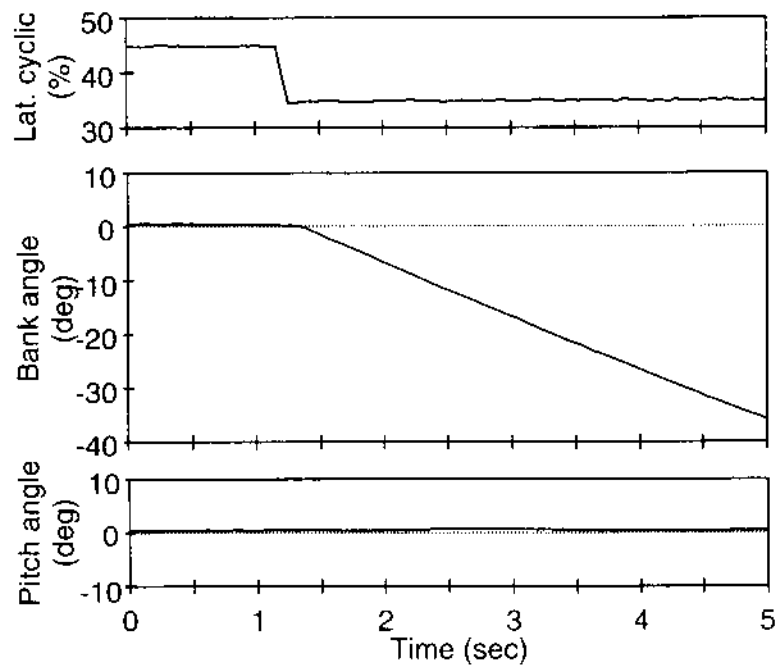


Figure 4.2. Response of ATHeS with a decoupled command model (baseline model) to a lateral control step input.

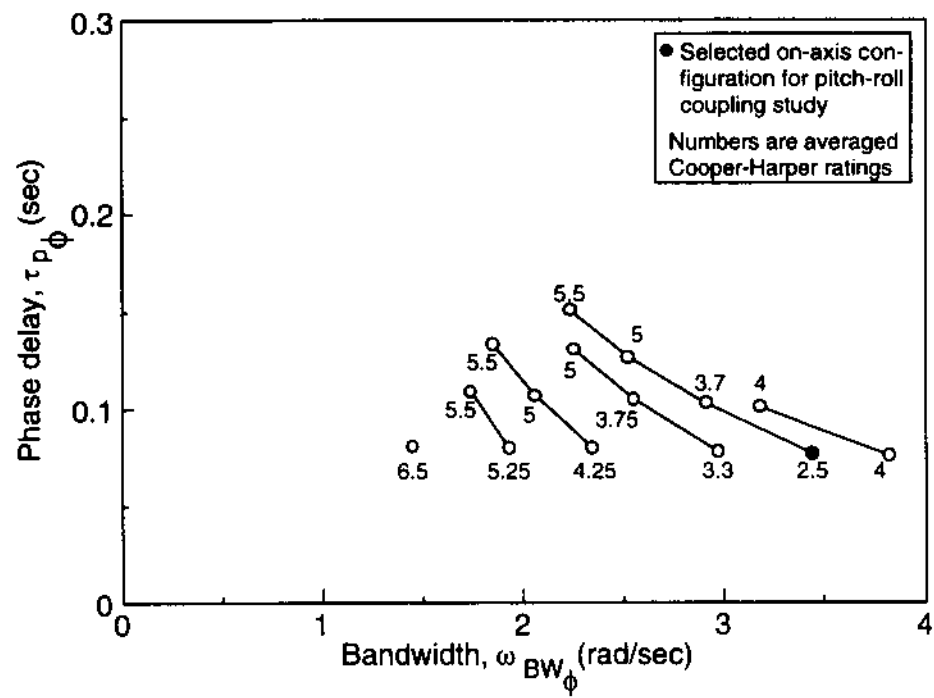


Figure 5.1. Rate command configurations evaluated during the bandwidth-time delay study (from ref. 14).

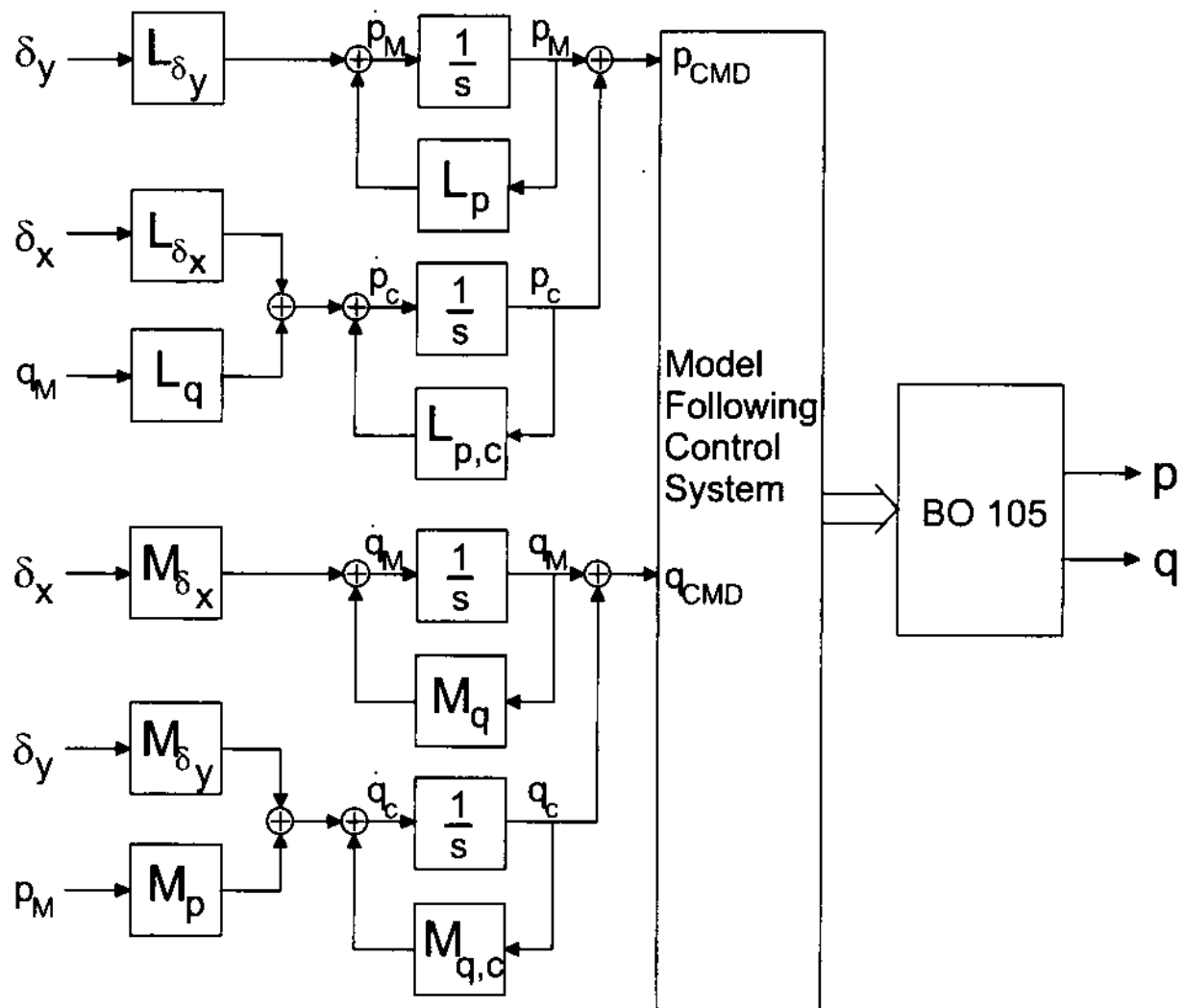


Figure 5.2. Cross-coupling models of pitch and roll axis.

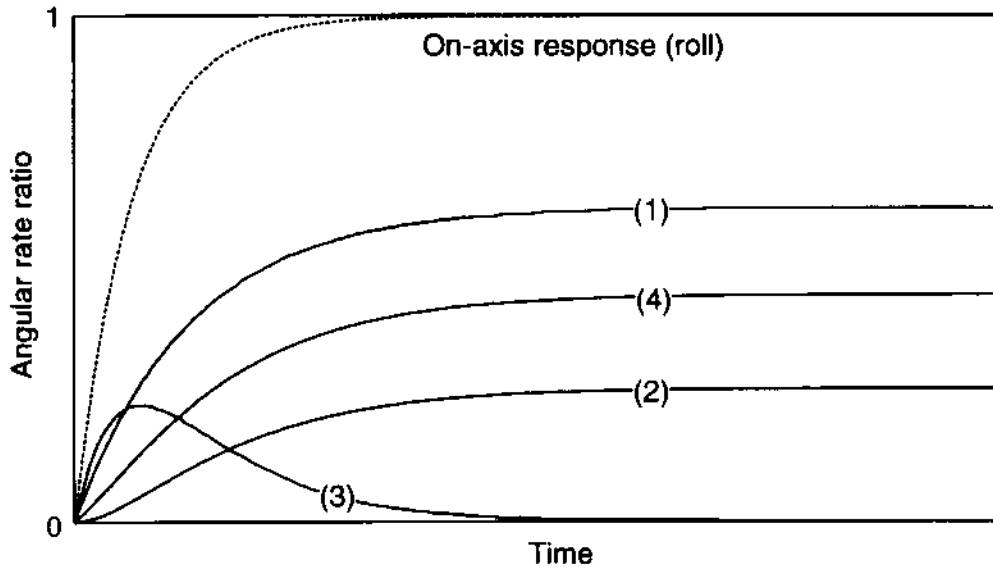


Figure 5.3. Roll and pitch rate responses to a lateral step input for different types of coupling: (1) control coupling, (2) rate coupling, (3) washed-out coupling, and (4) combined control and rate coupling.

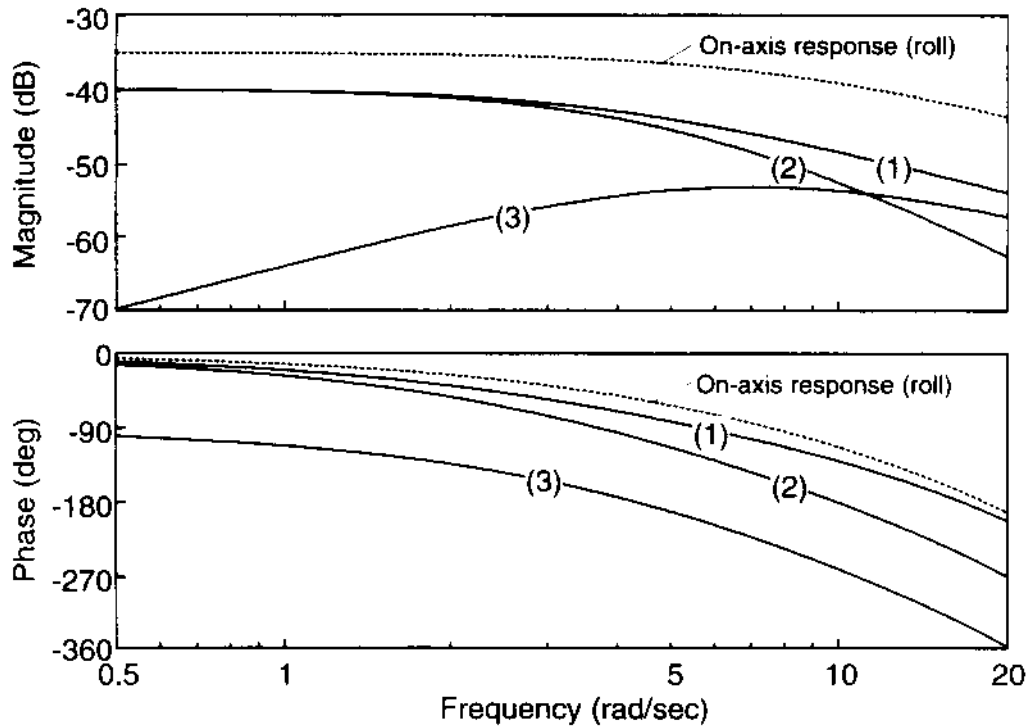


Figure 5.4. Bode plot of the roll and pitch rate responses to a lateral cyclic input, p/δ_y and q/δ_y , for three different types of coupling: (1) control coupling, (2) rate coupling, and (3) washed-out coupling.

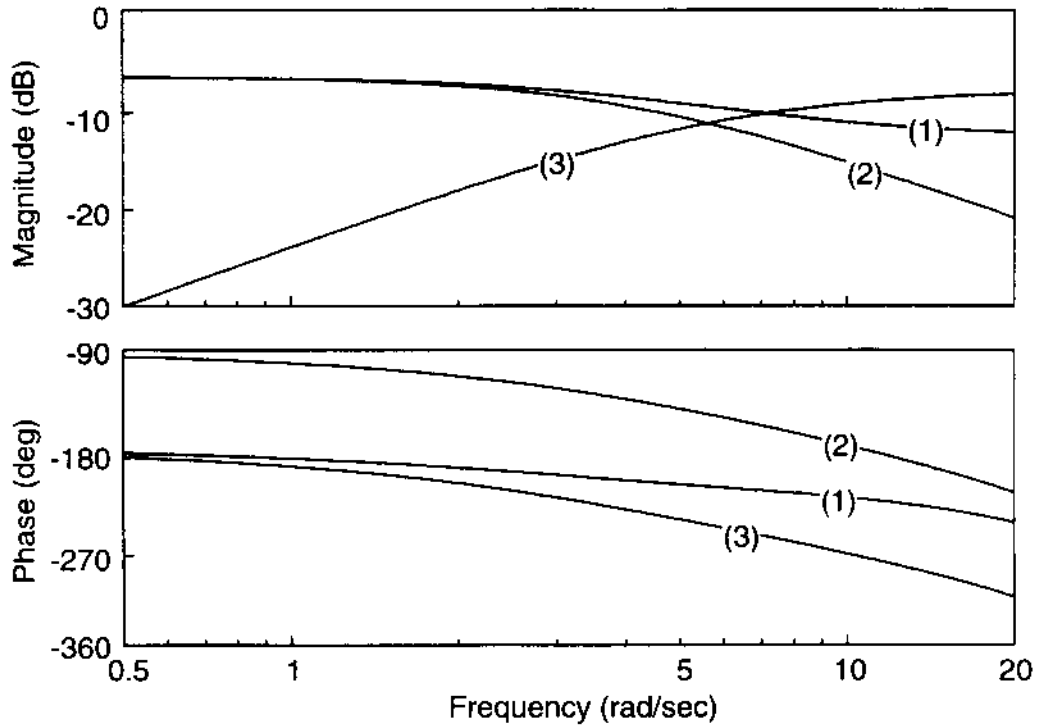


Figure 5.5. Bode plot of the pitch rate to roll rate response (lateral cyclic input), $q/p|\delta_y$, for three different types of coupling: (1) control coupling, (2) rate coupling, and (3) washed-out coupling.

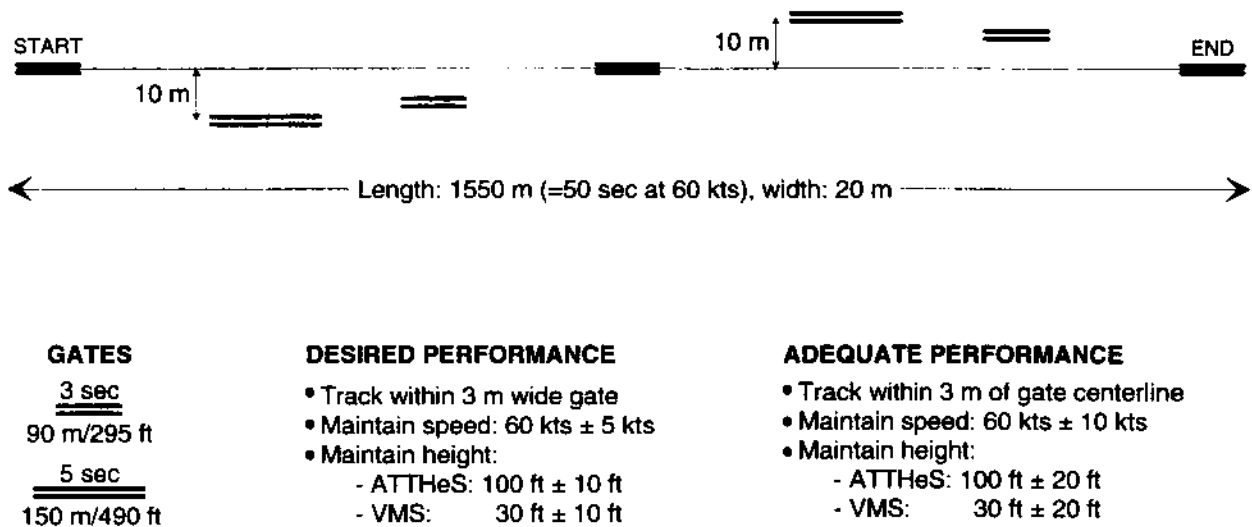


Figure 6.1. The slalom-tracking course used for the VMS ground-based and ATTheS in-flight simulations.

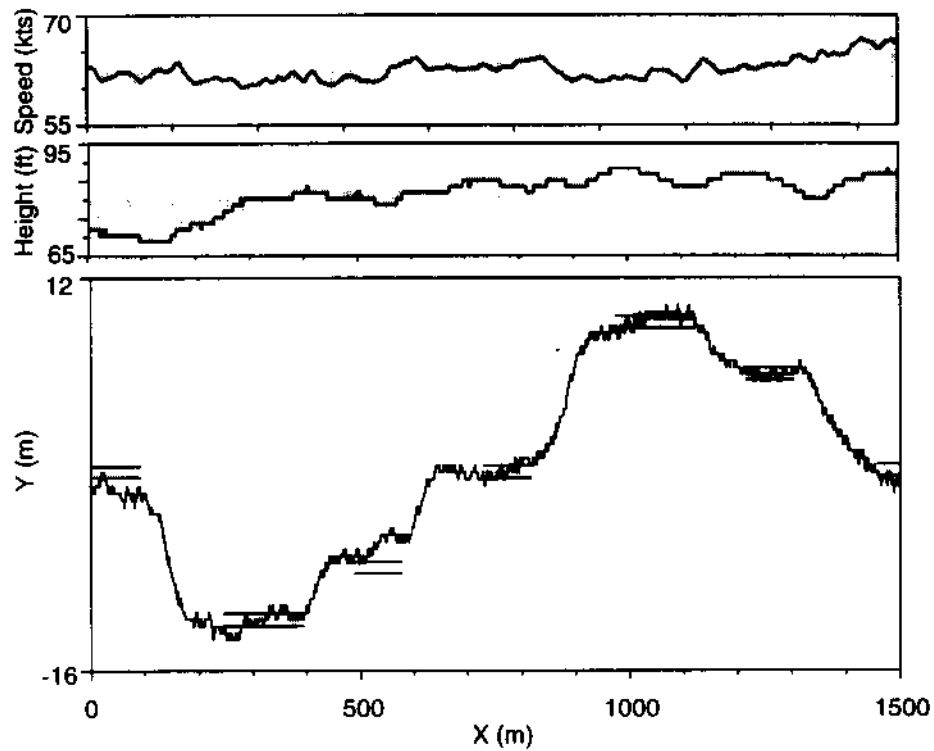


Figure 6.2. Typical task performance through the slalom-tracking course (ATTheS baseline configuration, no interaxis coupling, and Level 1 handling qualities).

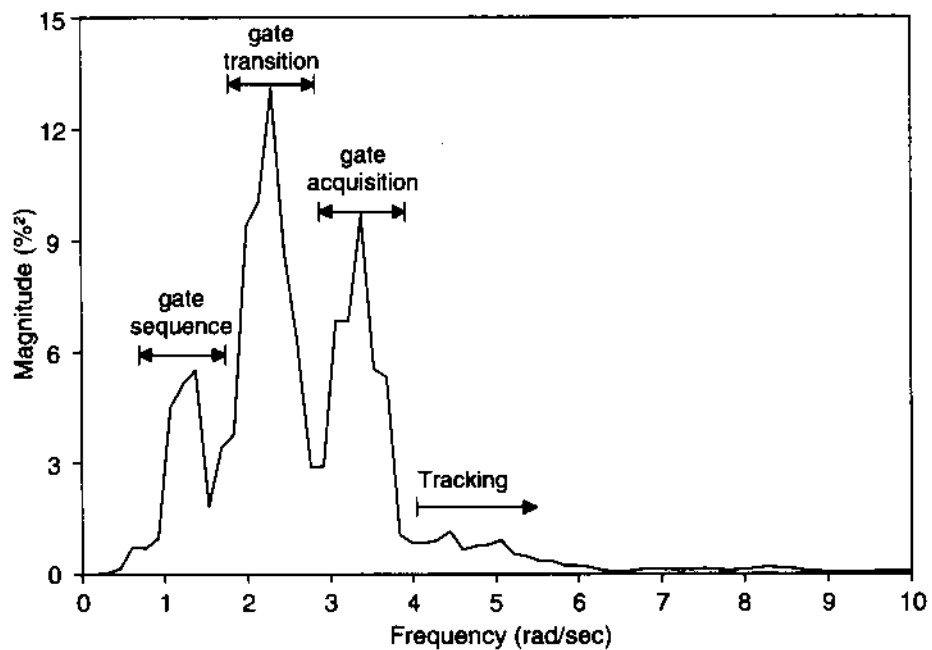


Figure 6.3. Power spectrum of the lateral control inputs for the slalom of figure 6.2.

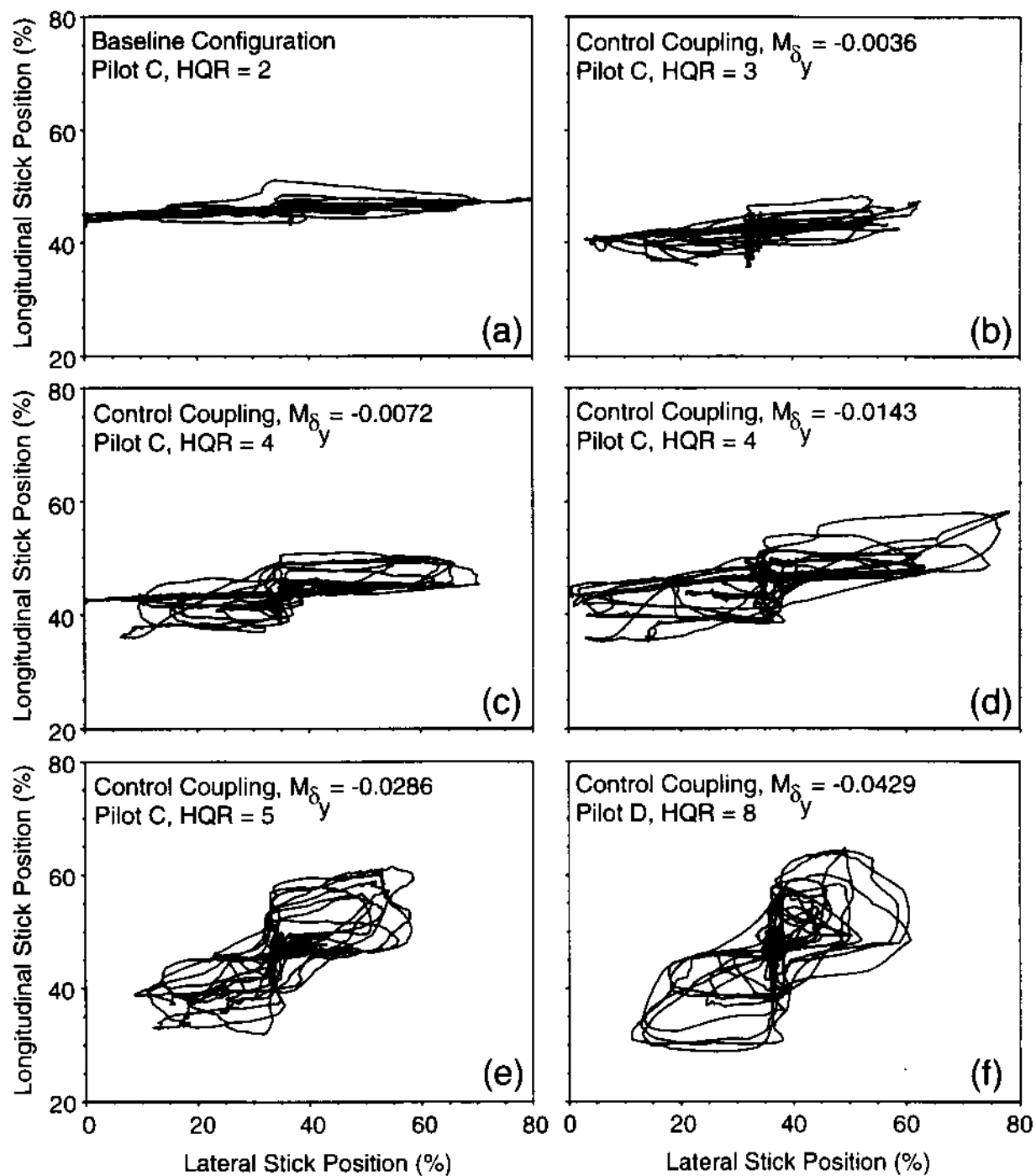


Figure 7.1. Representative control input positions for control coupling configurations (all data from the 1992 flight tests).

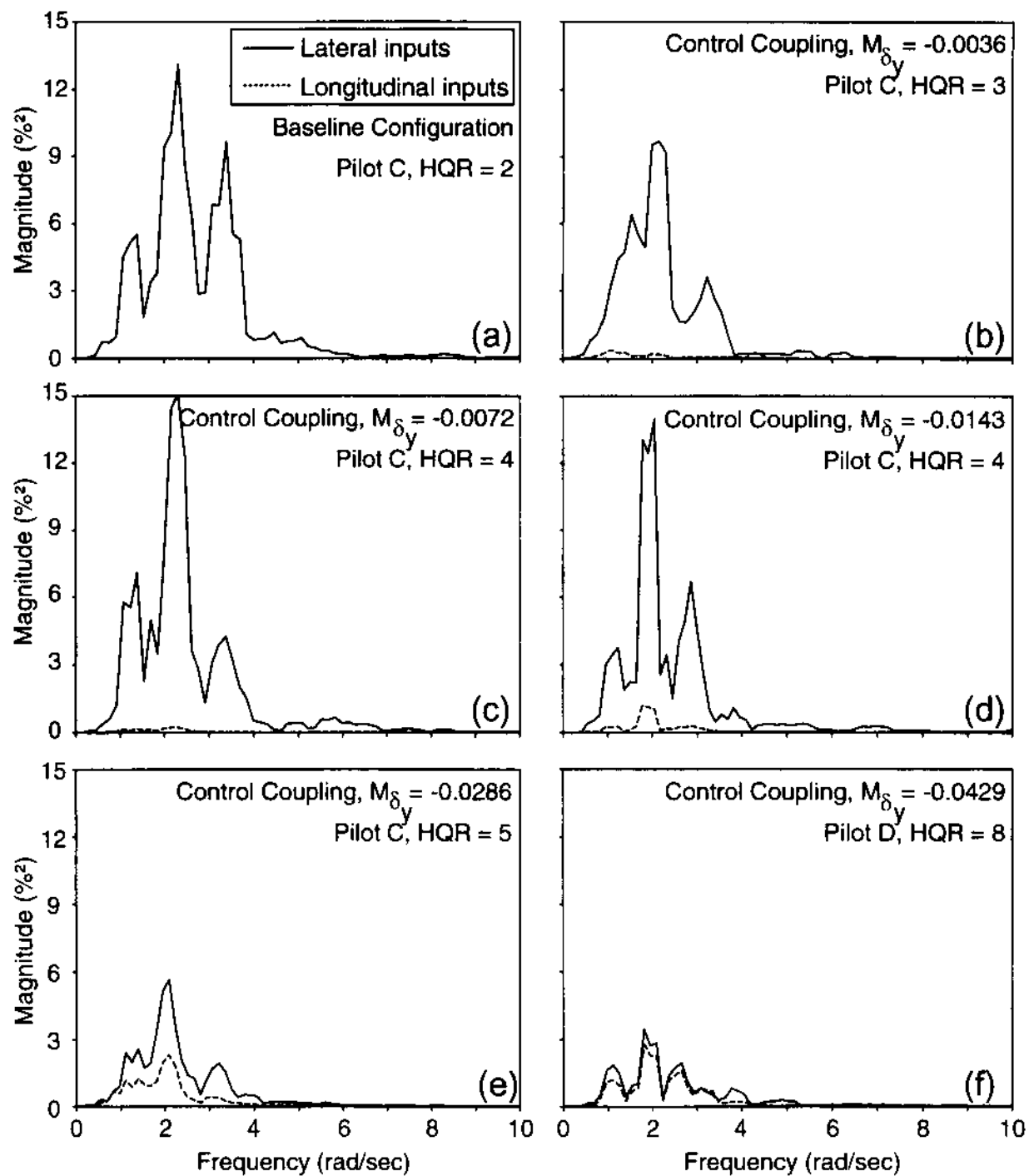


Figure 7.2. Power spectrum of the control inputs for typical control coupling configurations (all data from the 1992 flight tests).

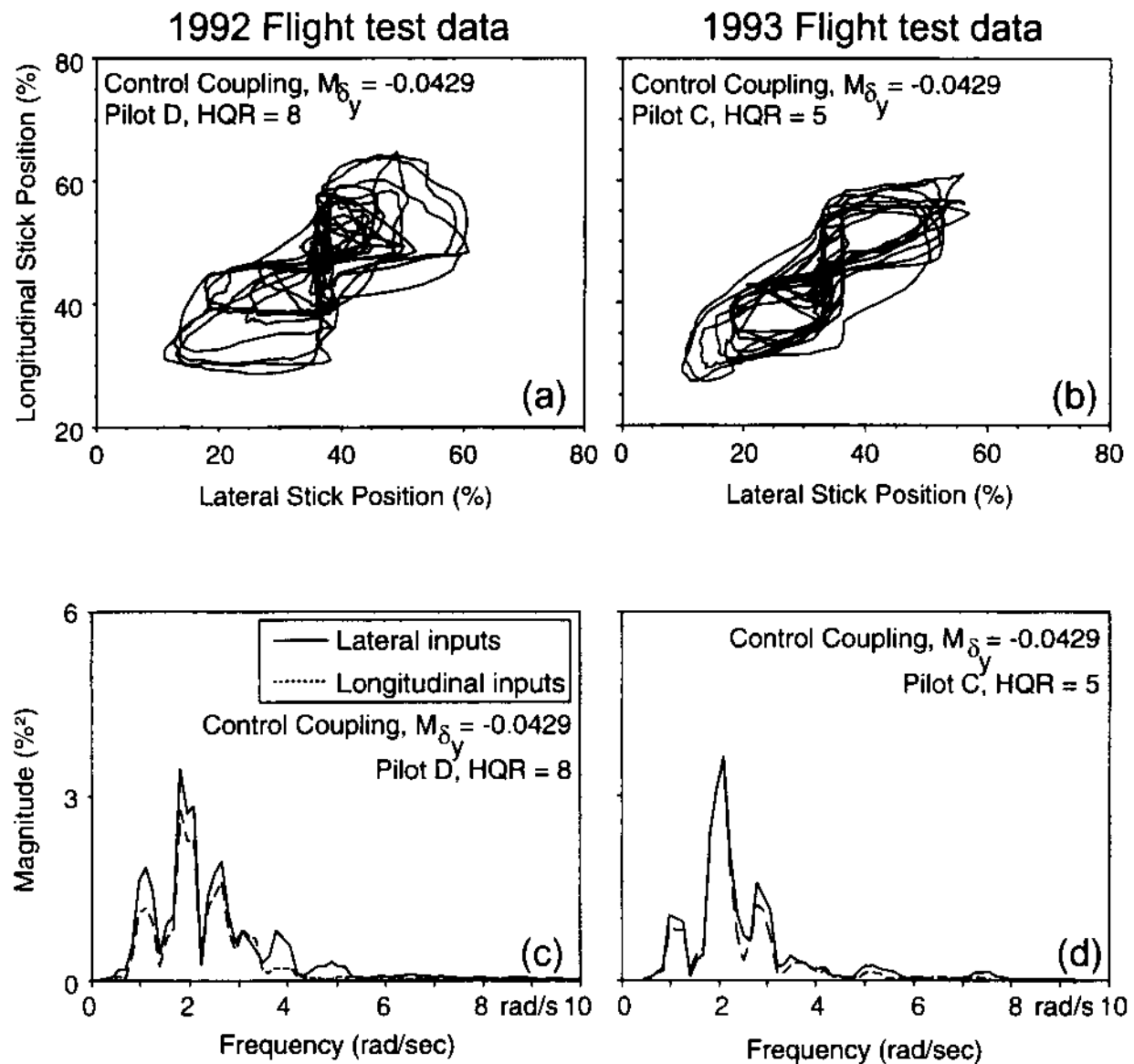


Figure 7.3. Comparison of the 1992 and 1993 flight test control inputs and power spectra of the control coupling configuration with $M_{\delta_y} = -0.0429 \text{ rad}\cdot\text{sec}^{-1}\cdot\text{percent}^{-1}$.

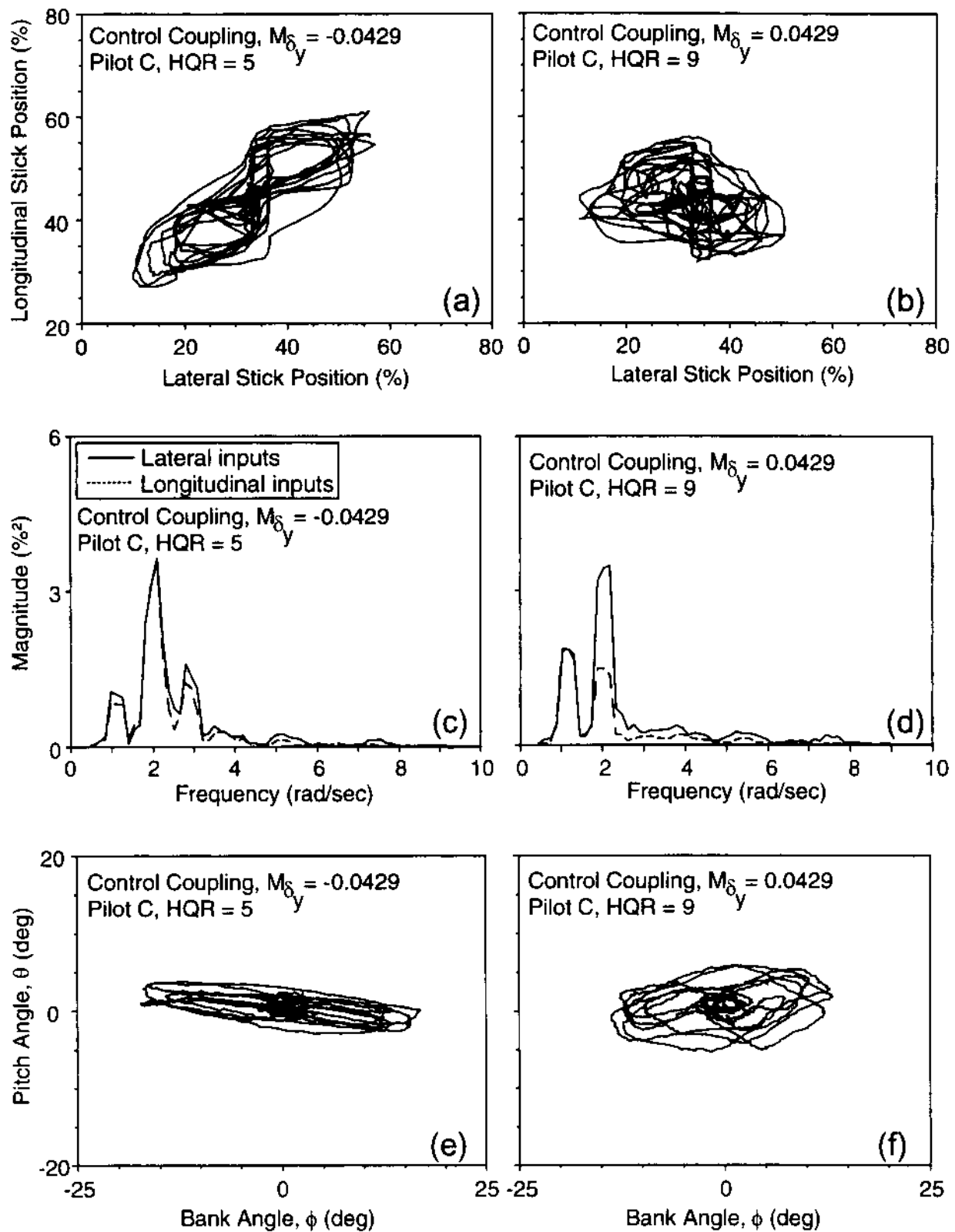


Figure 7.4. Comparison of the control coupling configurations with conventional and unconventional direction of coupling (both results from the 1993 flight tests).

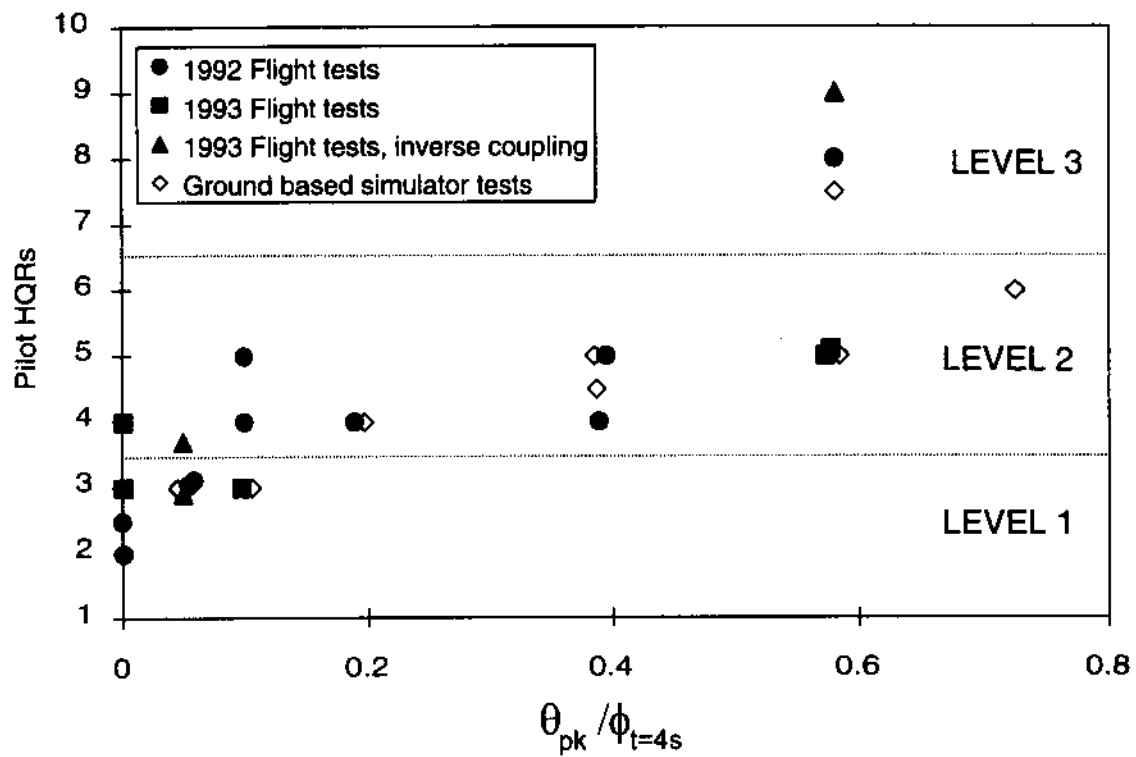


Figure 7.5. Comparison of the HQRs with the ADS-33C coupling parameters for control coupling configurations.

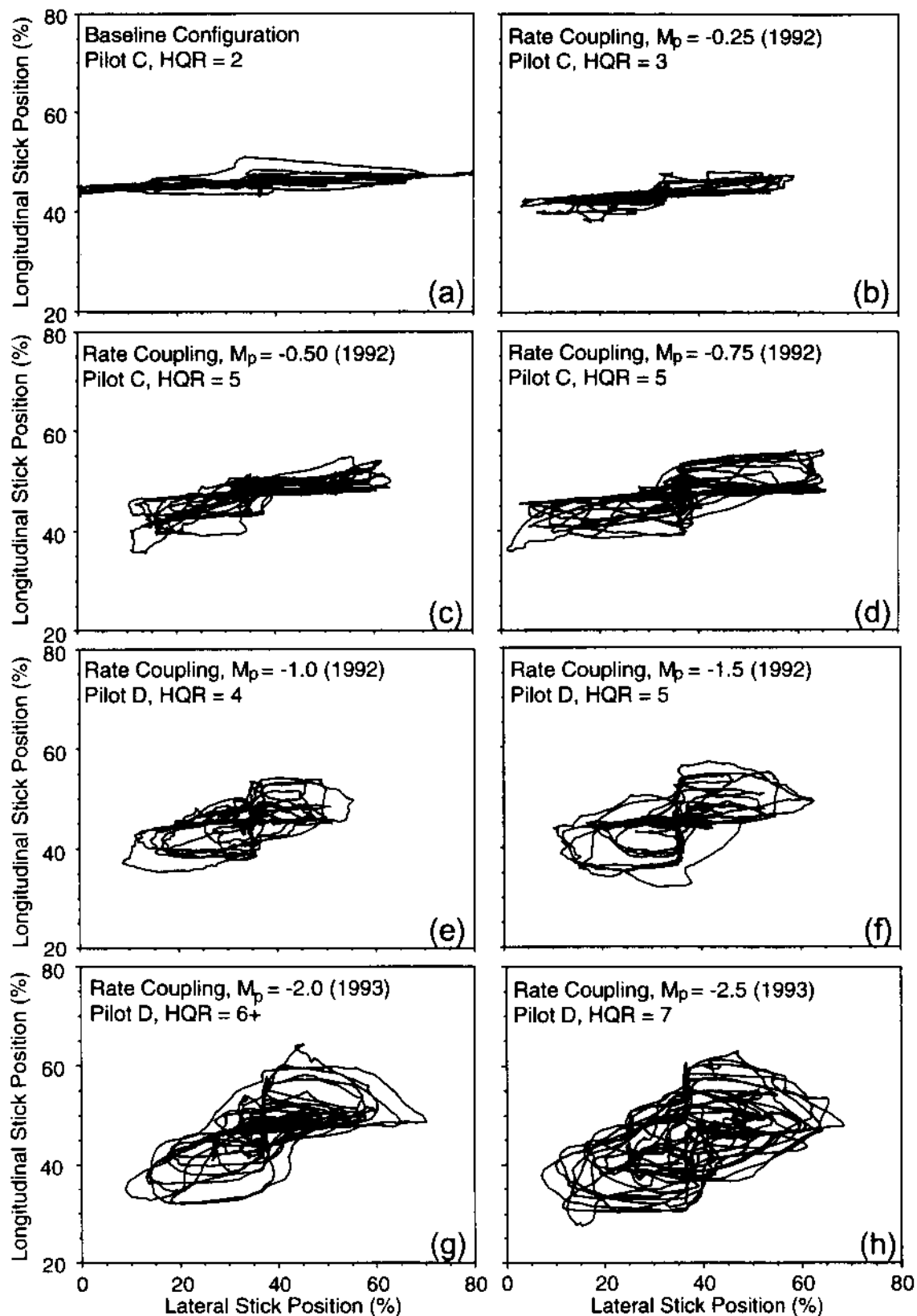


Figure 7.6. Representative control input positions for rate coupling configurations (data from 1992 and 1993 flight tests).

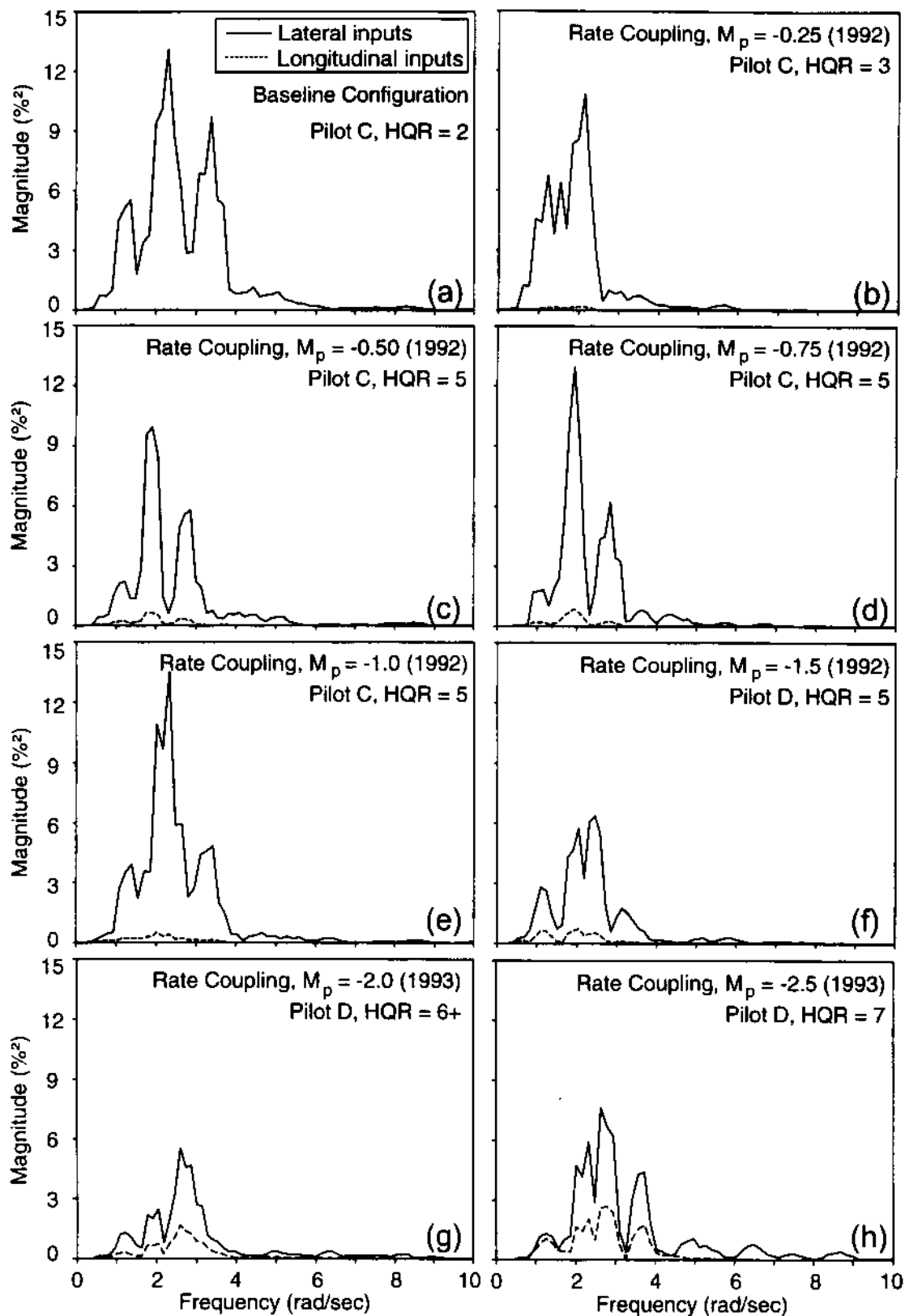


Figure 7.7. Representative power spectra of the control inputs for rate coupling configurations (data from 1992 and 1993 flight tests).

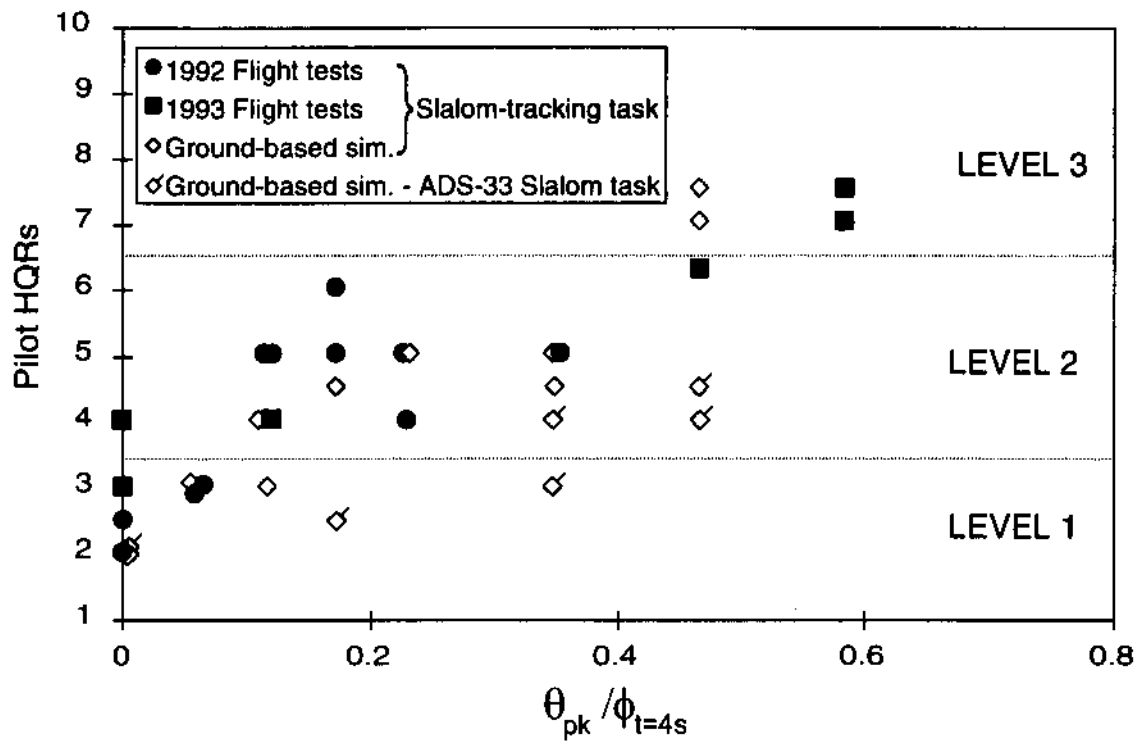


Figure 7.8. Comparison of the HQRs with the ADS-33C coupling parameter for two different slalom tasks with rate coupling configurations.

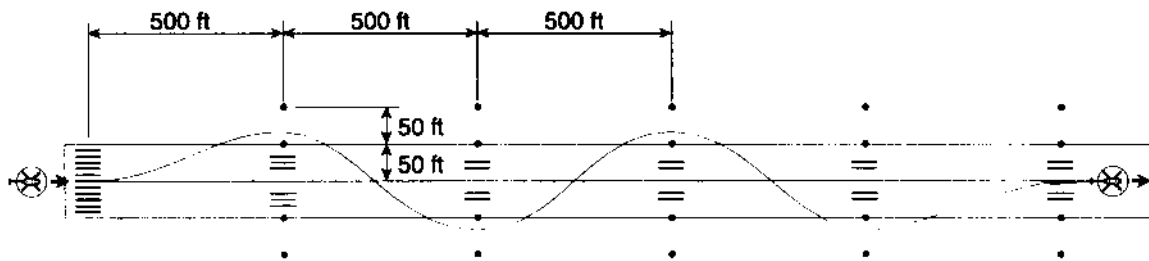


Figure 7.9. Modified ADS-33C slalom course (evaluated on the ground-based simulator only).

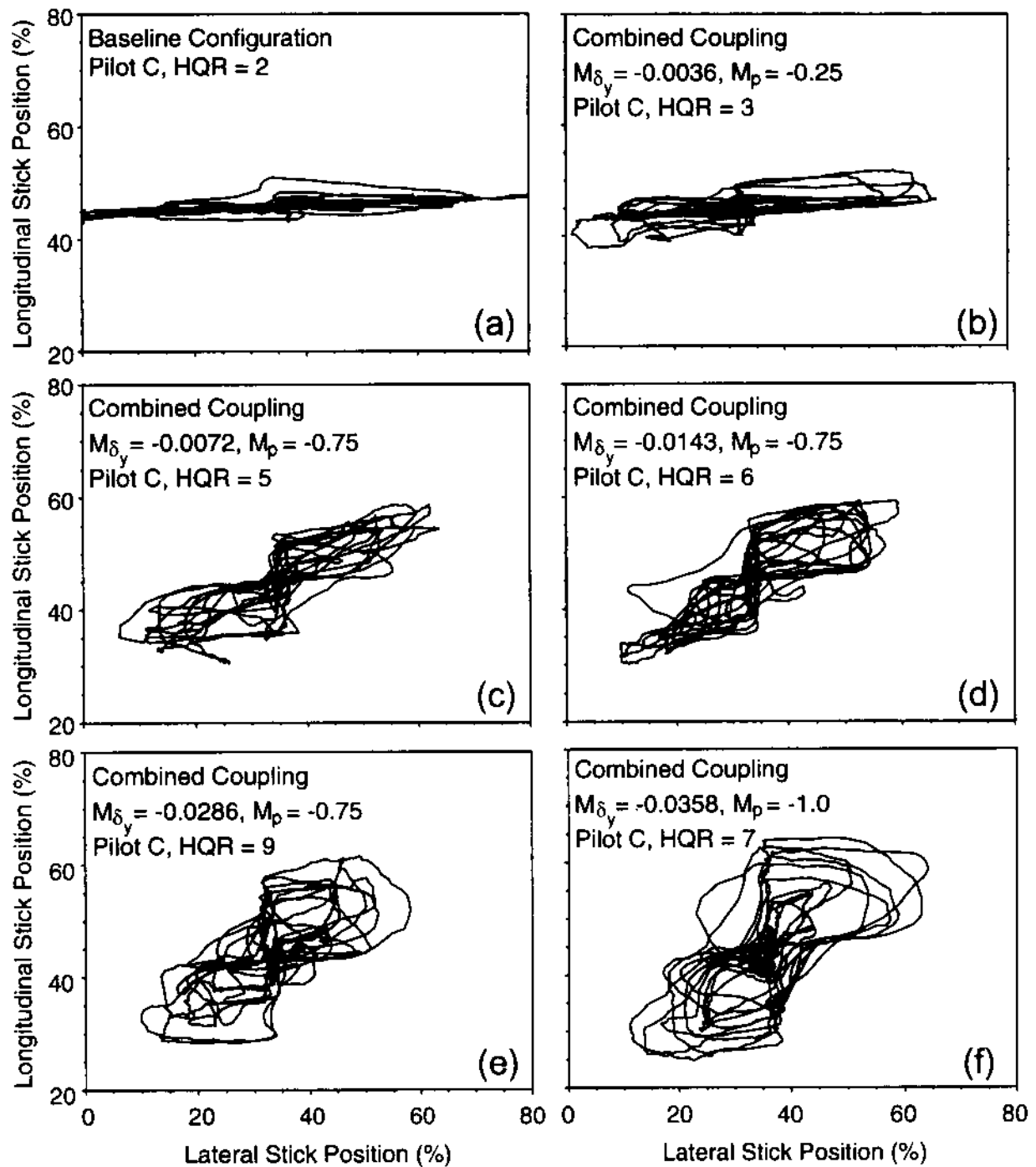


Figure 7.10. Representative control input positions for combined control-rate coupling configurations (data from 1992 flight tests).

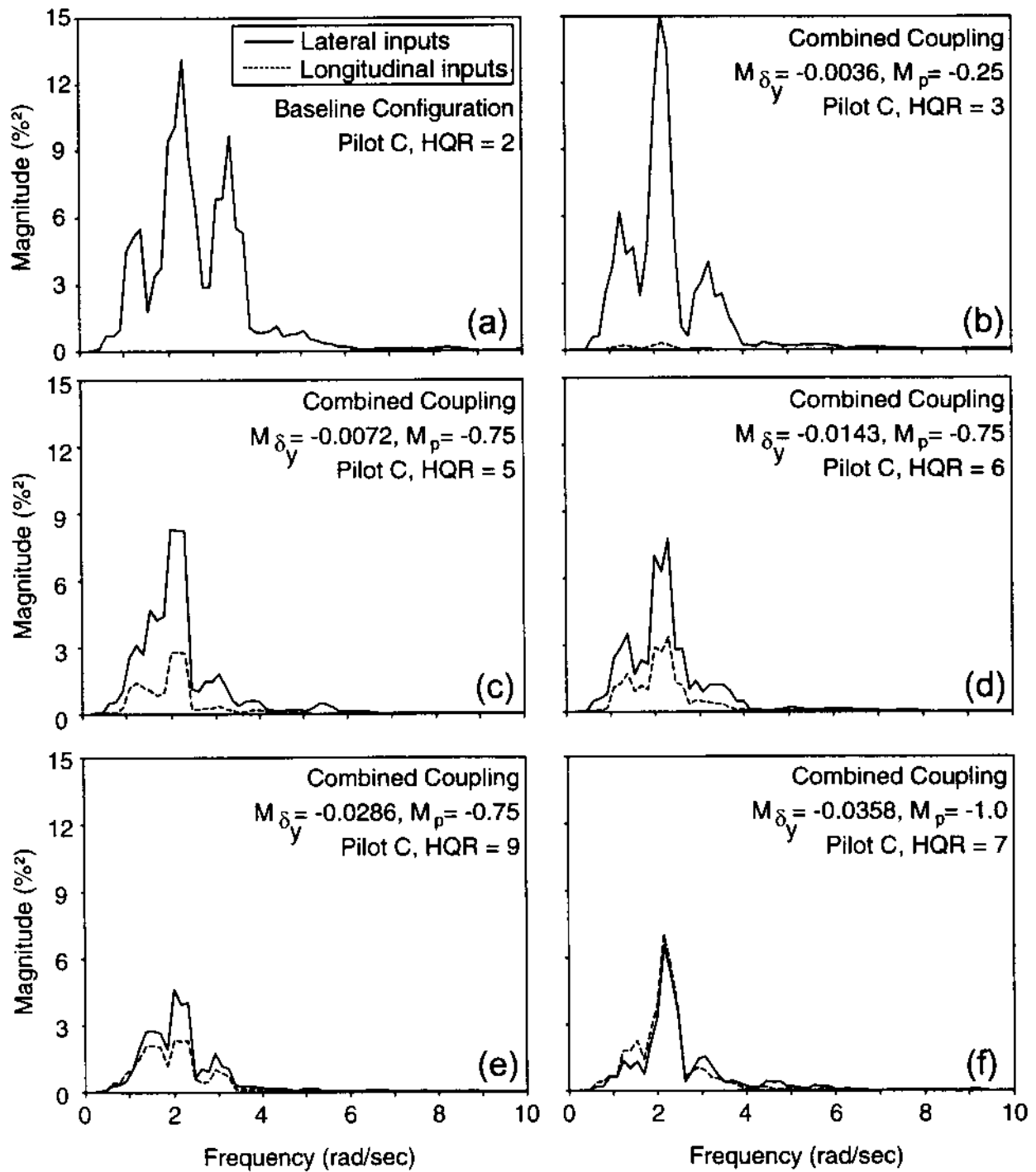


Figure 7.11. Representative power spectra of the control inputs for combined control-rate coupling configurations (data from 1992 flight tests).

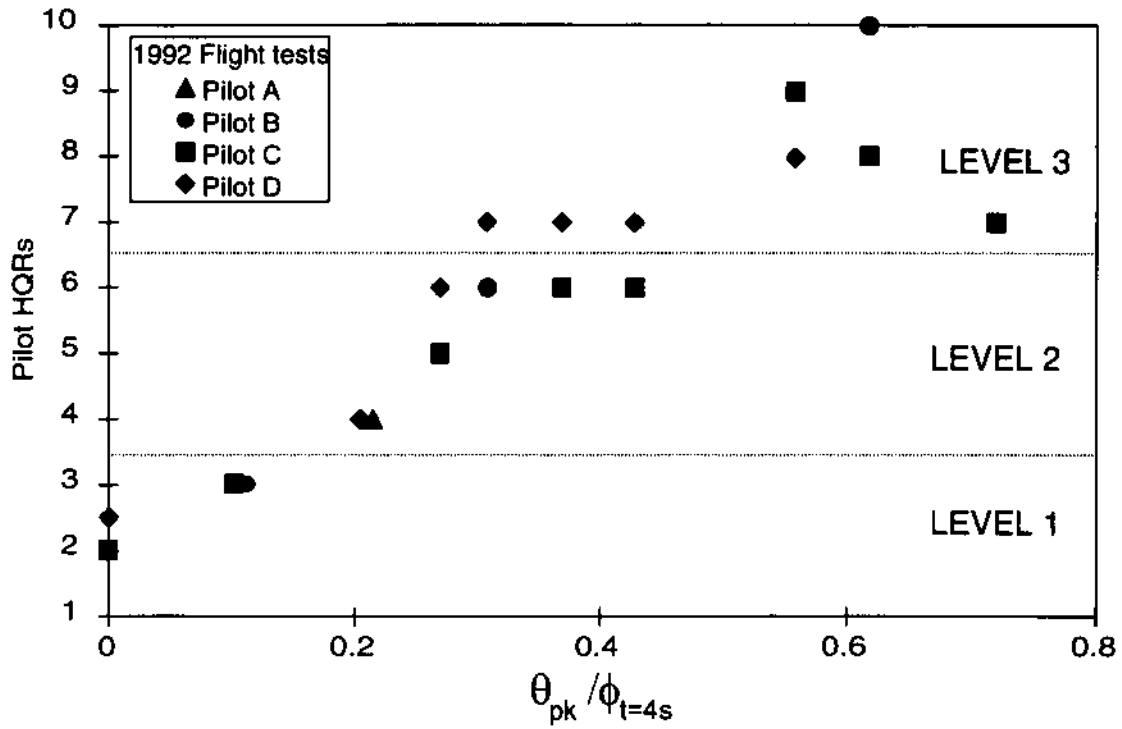


Figure 7.12. Comparison of the HQRs with the ADS-33C coupling parameters for combined control and rate coupling configurations.

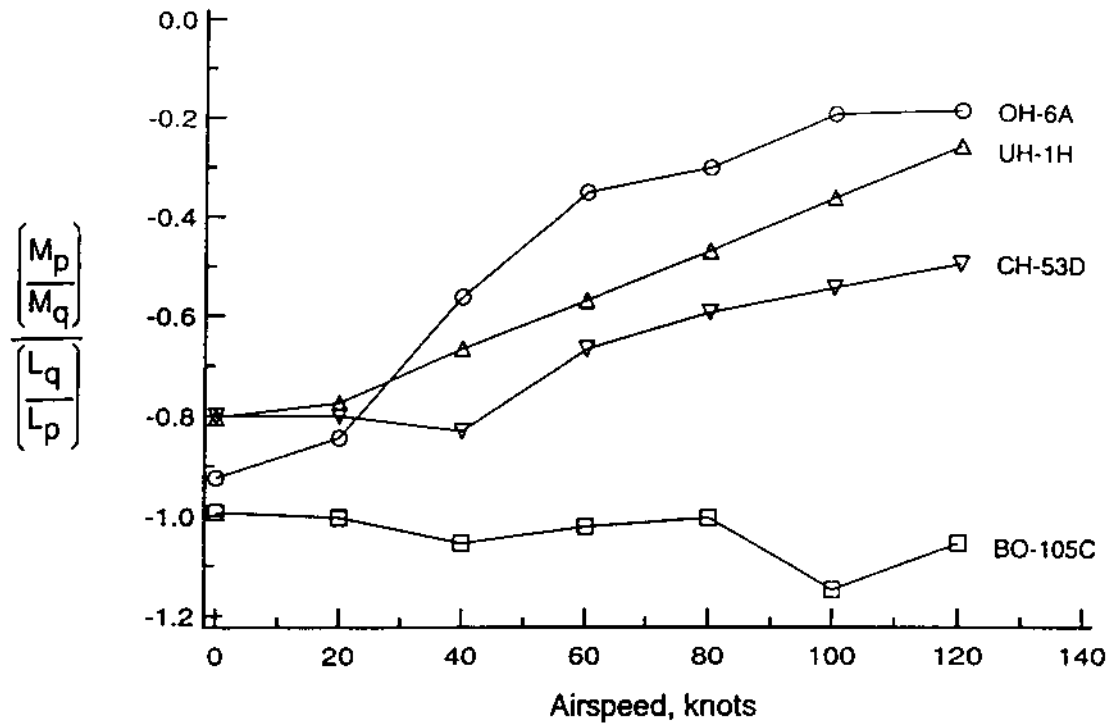


Figure 7.13. Ratio of off-to-on axis derivatives for several helicopters vs. airspeed (data from ref. 20).

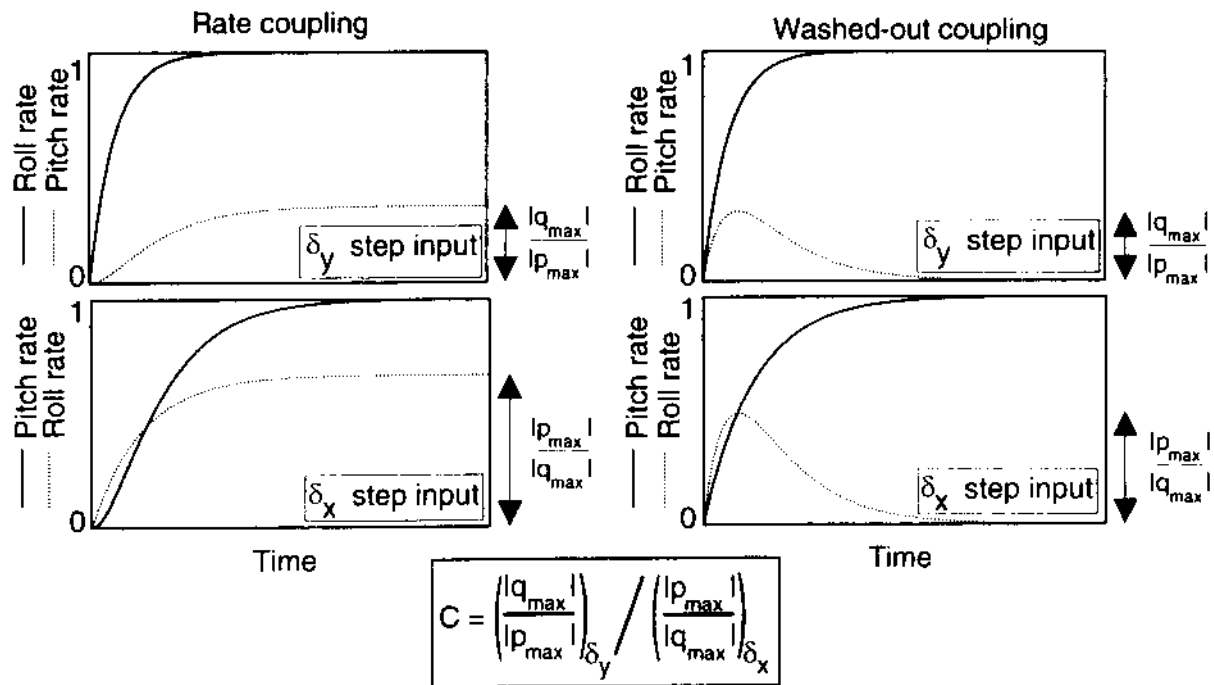


Figure 7.14. Definition of the off-to-on axis coupling ratio, C , for two examples.

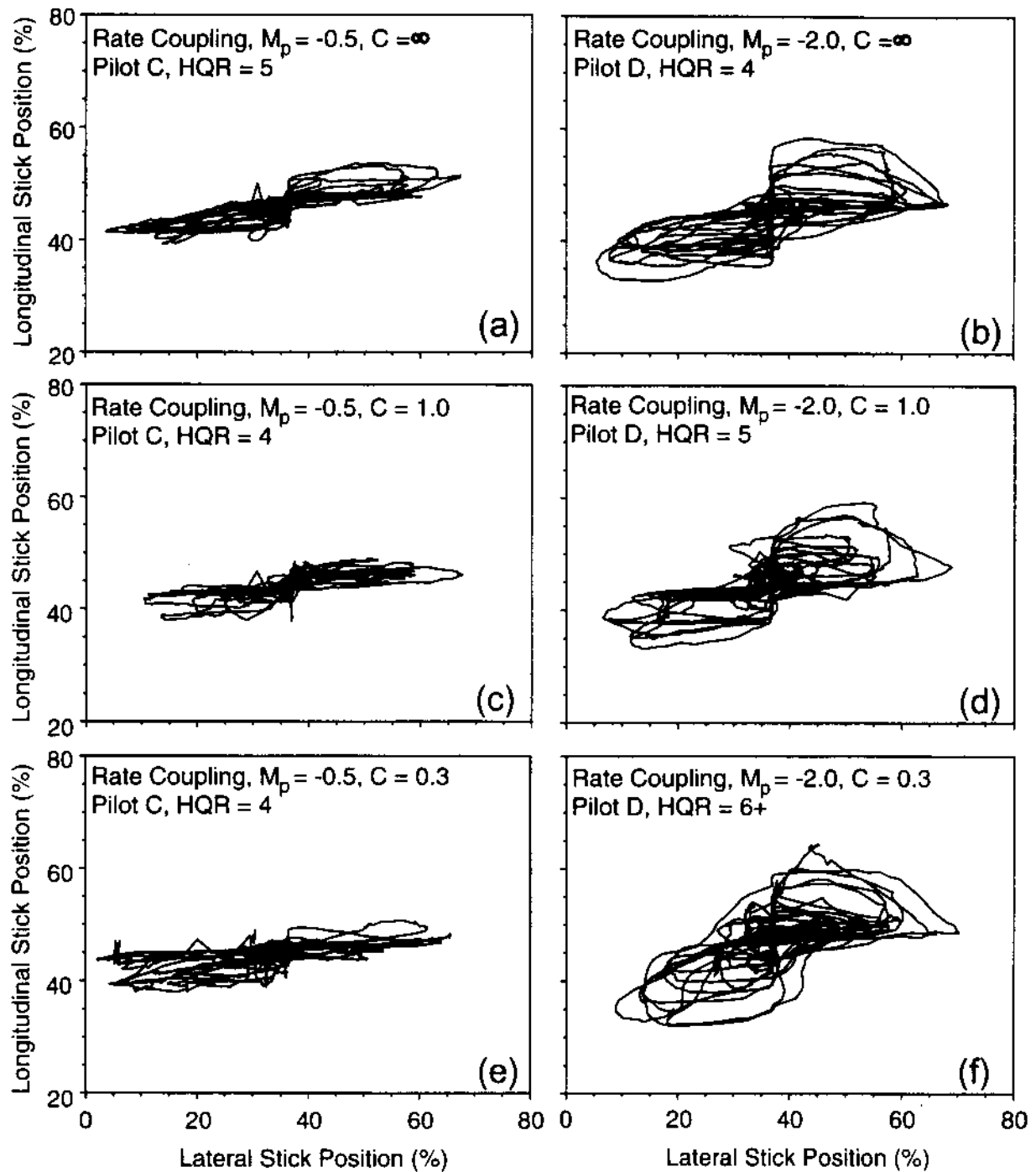


Figure 7.15. Control input positions for two rate coupling configurations with different amounts of off-to-on axis coupling ratios, C (data from 1993 flight tests).

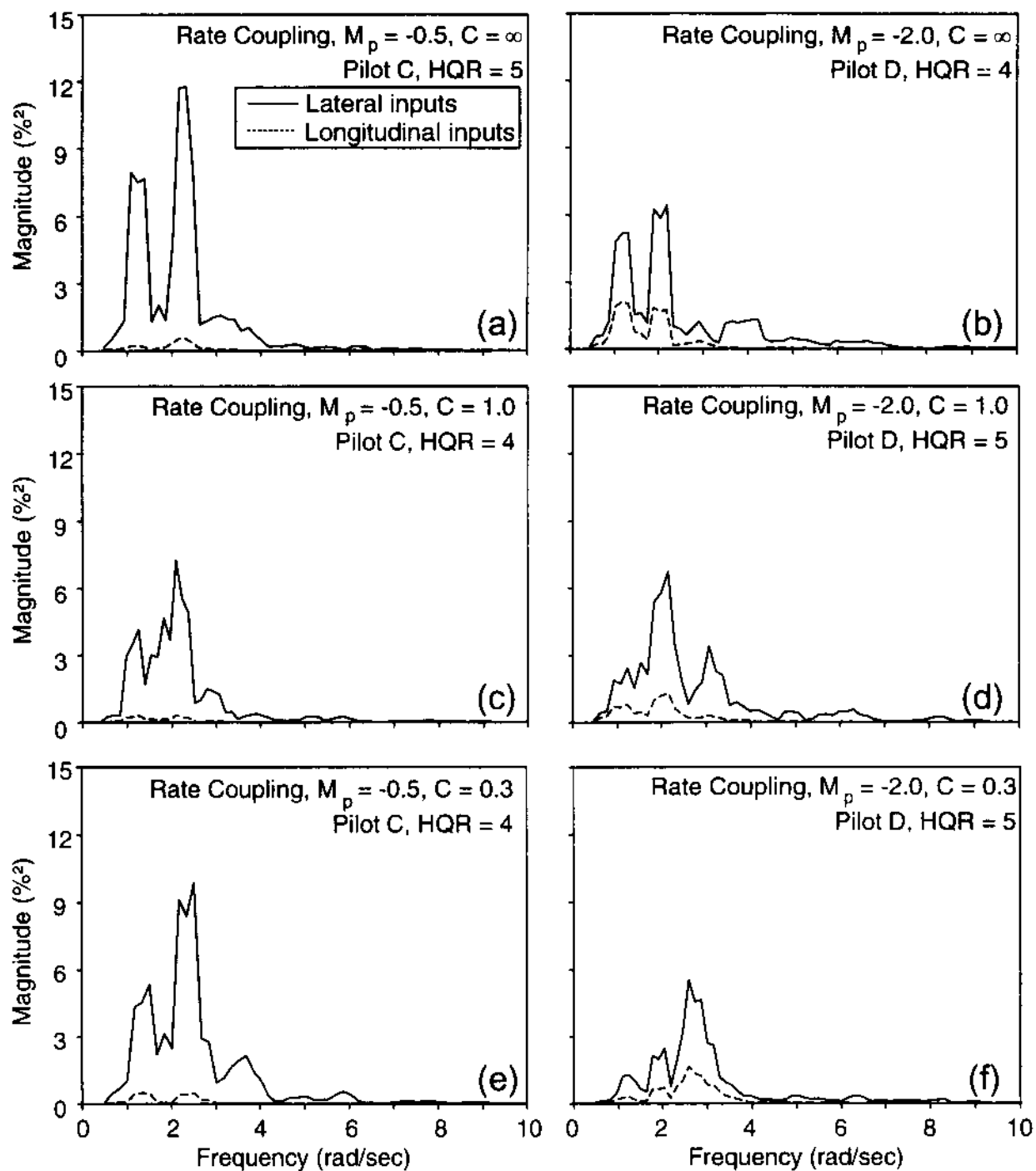


Figure 7.16. Power spectrum of the control inputs for typical rate coupling configurations with different amounts of off-to-on axis coupling ratios, C (data from 1993 flight tests).

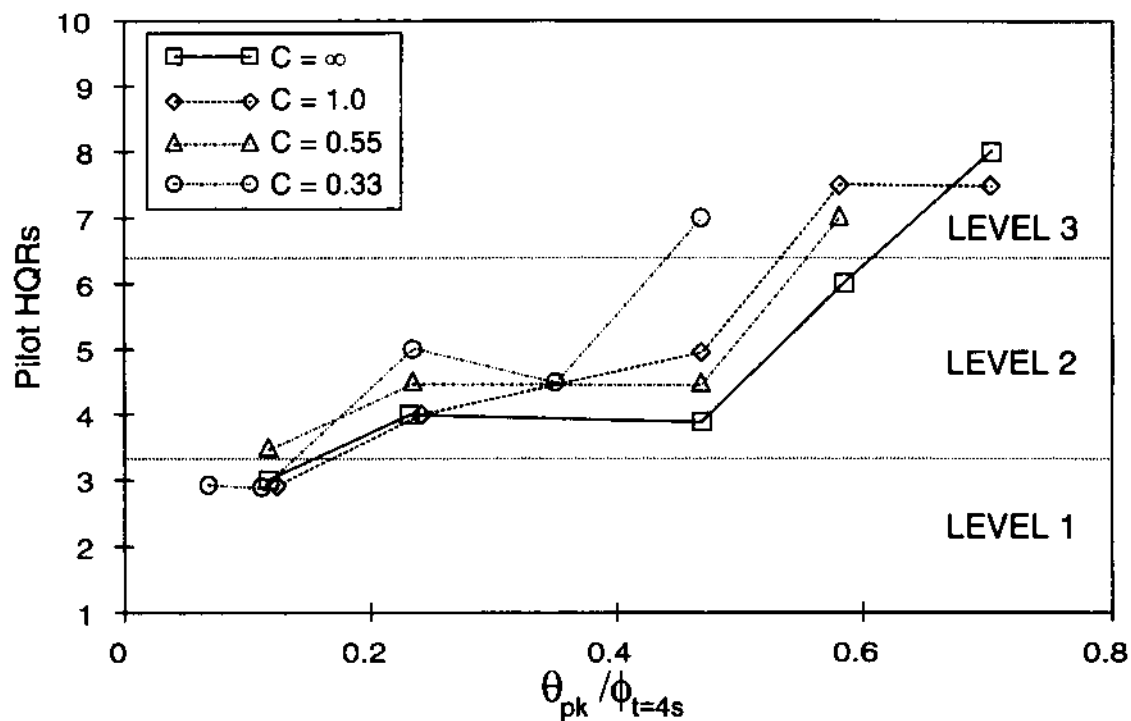


Figure 7.17. Comparison of the HQRs with the ADS-33C coupling parameters for cases with different off-to-on axis coupling ratios, C (data from fixed-base simulator).

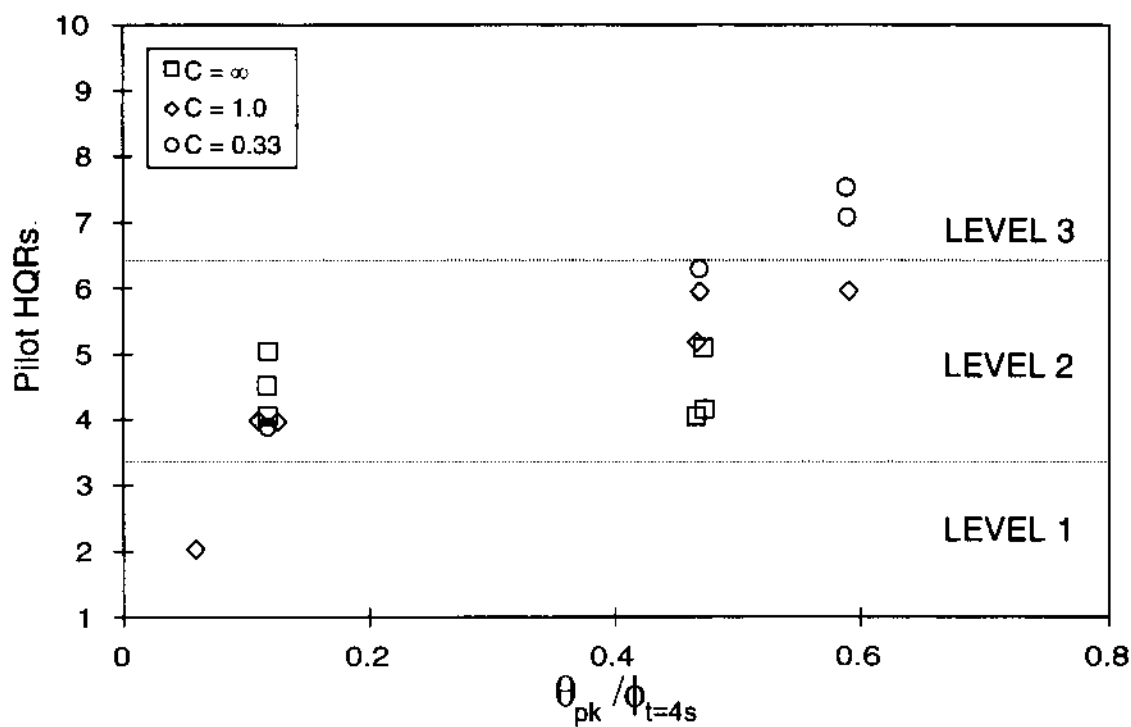


Figure 7.18. Comparison of the HQRs with the ADS-33C coupling parameter for cases with different off-to-on axis coupling ratios, C (data from 1993 flight tests).

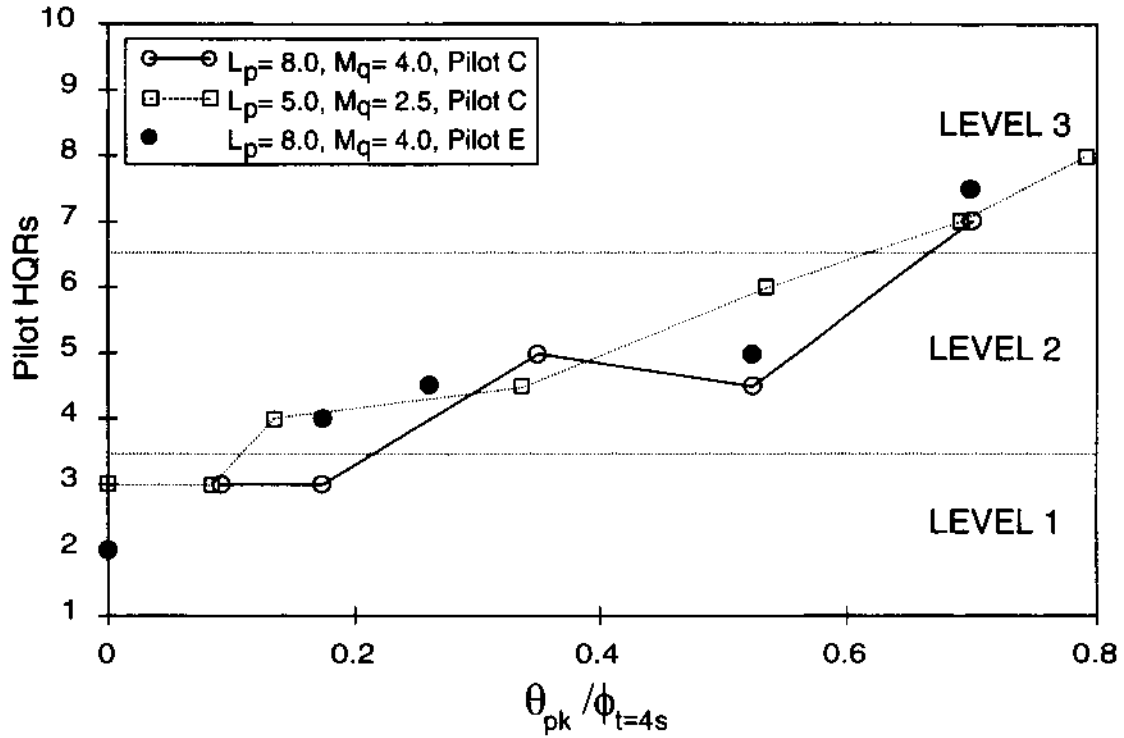


Figure 7.19. Comparison of the pilot HQRs with the ADS-33C coupling parameters for rate coupling configurations with different on-axis damping (fixed-base simulator data).

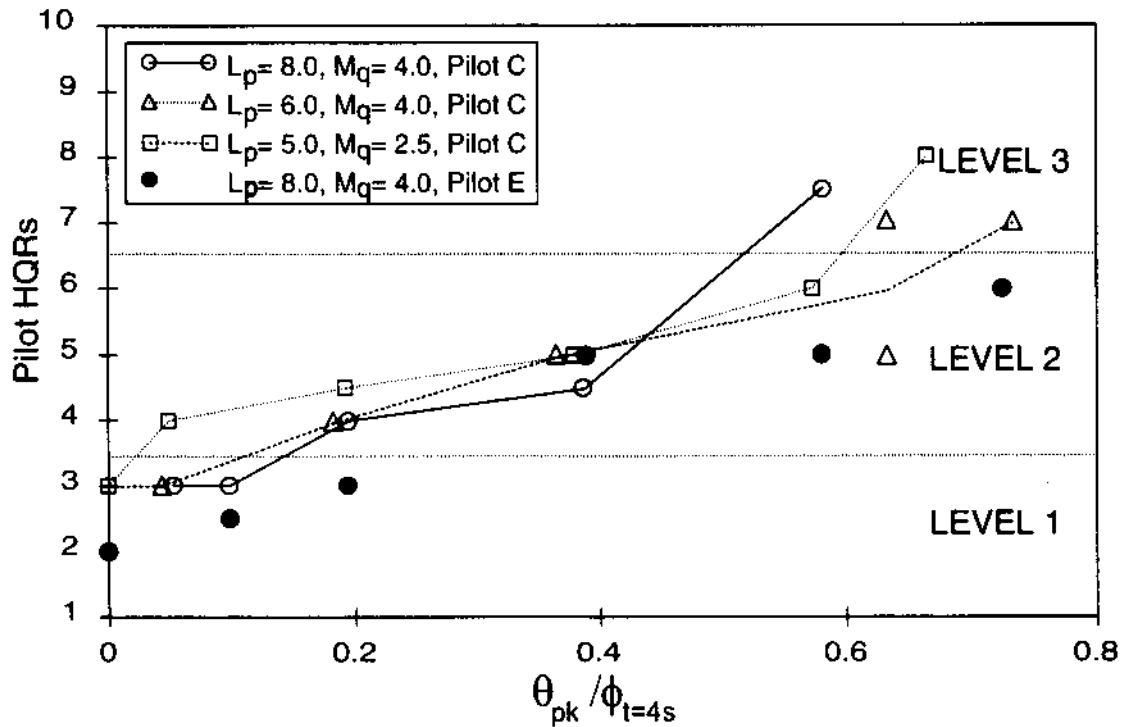


Figure 7.20. Comparison of the pilot HQRs with the ADS-33C coupling parameters for control coupling configurations with different on-axis damping (fixed-base simulator data).

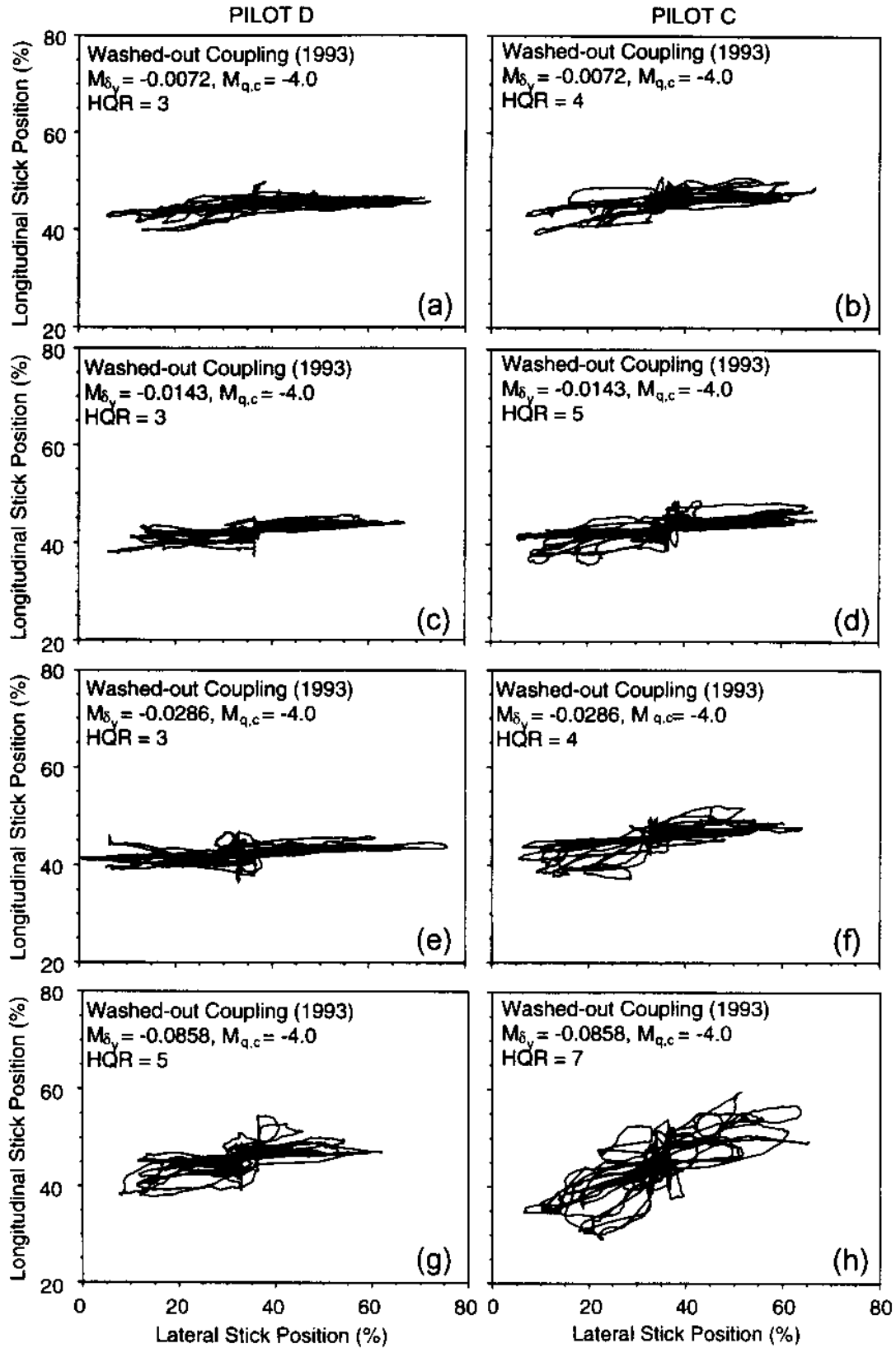


Figure 7.21. Control input positions for typical washed-out coupling configurations. All data for $M_{\delta_x}/L_{\delta_y} = -1.0$ and $M_{q,c} = -4.0 \text{ sec}^{-1}$, except for (a) which has $M_{\delta_x}/L_{\delta_y} = -1.8$ (data from 1993 flight tests).

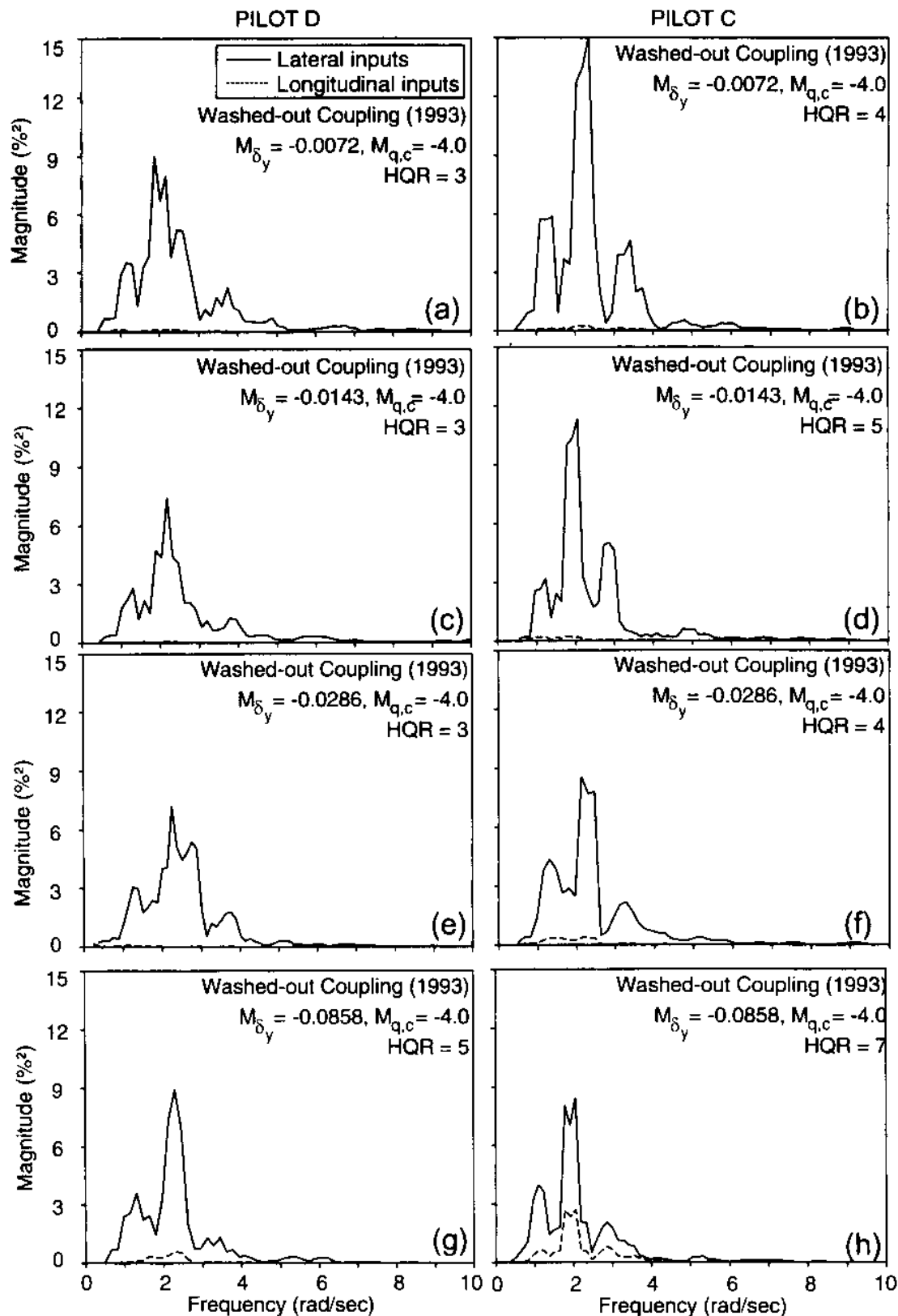


Figure 7.22. Power spectrum of the control inputs for typical washed-out coupling configurations. All data for $M_{\delta_x}/L_{\delta_y} = -1.0$ and $M_{q,c} = -4.0 \text{ sec}^{-1}$, except for (a) which has $M_{\delta_x}/L_{\delta_y} = -1.8$ (data from 1993 flight tests).

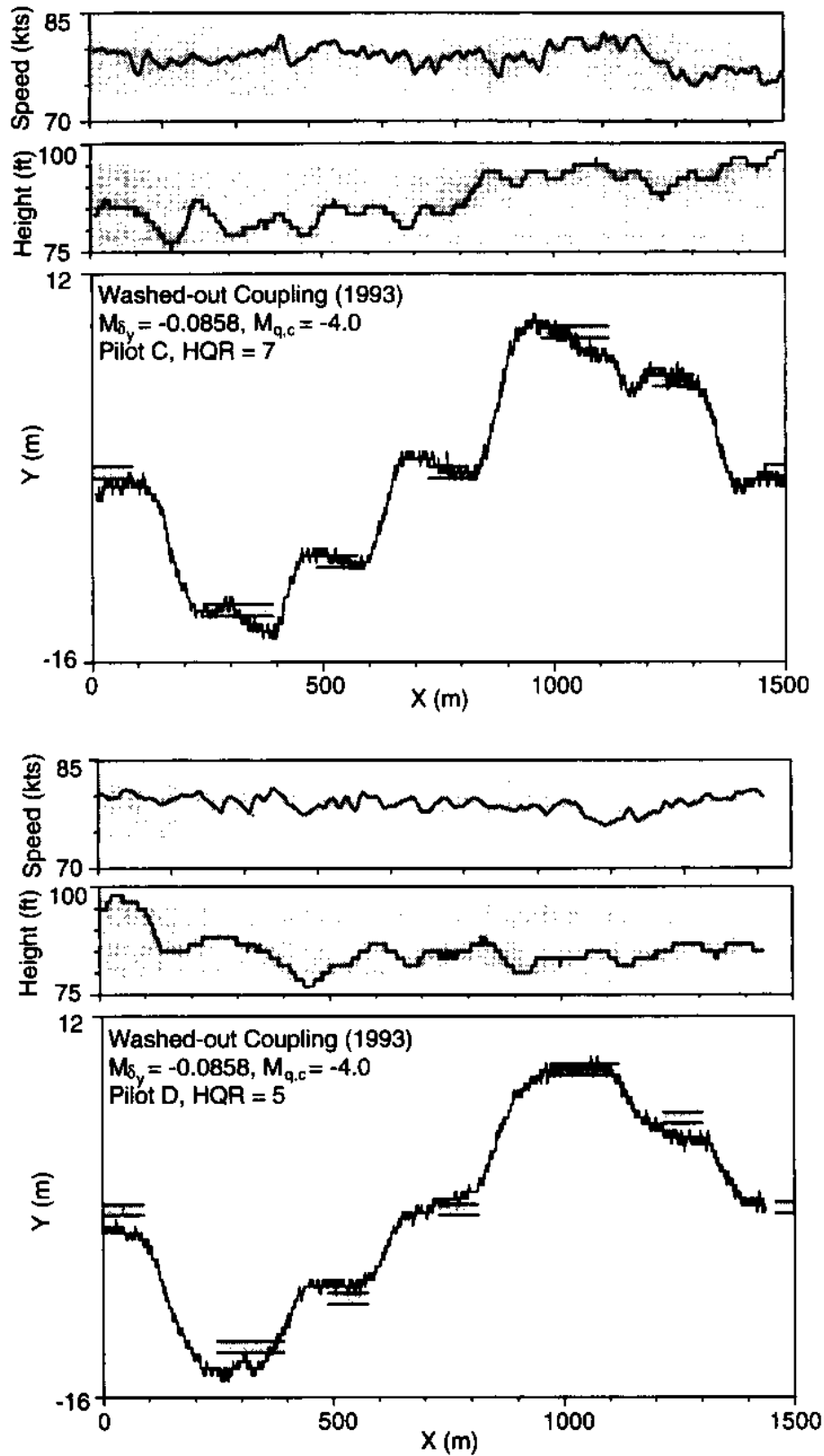


Figure 7.23. Comparison of the task performance of pilots C and D for a washed-out coupling configuration (data from 1993 flight tests).

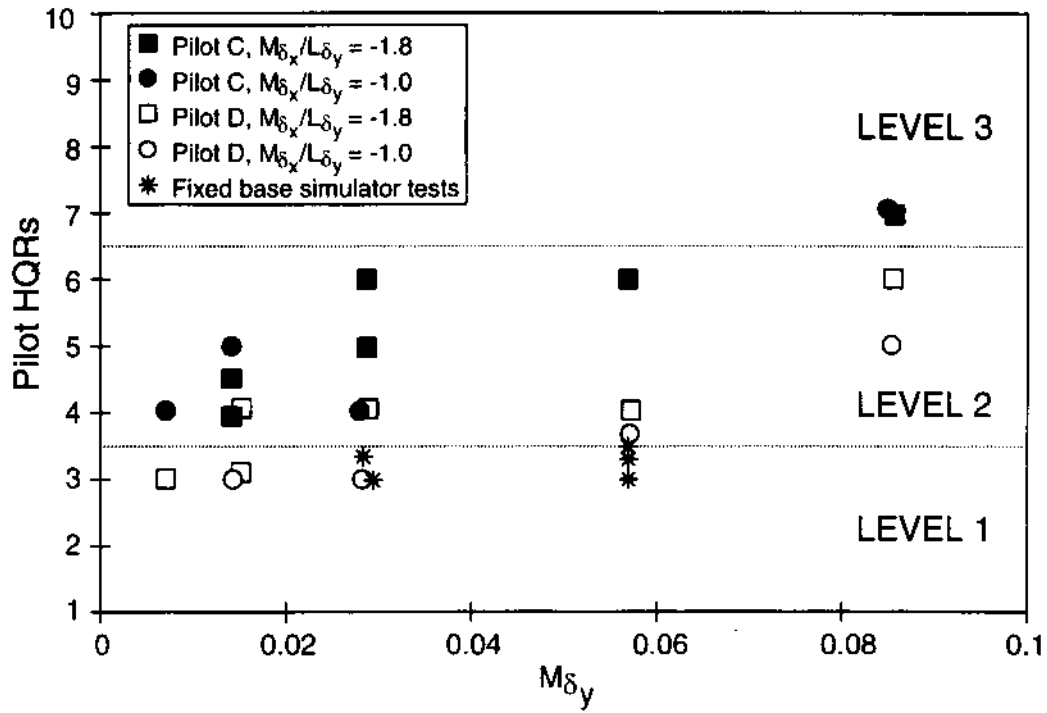


Figure 7.24. Pilot ratings vs. M_{δ_y} for the washed-out coupling configurations with $M_{q,c} = -4.0 \text{ sec}^{-1}$.

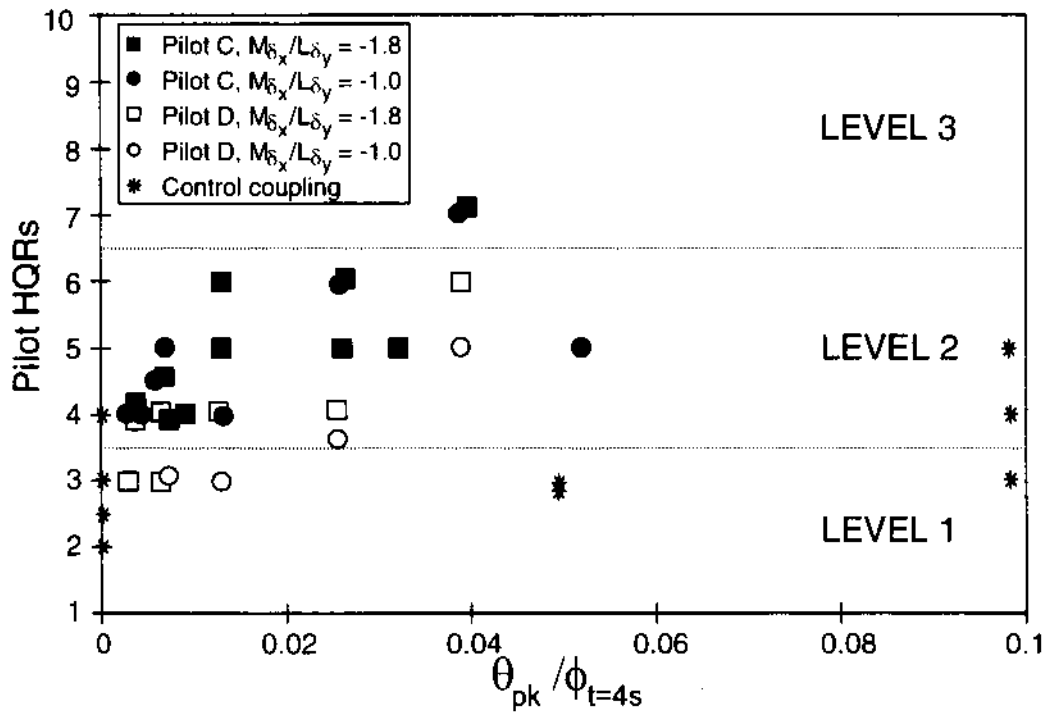


Figure 7.25. Comparison of the HQRs with the ADS-33C coupling parameters for washed-out coupling configurations.

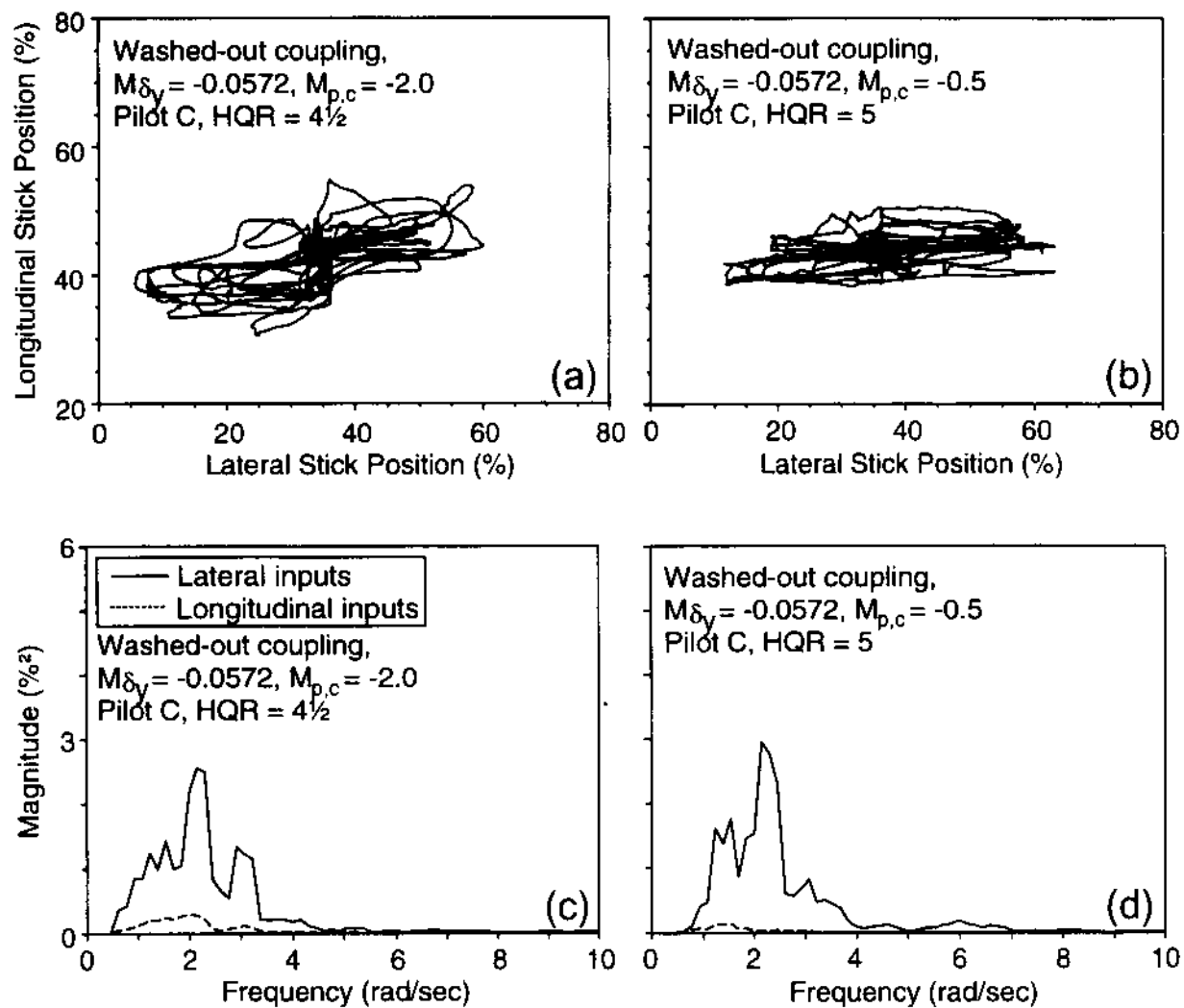


Figure 7.26. Control input positions and power spectra for the washed-out coupling configuration with $L_{p,c} = M_{q,c}$ (data from 1993 flight tests).

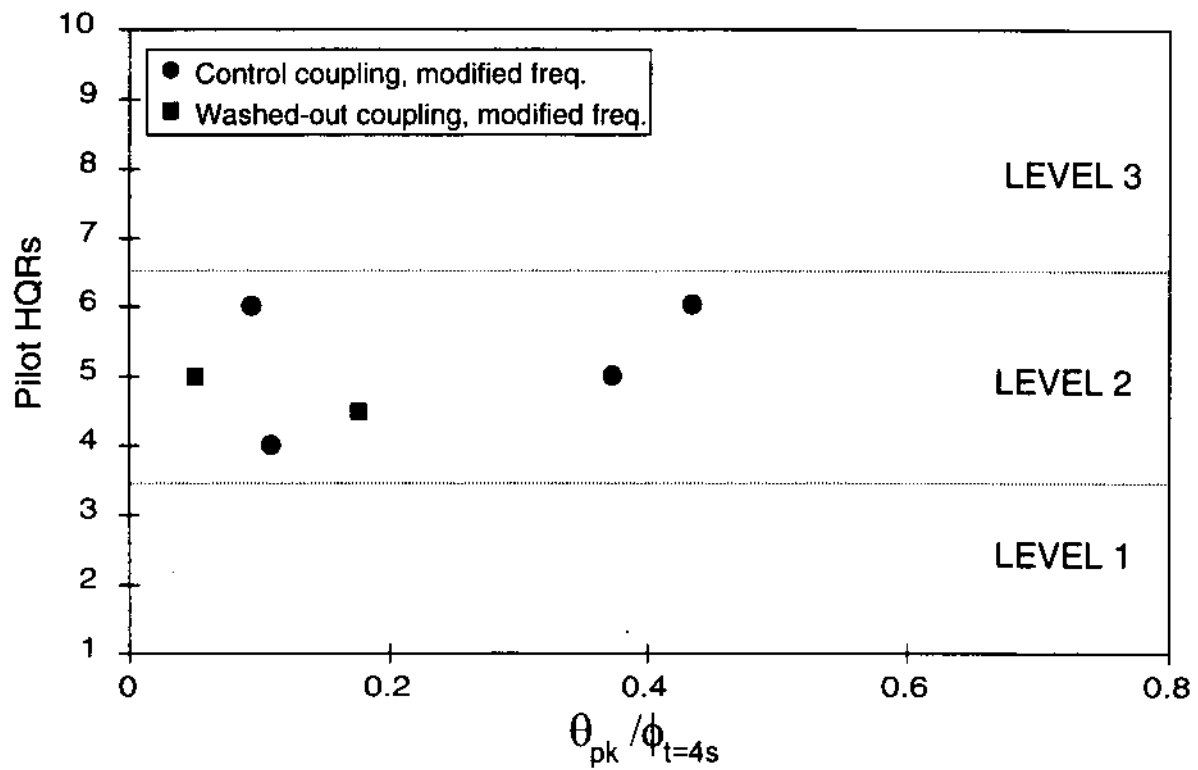


Figure 7.27. Comparison of the HQRs with the ADS-33C coupling parameters for control coupling and washed-out coupling configurations with modified frequency characteristics.

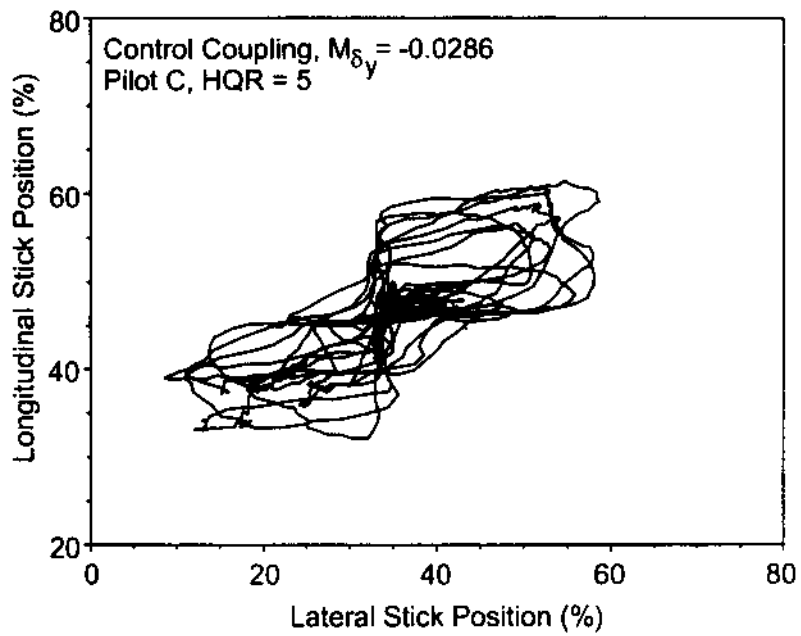


Figure 8.1. Typical figure eight cyclic control path for a control coupling configuration.

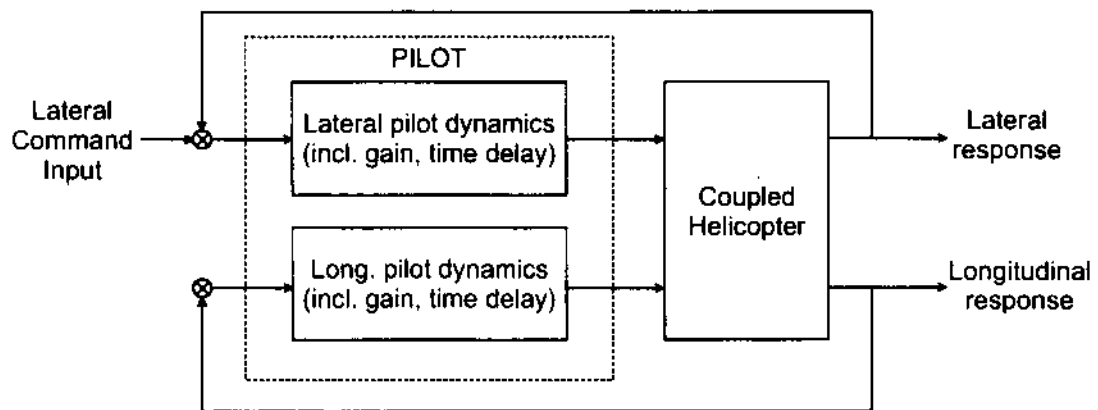


Figure 8.2. Simplified model of the pilot as a two-axis single loop feedback system.

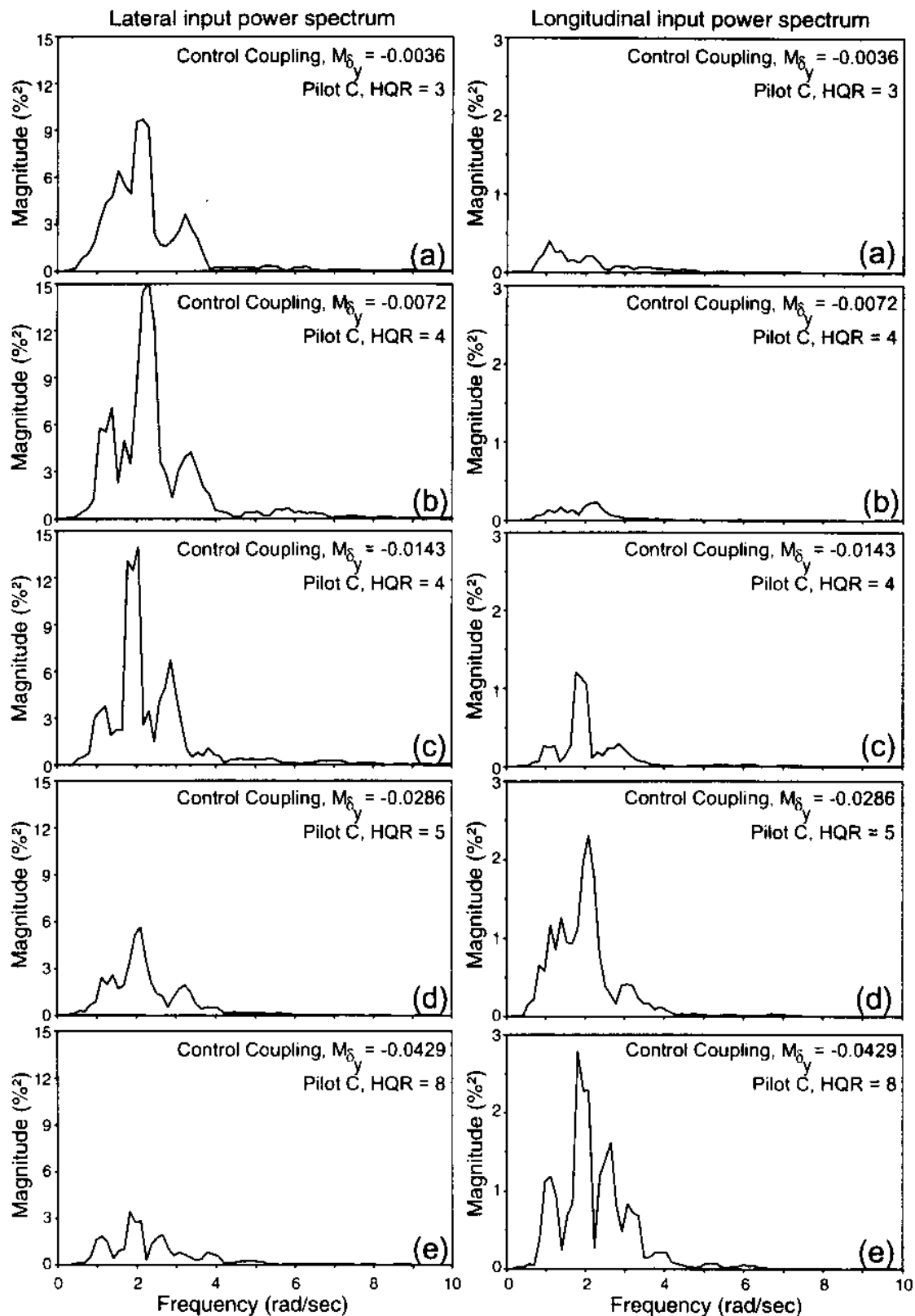


Figure 8.3. Lateral and longitudinal power spectra for selected control coupling configurations (notice differences in scale between lateral and longitudinal spectra; data from the 1992 flight tests).

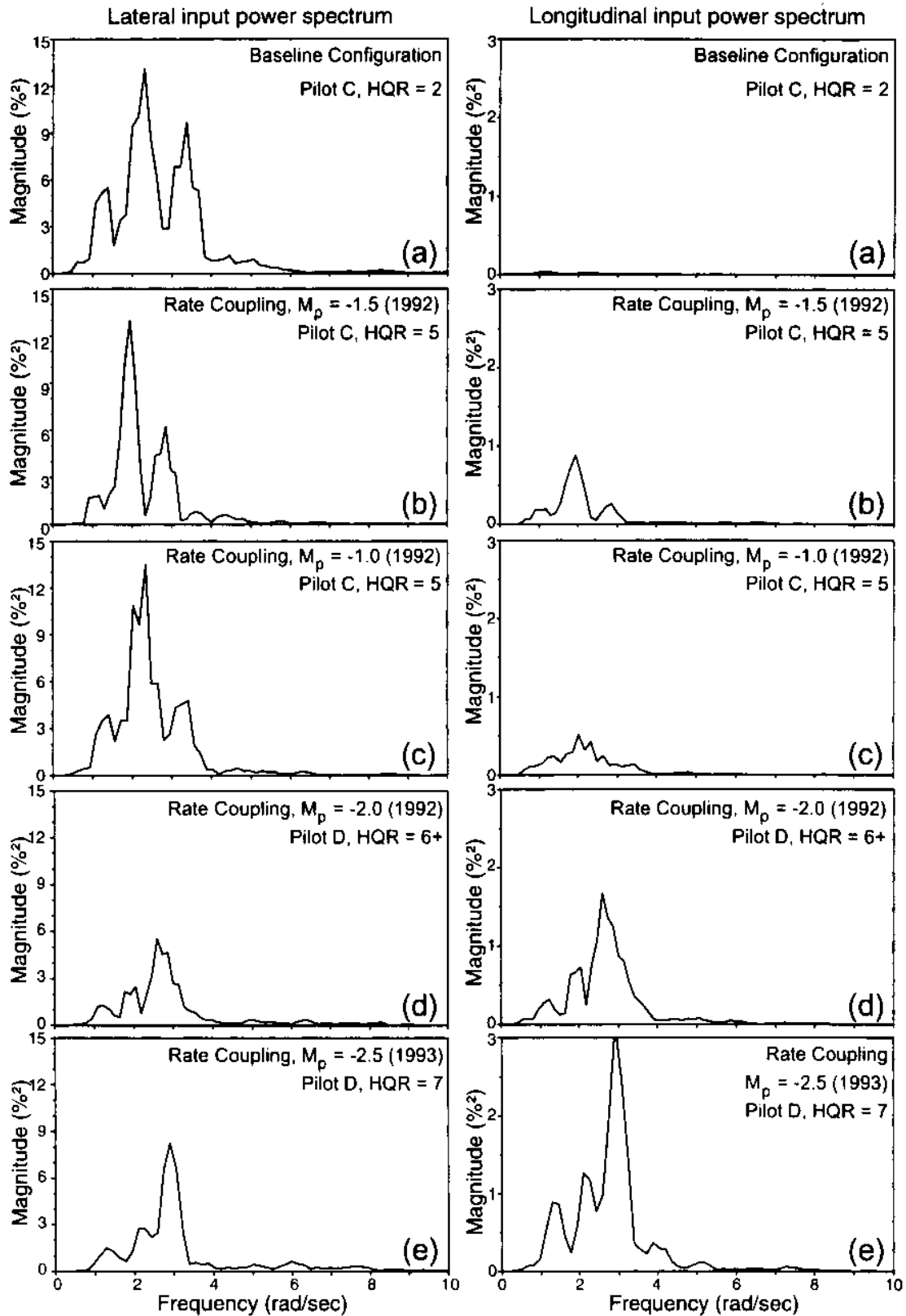


Figure 8.4. Lateral and longitudinal power spectra for selected rate coupling configurations (notice differences in scale between lateral and longitudinal spectra; data from flight tests).

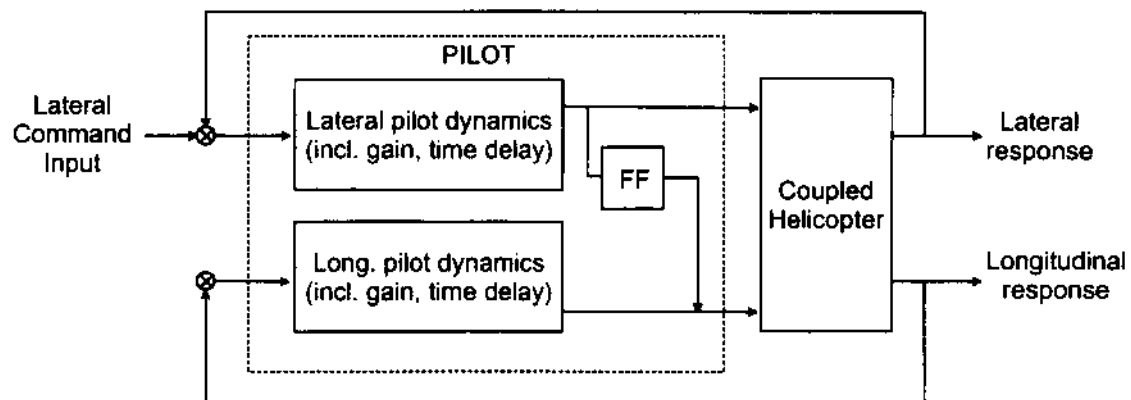


Figure 8.5. Simplified model of the pilot using a feedforward control strategy.

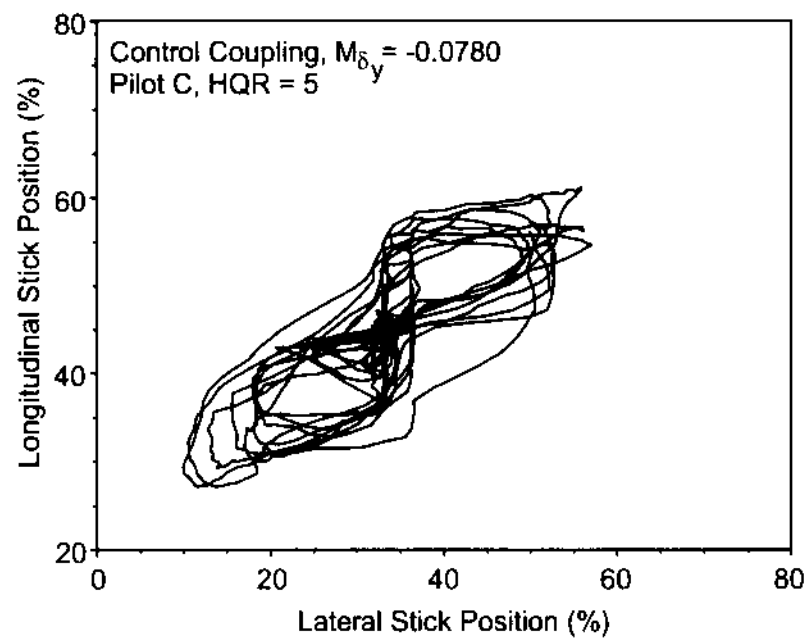


Figure 8.6. Typical cyclic control crossplot for diagonalized inputs.

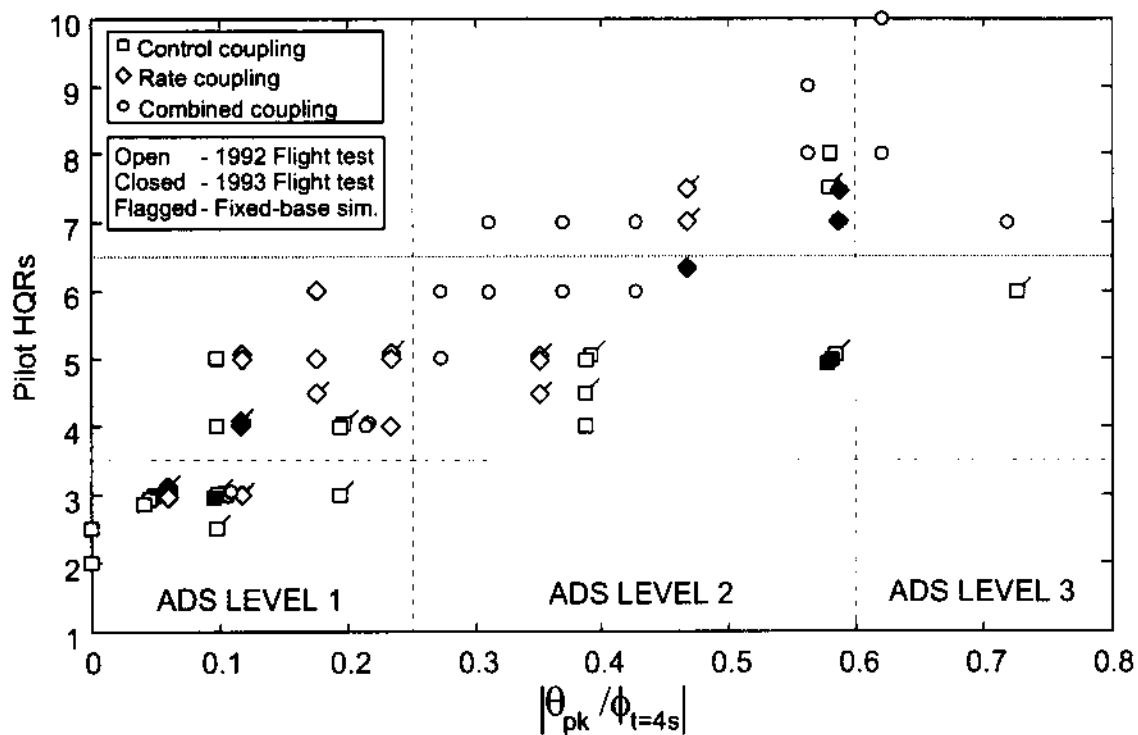


Figure 8.7. Four-second ADS-33C time domain coupling parameters vs. individual pilot ratings for the control, rate, and combined coupling cases with an L_q/M_p and/or $L_{\delta_x}/M_{\delta_y}$ ratio close to that of the BO 105.

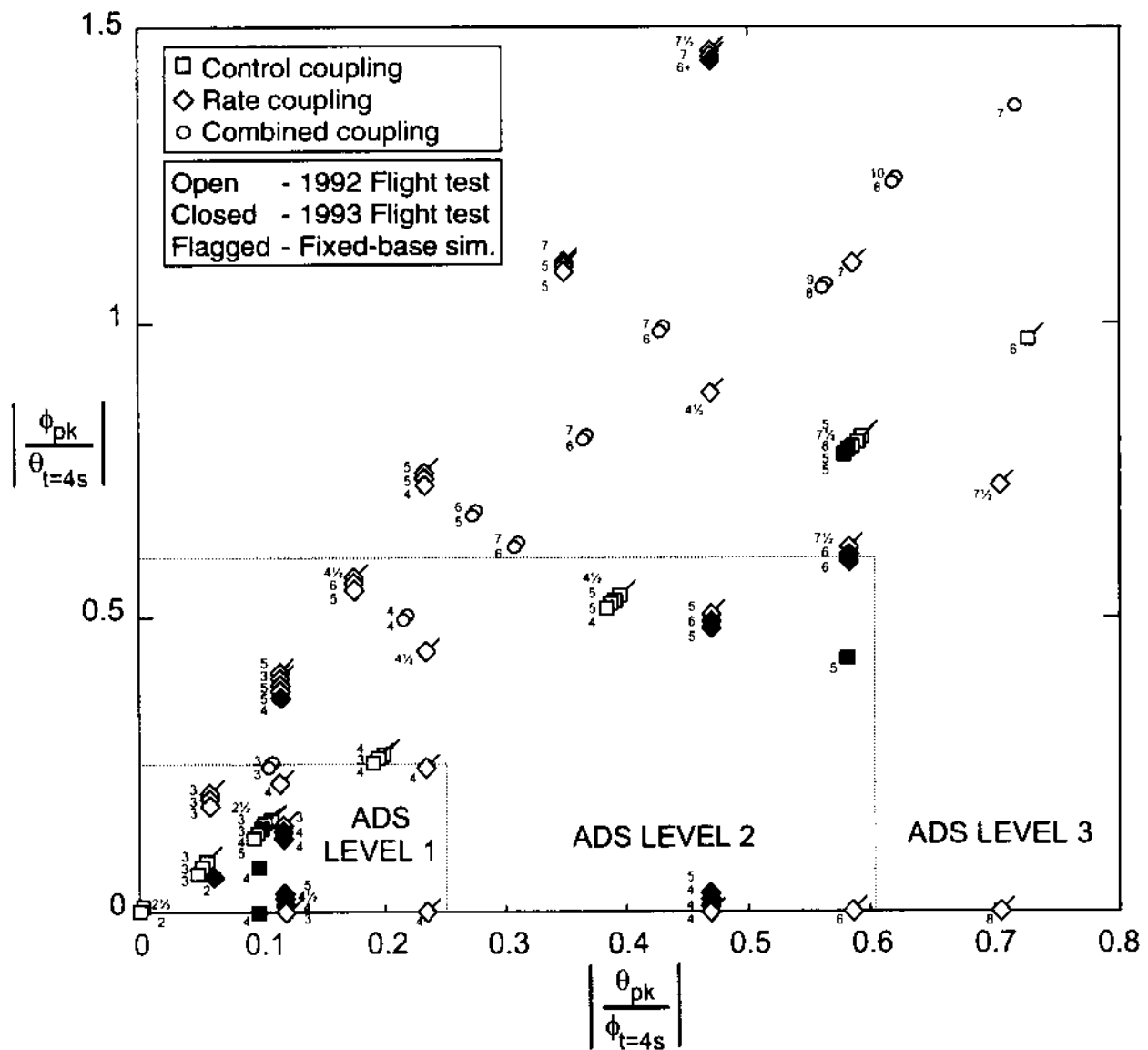


Figure 8.8. Two-sided representation of the ADS-33C time domain coupling parameters for all control, rate, and combined coupling cases. Individual pilot ratings and the ADS-33C level boundaries are shown.

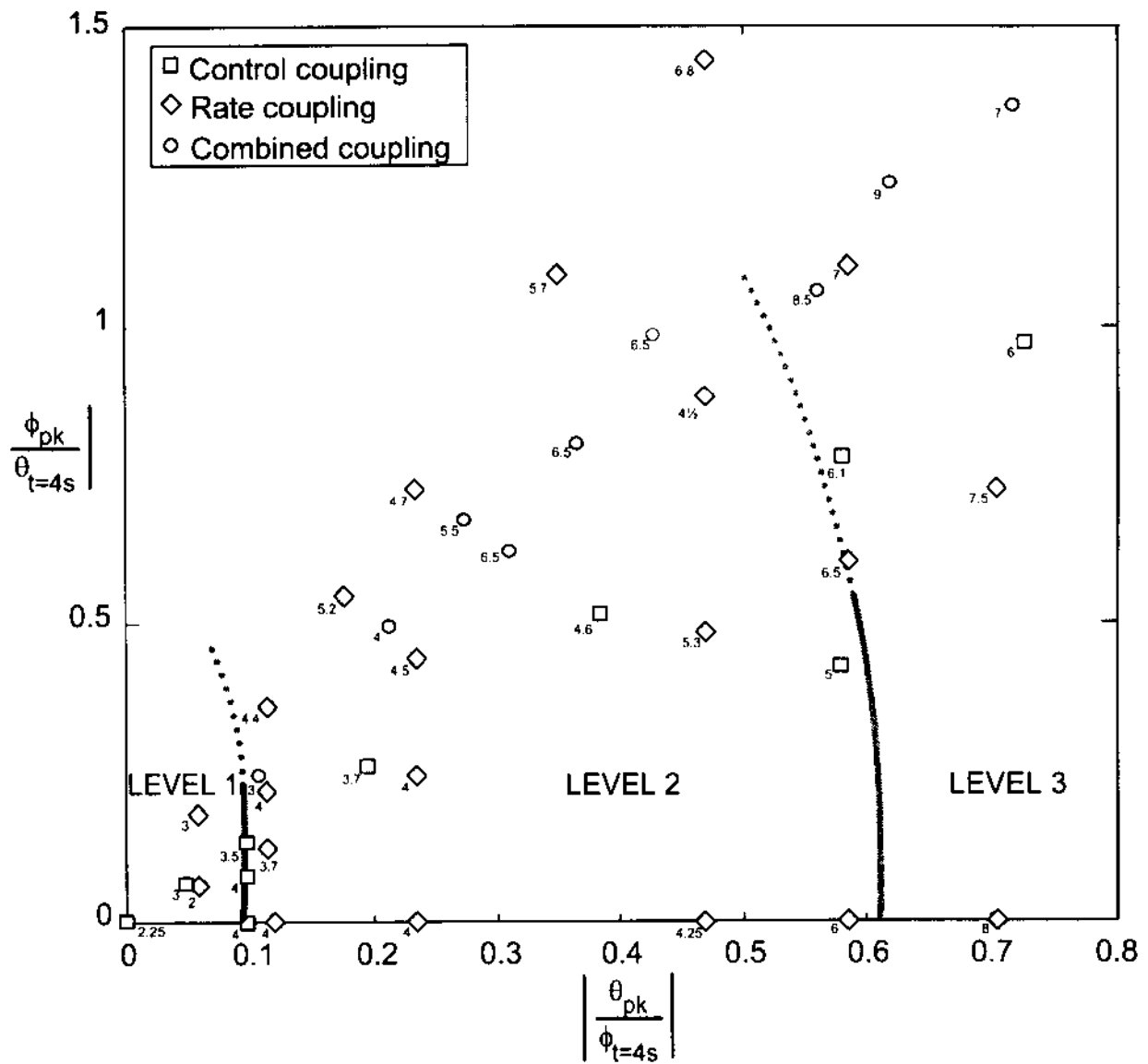


Figure 8.9. Two-sided representation of the ADS-33C time domain coupling parameters for all control, rate, and combined coupling cases. Averaged HQRs and suggested level boundaries are shown.

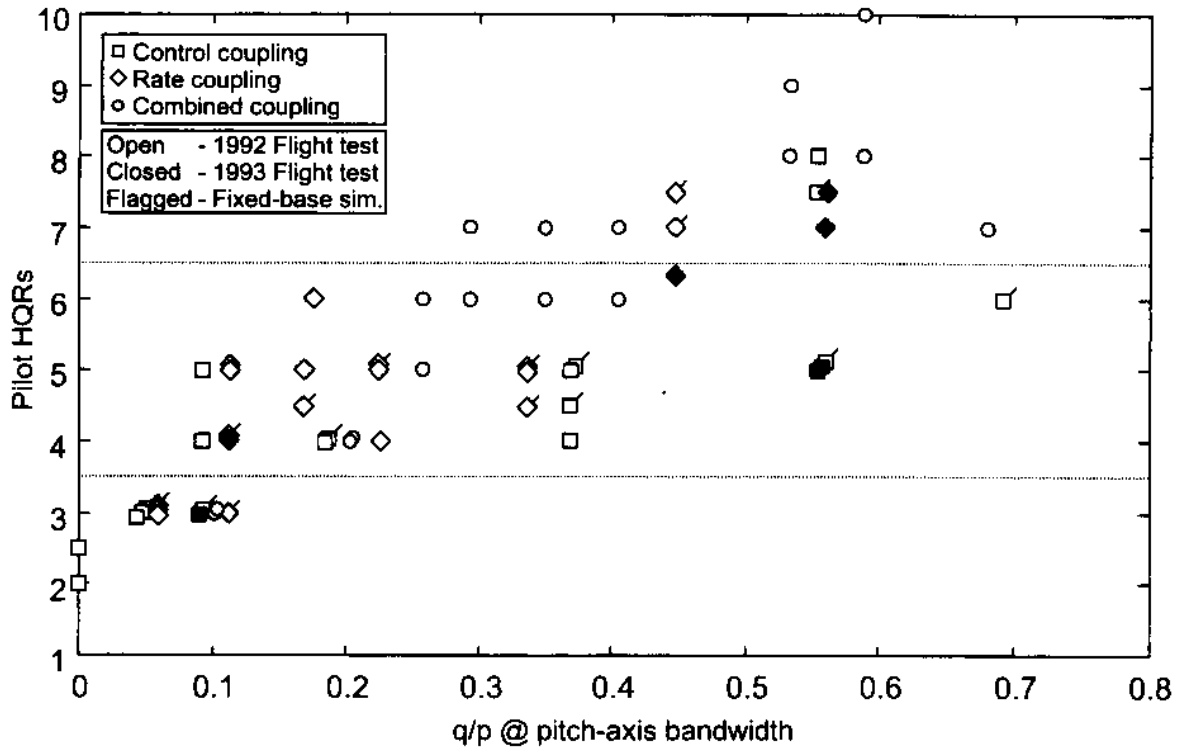


Figure 8.10. Magnitude of q/p at the pitch bandwidth frequency vs. individual pilot ratings for the control, rate, and combined coupling cases with an L_q/M_p and/or $L_{\delta_x}/M_{\delta_y}$ ratio close to that of the BO 105.

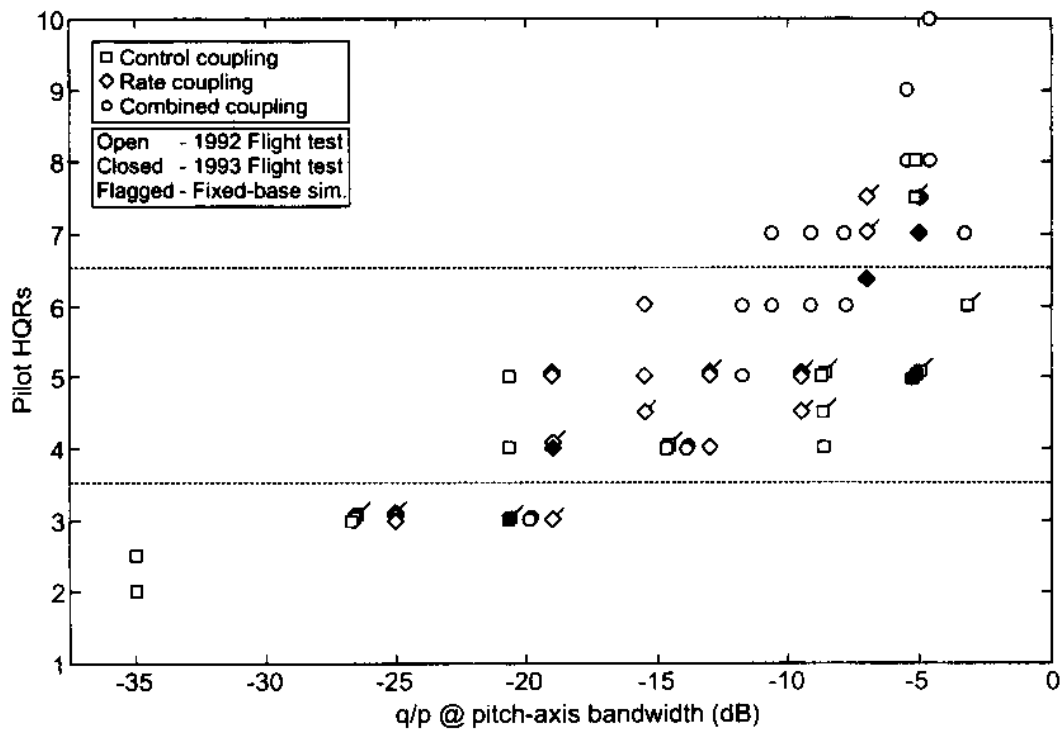


Figure 8.11. Magnitude (in decibels) of q/p at the pitch bandwidth frequency vs. individual pilot ratings for the control, rate, and combined coupling cases of figure 8.10.

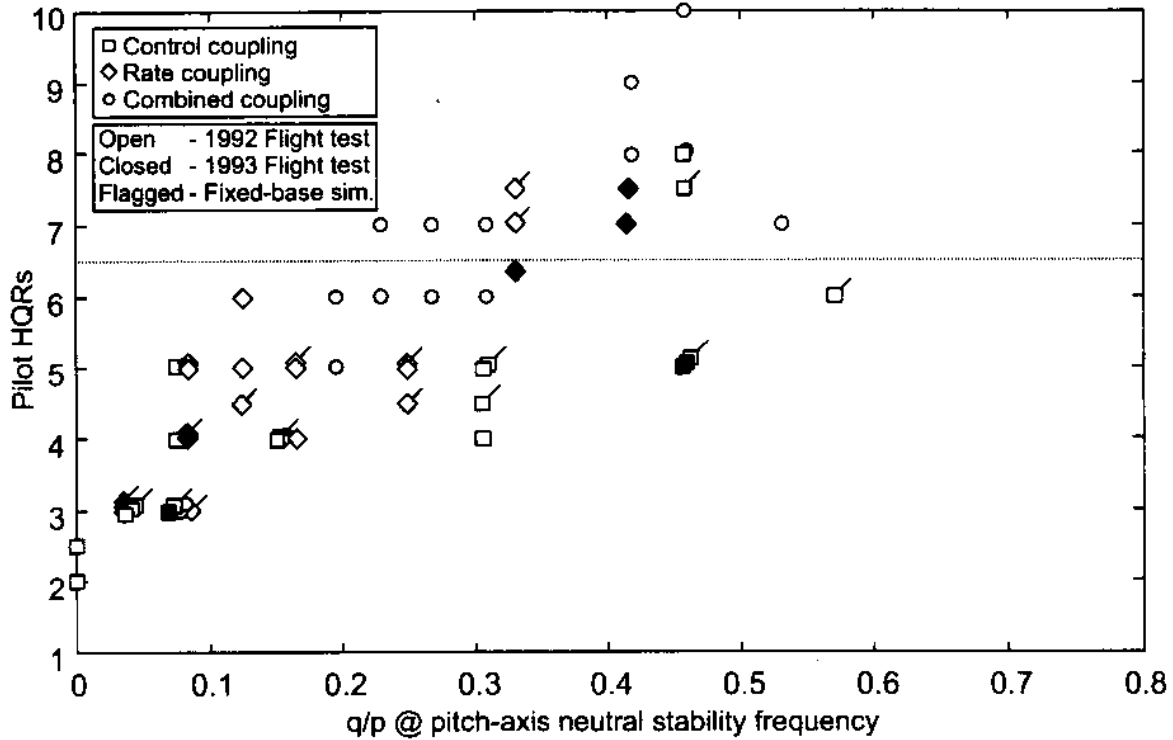


Figure 8.12. Magnitude of q/p at the pitch neutral stability frequency vs. individual pilot ratings for the control, rate, and combined coupling cases with an L_q/M_p and/or $L_{\delta_x}/M_{\delta_y}$ ratio close to that of the BO 105.

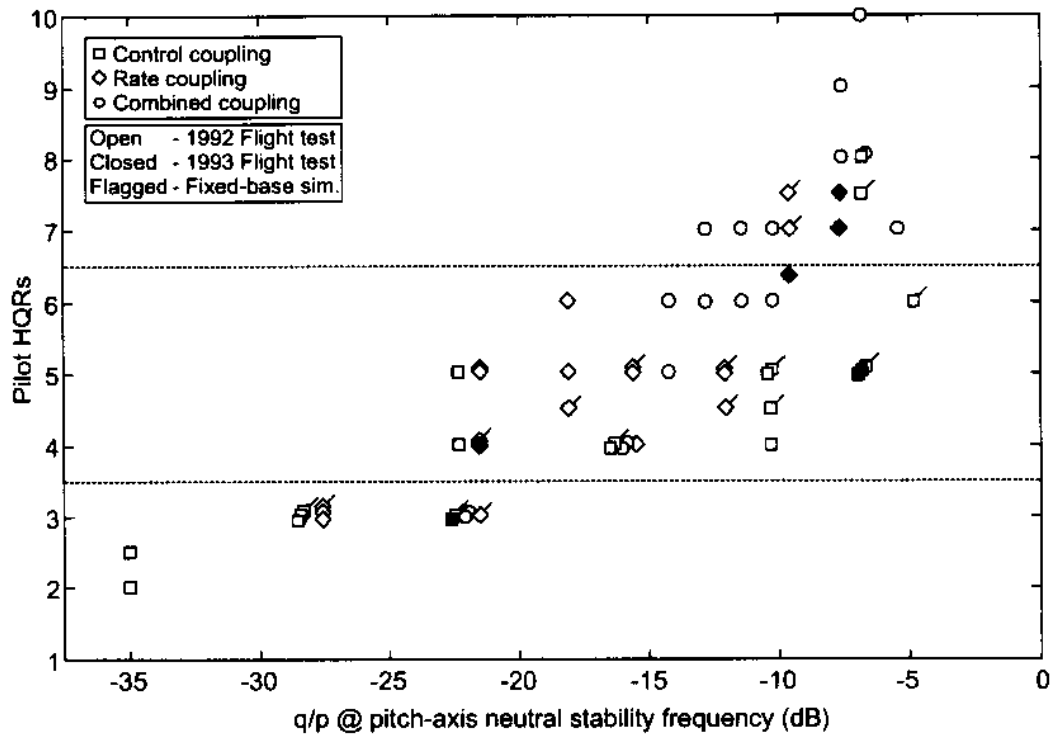


Figure 8.13. Magnitude (in decibels) of q/p at the pitch neutral stability frequency vs. individual pilot ratings for the control, rate, and combined coupling cases of figure 8.12.

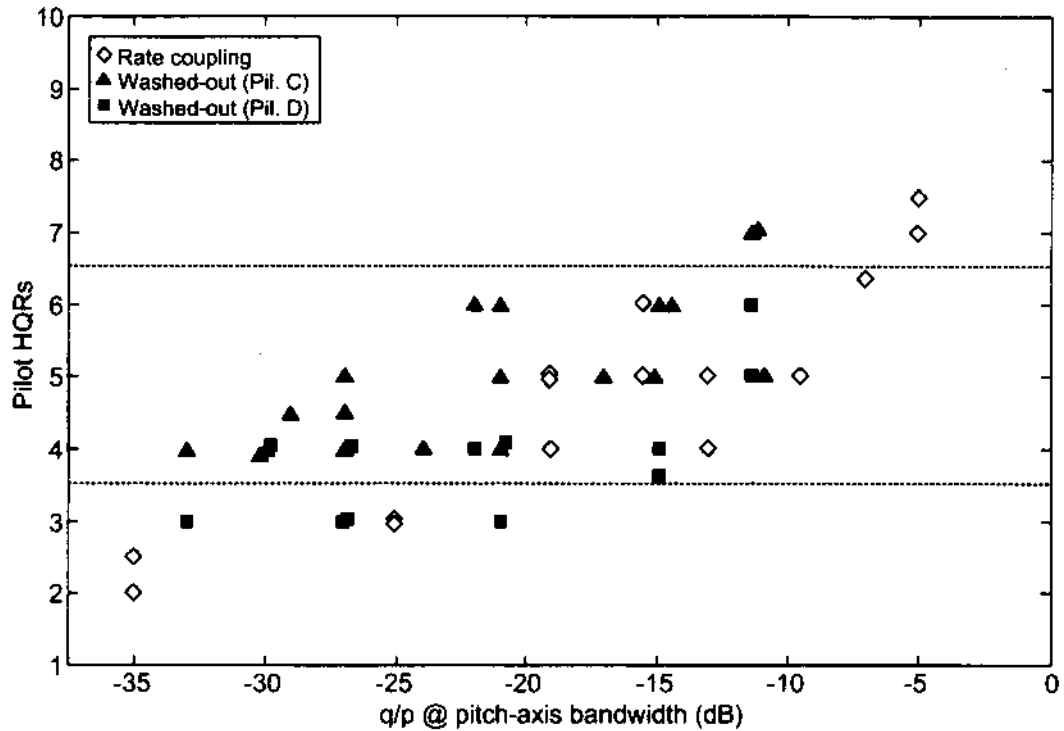


Figure 8.14. Magnitude of q/p at the pitch bandwidth frequency vs. individual pilot ratings for the washed-out coupling cases and some selected rate coupling cases (flight data only).

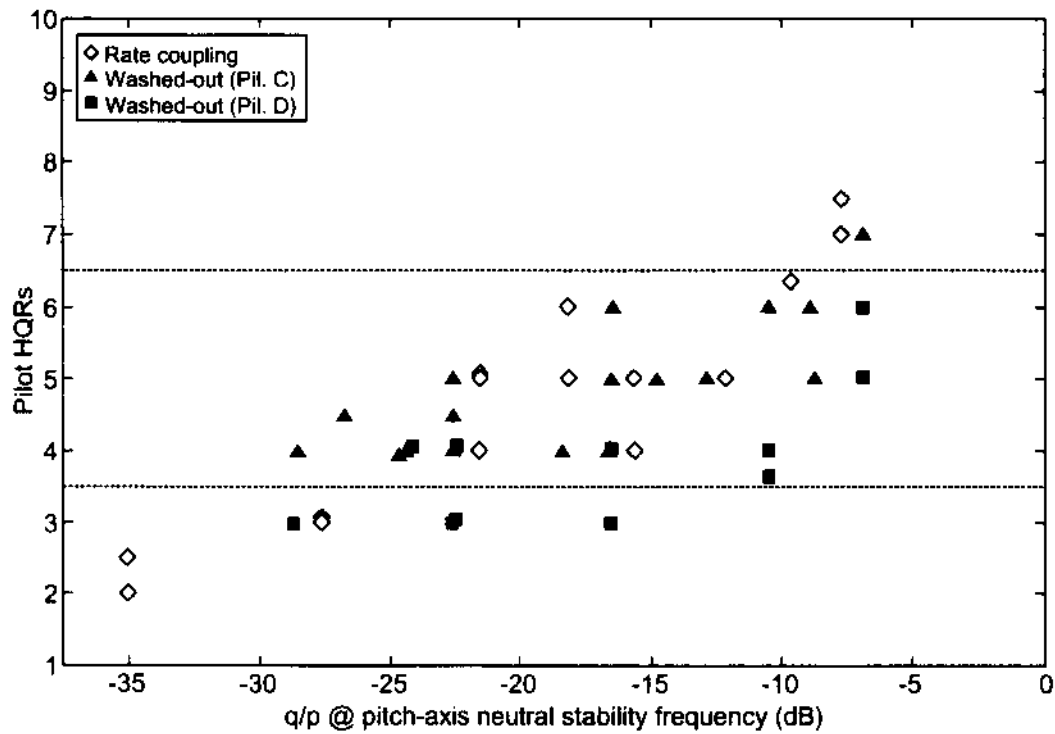


Figure 8.15. Magnitude of q/p at the pitch neutral stability frequency vs. individual pilot ratings for the washed-out coupling cases and some selected rate coupling cases (flight data only).

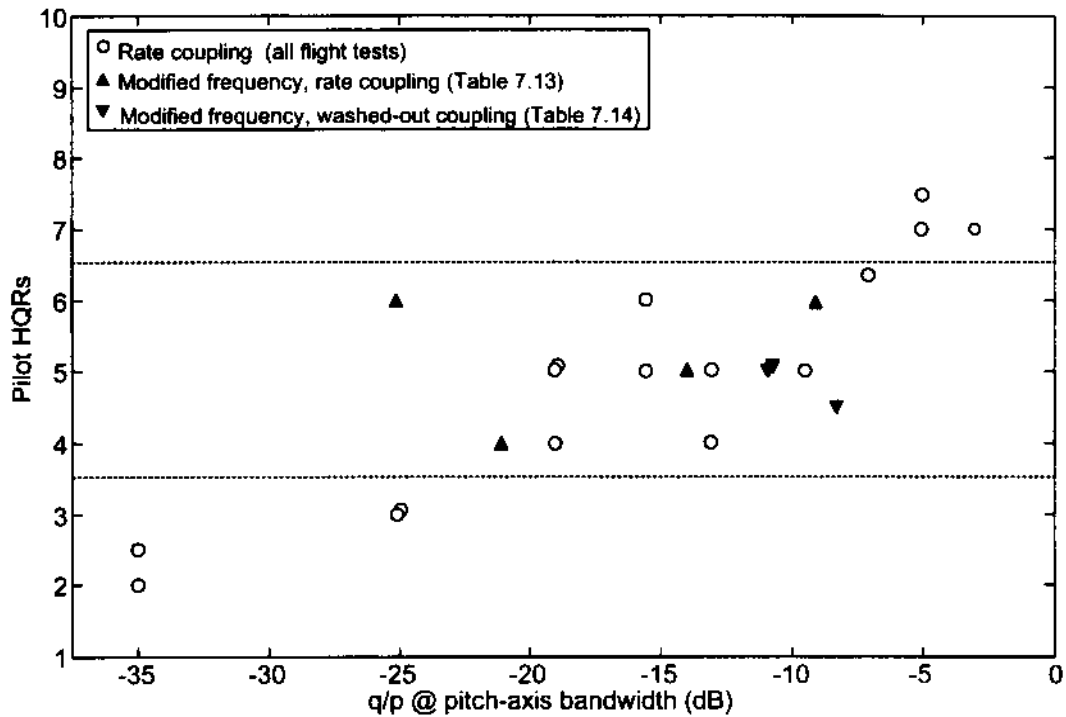


Figure 8.16. Magnitude of q/p at the pitch bandwidth frequency vs. individual pilot ratings for the modified frequency cases and some selected rate coupling cases.

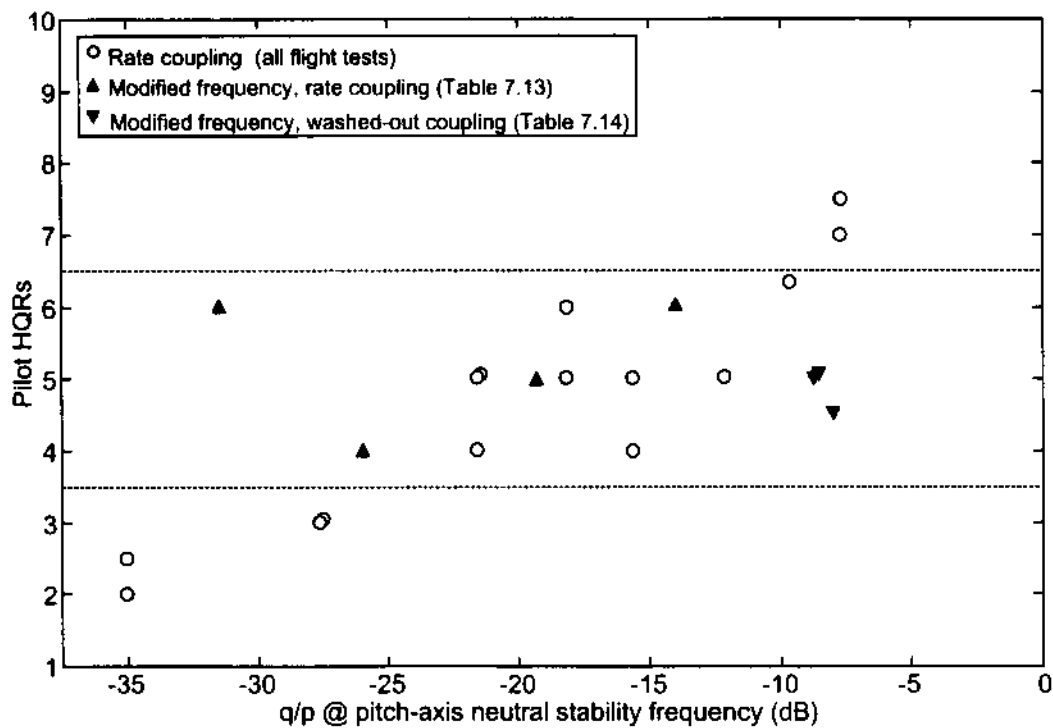


Figure 8.17. Magnitude of q/p at the pitch neutral stability frequency vs. individual pilot ratings for the modified frequency cases and some selected rate coupling cases.

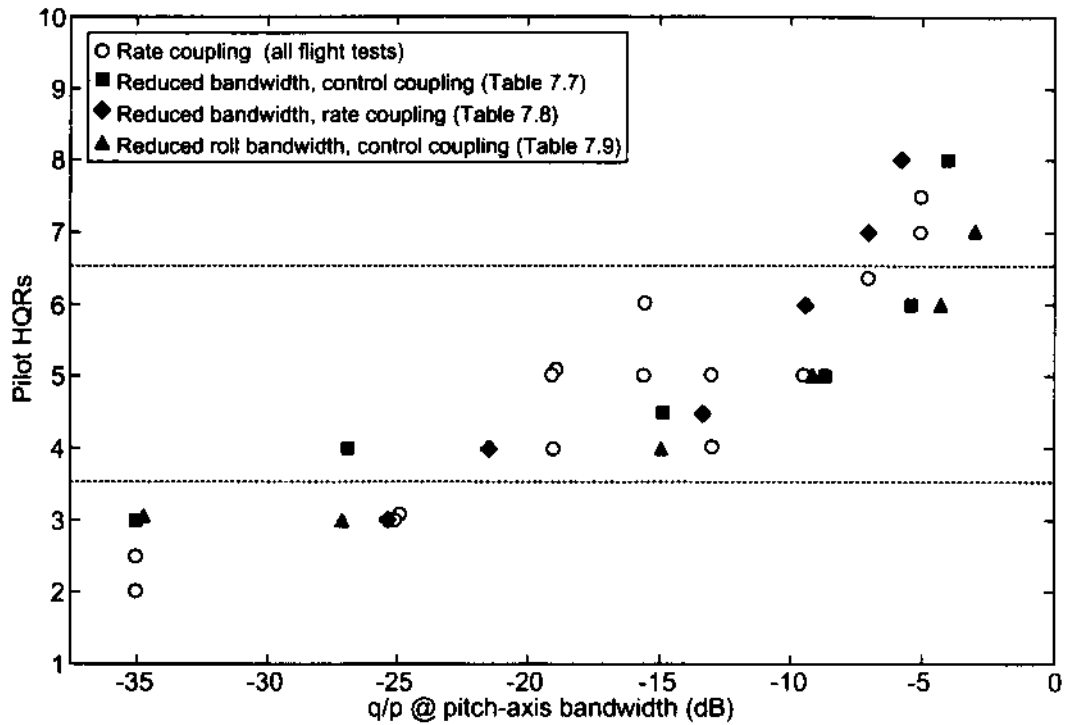


Figure 8.18. Magnitude of q/p at the pitch bandwidth frequency vs. individual pilot ratings for the reduced on-axis bandwidth frequency cases and some selected rate coupling cases.

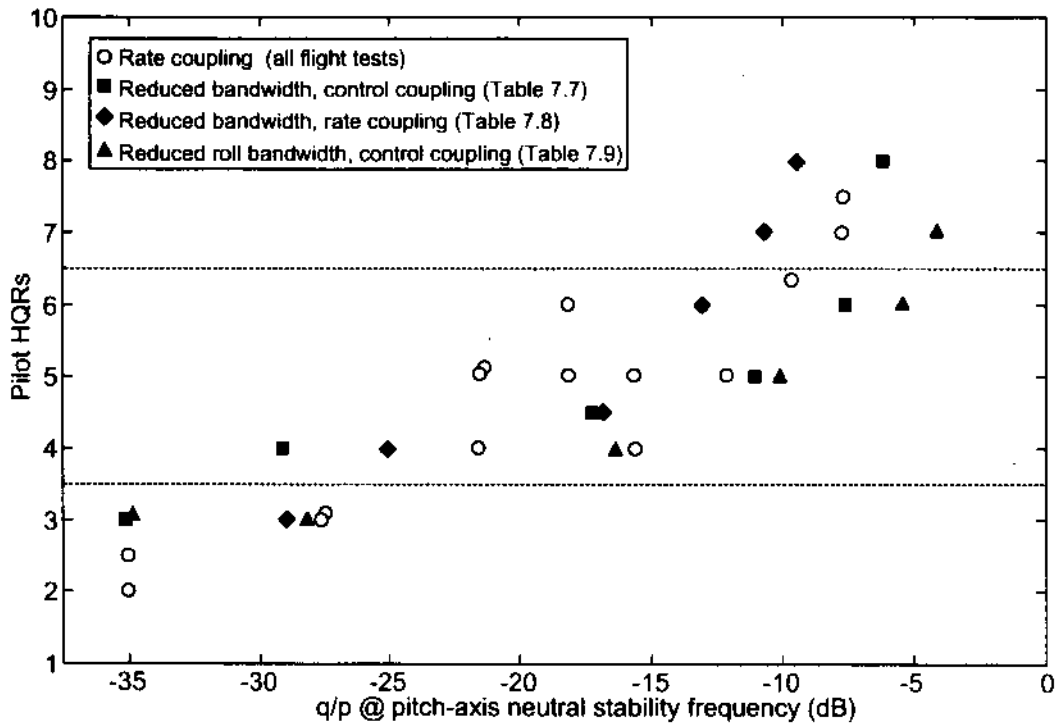


Figure 8.19. Magnitude of q/p at the pitch neutral stability frequency vs. individual pilot ratings for the reduced on-axis bandwidth frequency cases and some selected rate coupling cases.

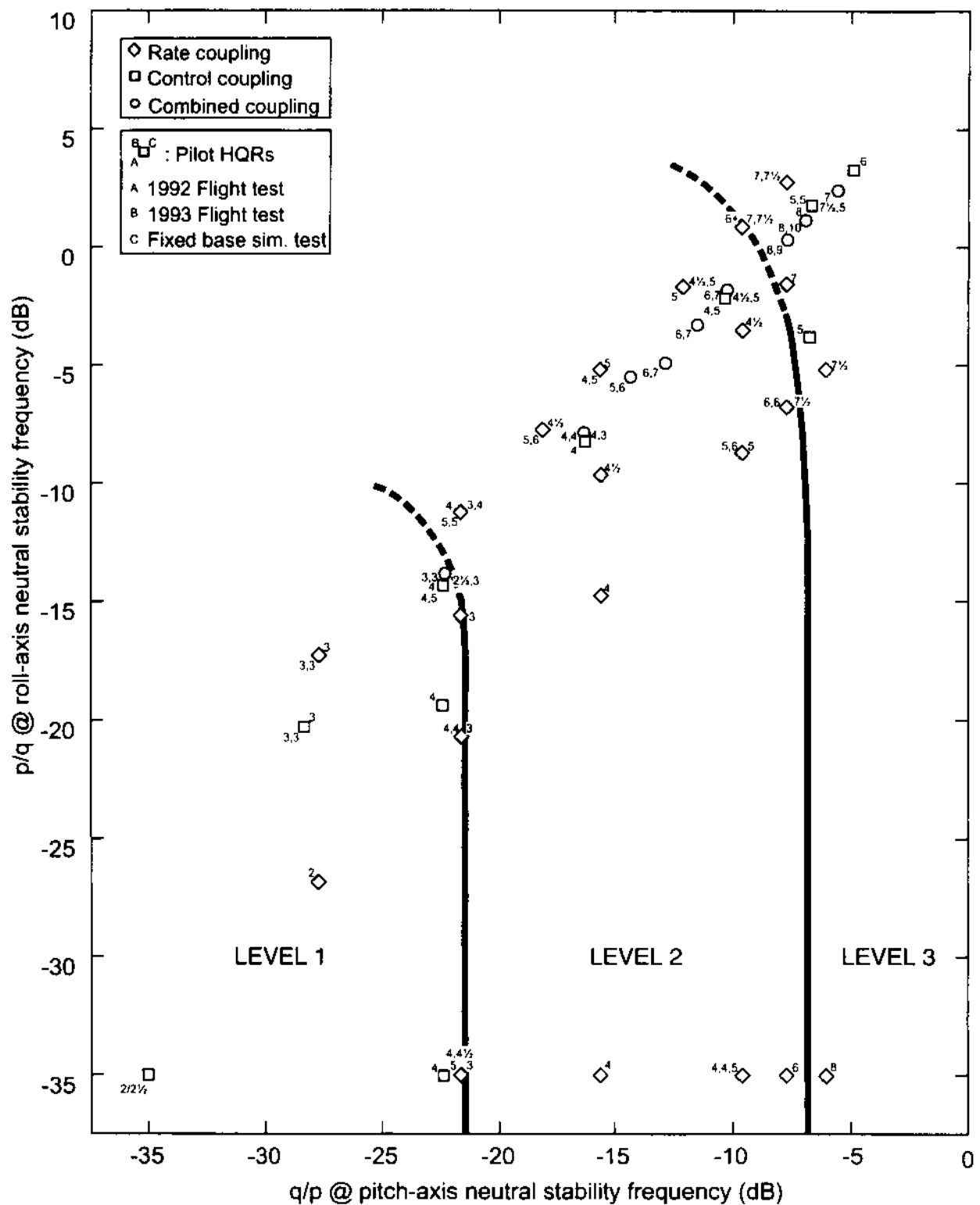


Figure 8.21. Two-sided representation of the pitch neutral stability frequency criterion for all control, rate, and combined coupling cases. Individual pilot ratings and suggested level boundaries are shown.

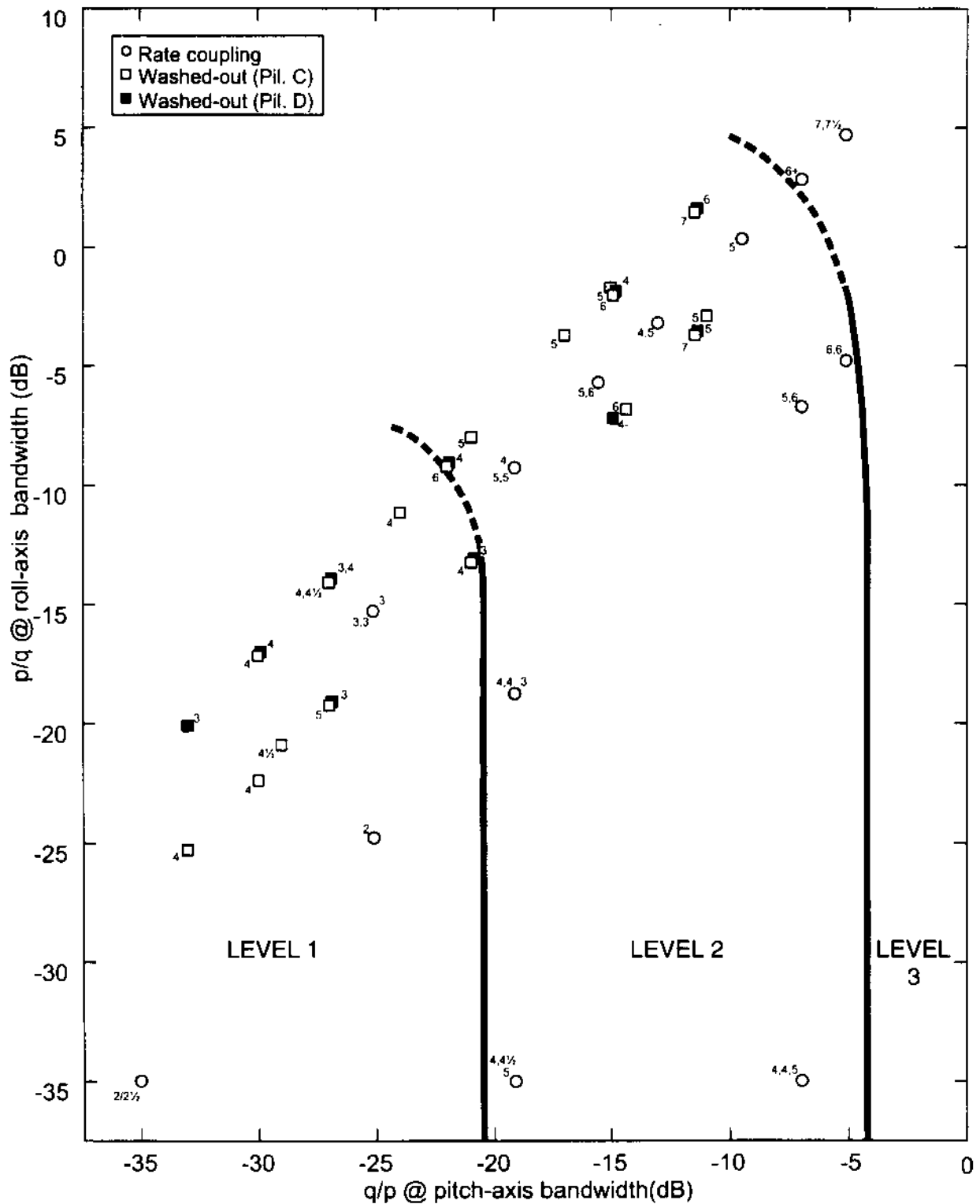


Figure 8.22. Two-sided representation of the pitch bandwidth frequency criterion for all washed-out coupling cases and some selected rate coupling cases. Individual pilot ratings and suggested level boundaries are shown.

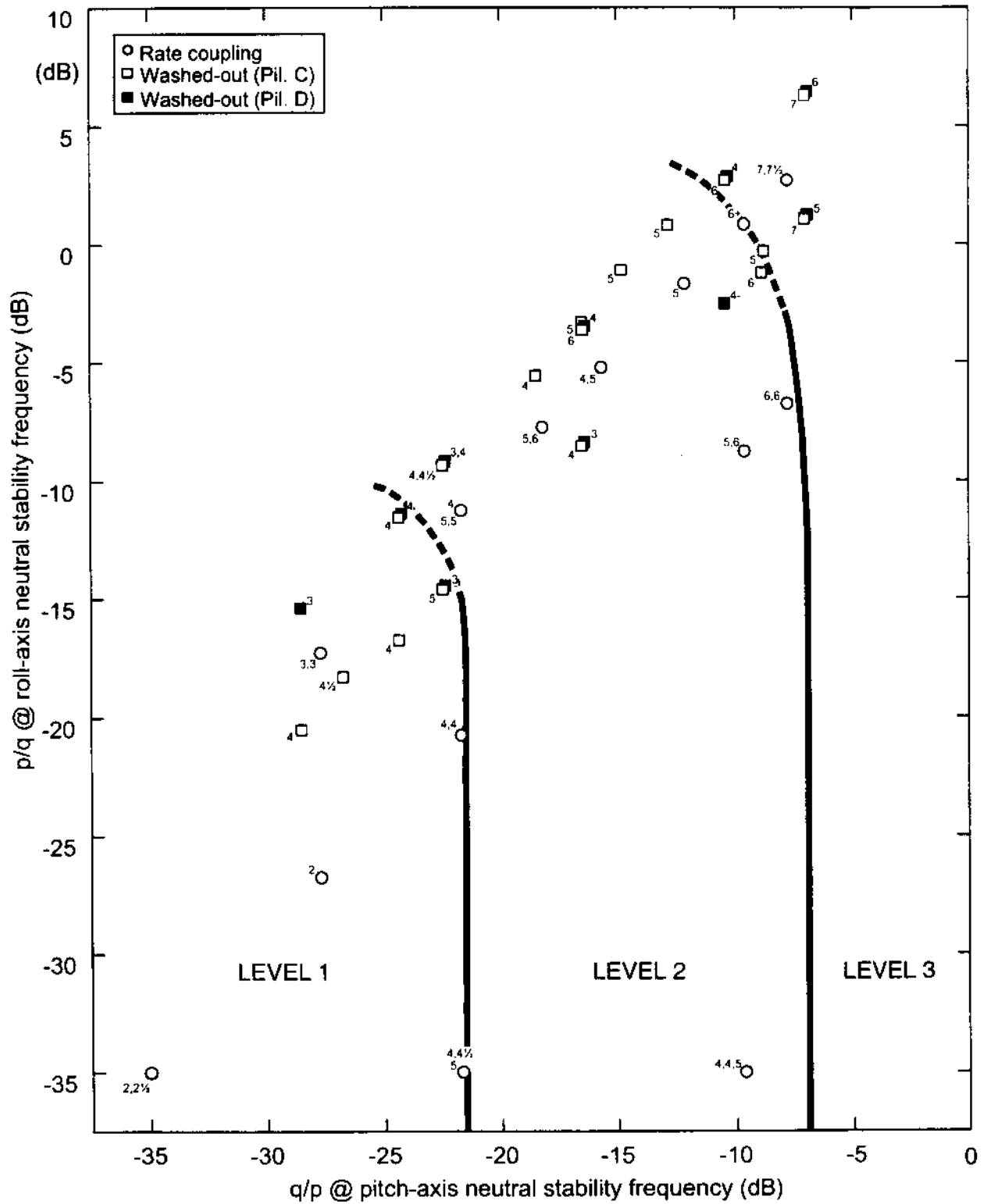


Figure 8.23. Two-sided representation of the pitch neutral stability frequency criterion for all washed-out coupling cases and some selected rate coupling cases. Individual pilot ratings and suggested level boundaries are shown.

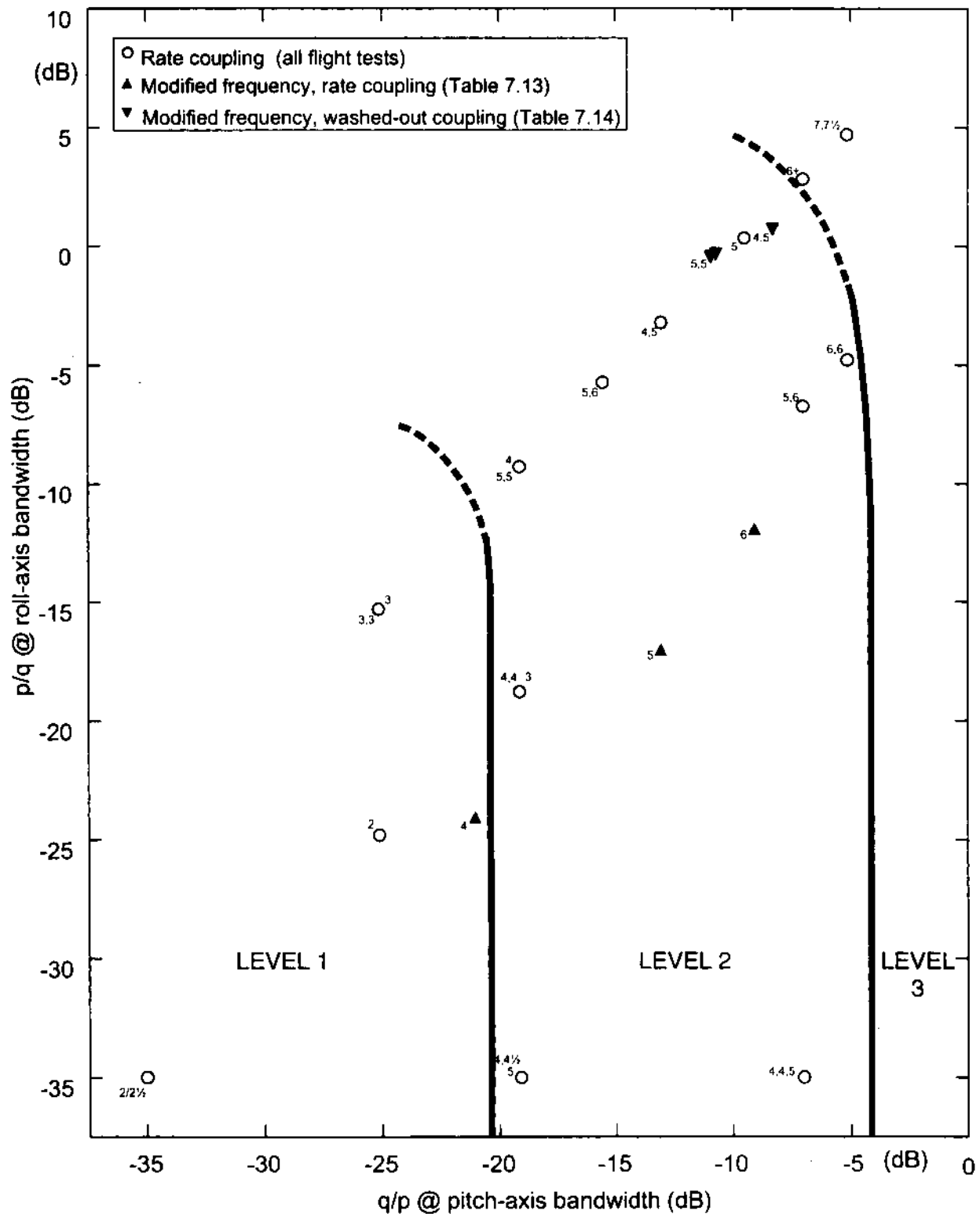


Figure 8.24. Two-sided representation of the pitch bandwidth frequency criterion for all modified frequency coupling cases and some selected rate coupling cases. Individual pilot ratings and suggested level boundaries are shown.

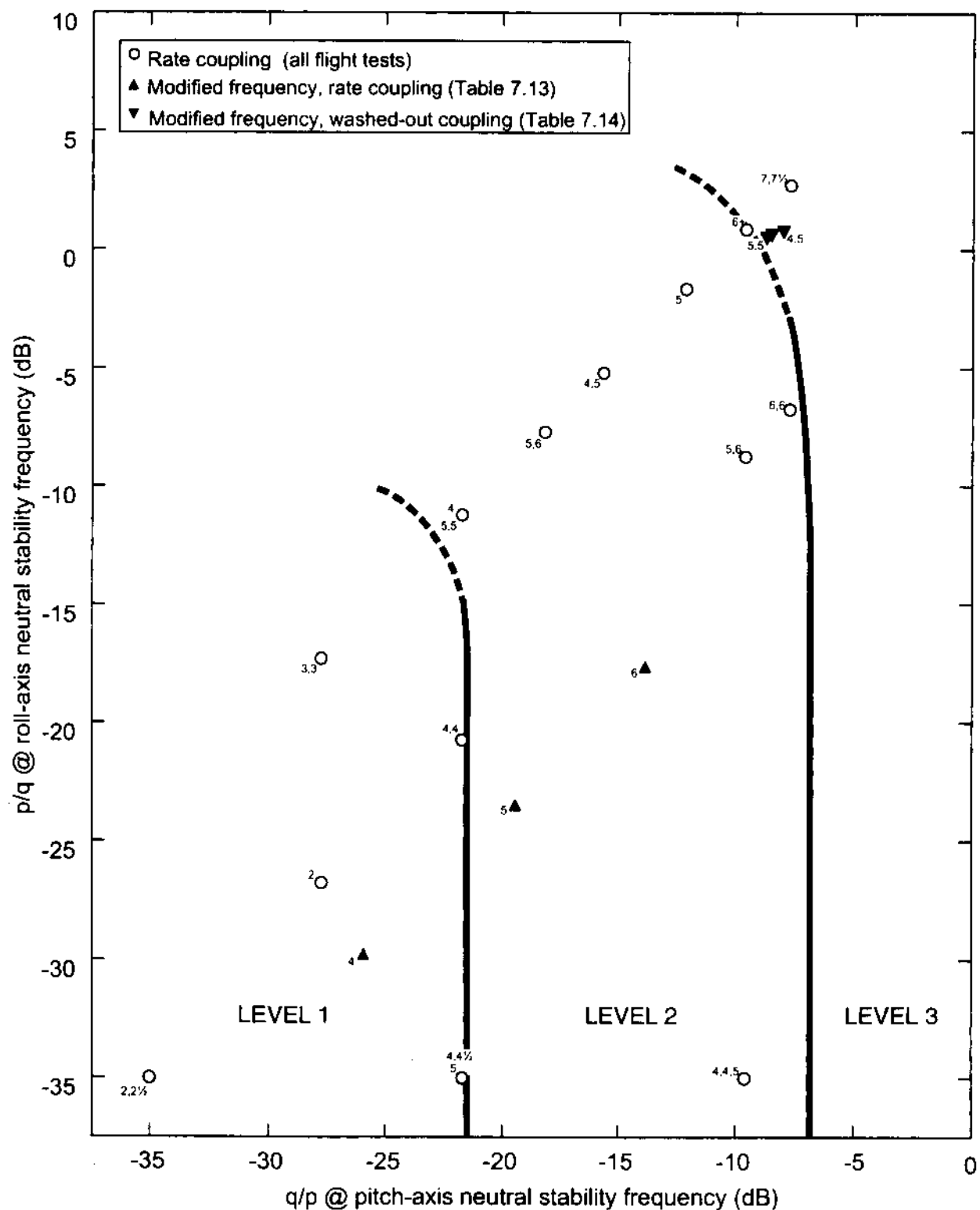


Figure 8.25. Two-sided representation of the pitch neutral stability frequency criterion for all modified frequency coupling cases and some selected rate coupling cases. Individual pilot ratings and suggested level boundaries are shown.

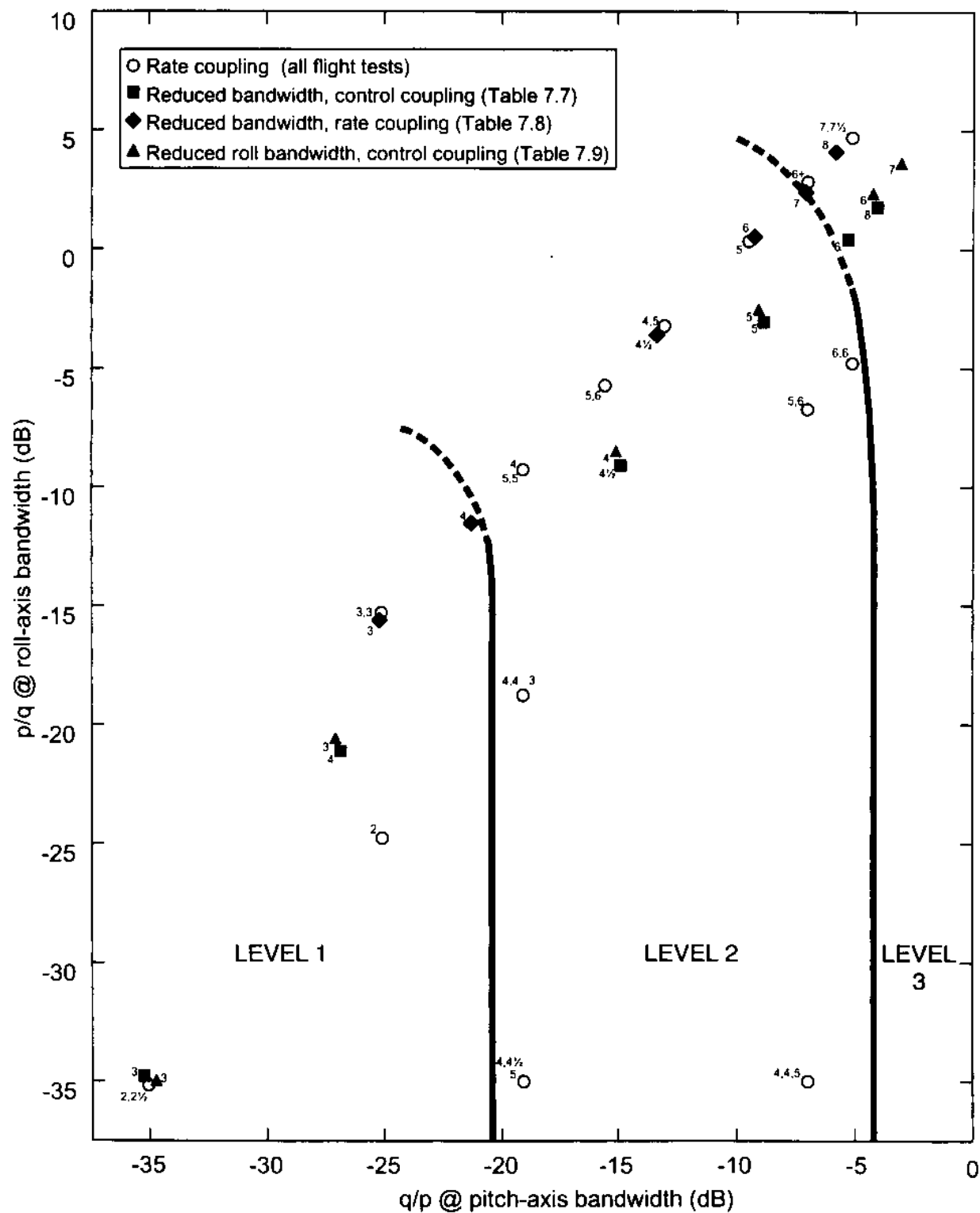


Figure 8.26. Two-sided representation of the pitch bandwidth frequency criterion for all reduced on-axis bandwidth coupling cases and some selected rate coupling cases. Individual pilot ratings and suggested level boundaries are shown.

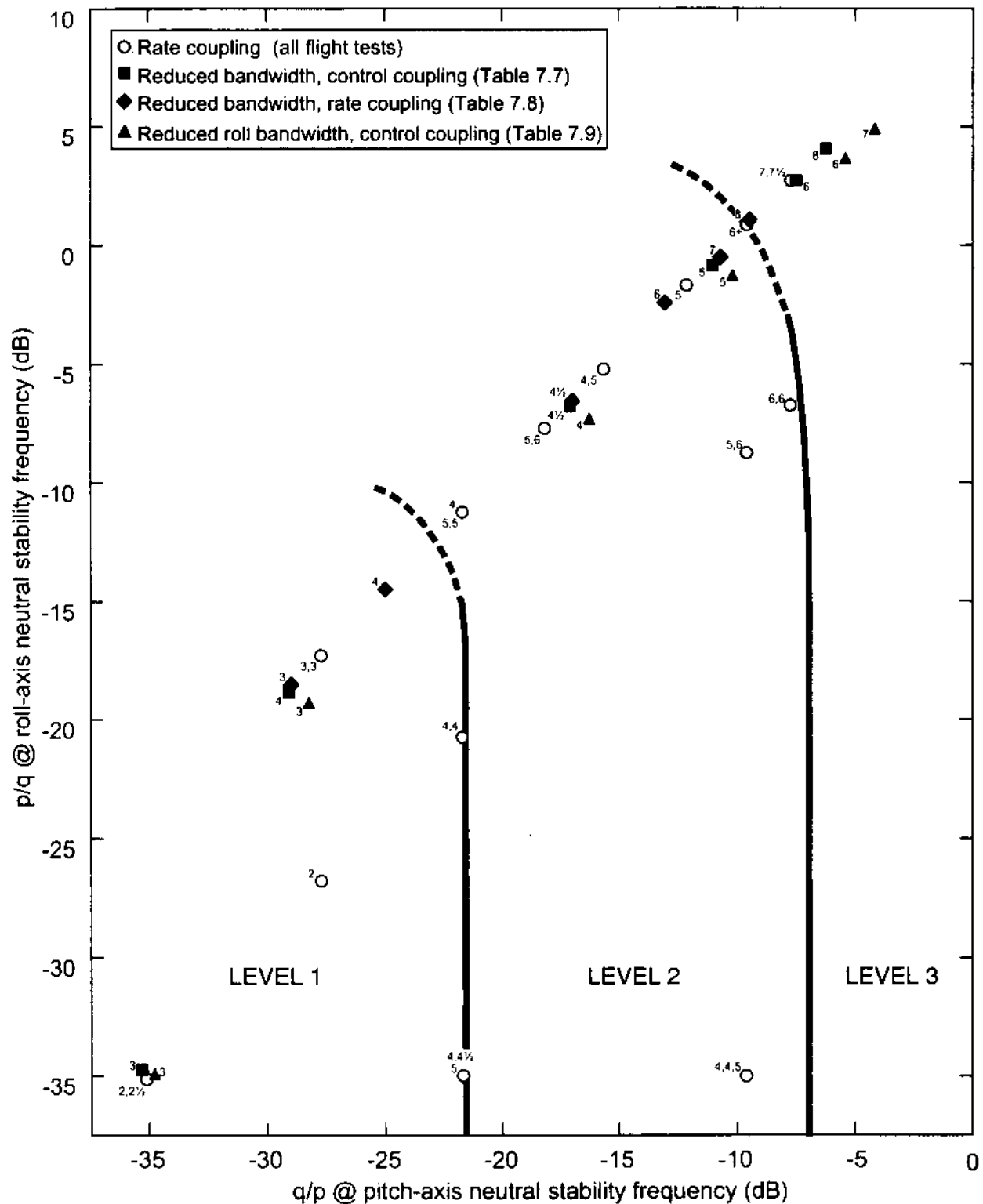


Figure 8.27. Two-sided representation of the pitch neutral stability frequency criterion for all reduced on-axis bandwidth coupling cases and some selected rate coupling cases. Individual pilot ratings and suggested level boundaries are shown.

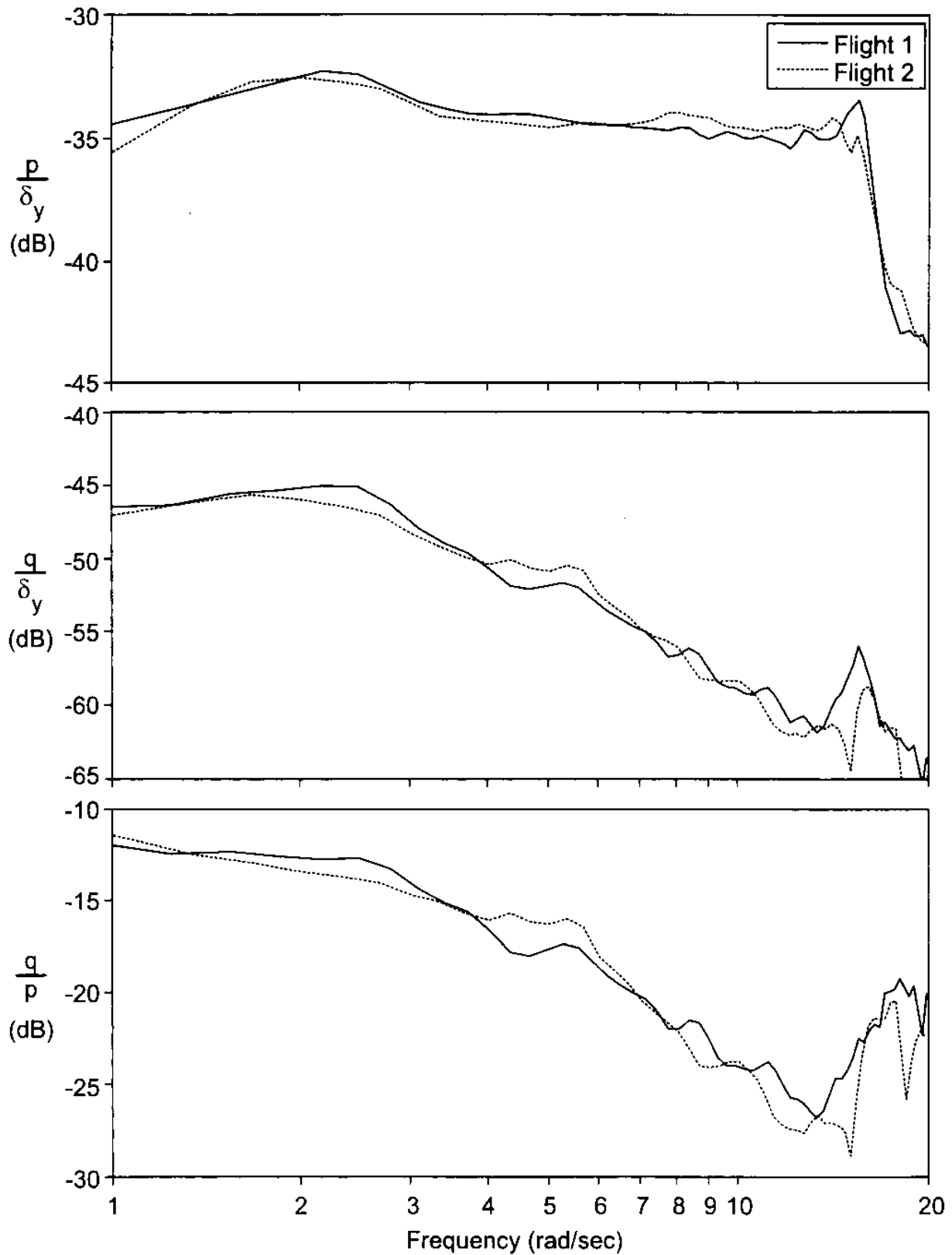


Figure 8.28. Amplitude of the frequency response of p/δ_y , q/δ_y , and q/p for two data sets obtained from two separate flight tests with the BO 105 S-123 (80 knots).

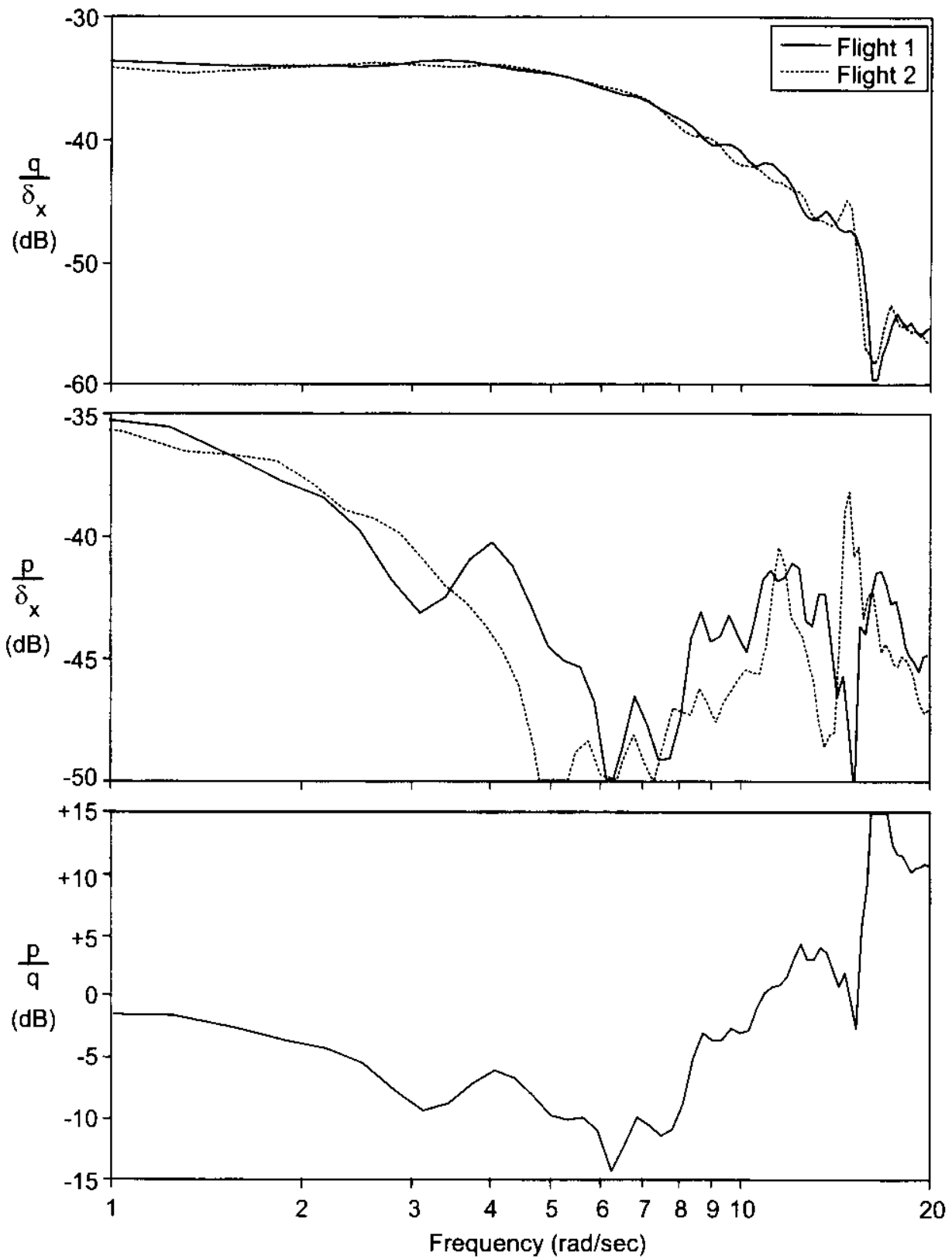


Figure 8.29. Amplitude of the frequency response of q/δ_x , p/δ_x , and p/q for two data sets obtained from two separate flight tests with the BO 105 S-123 (80 knots).

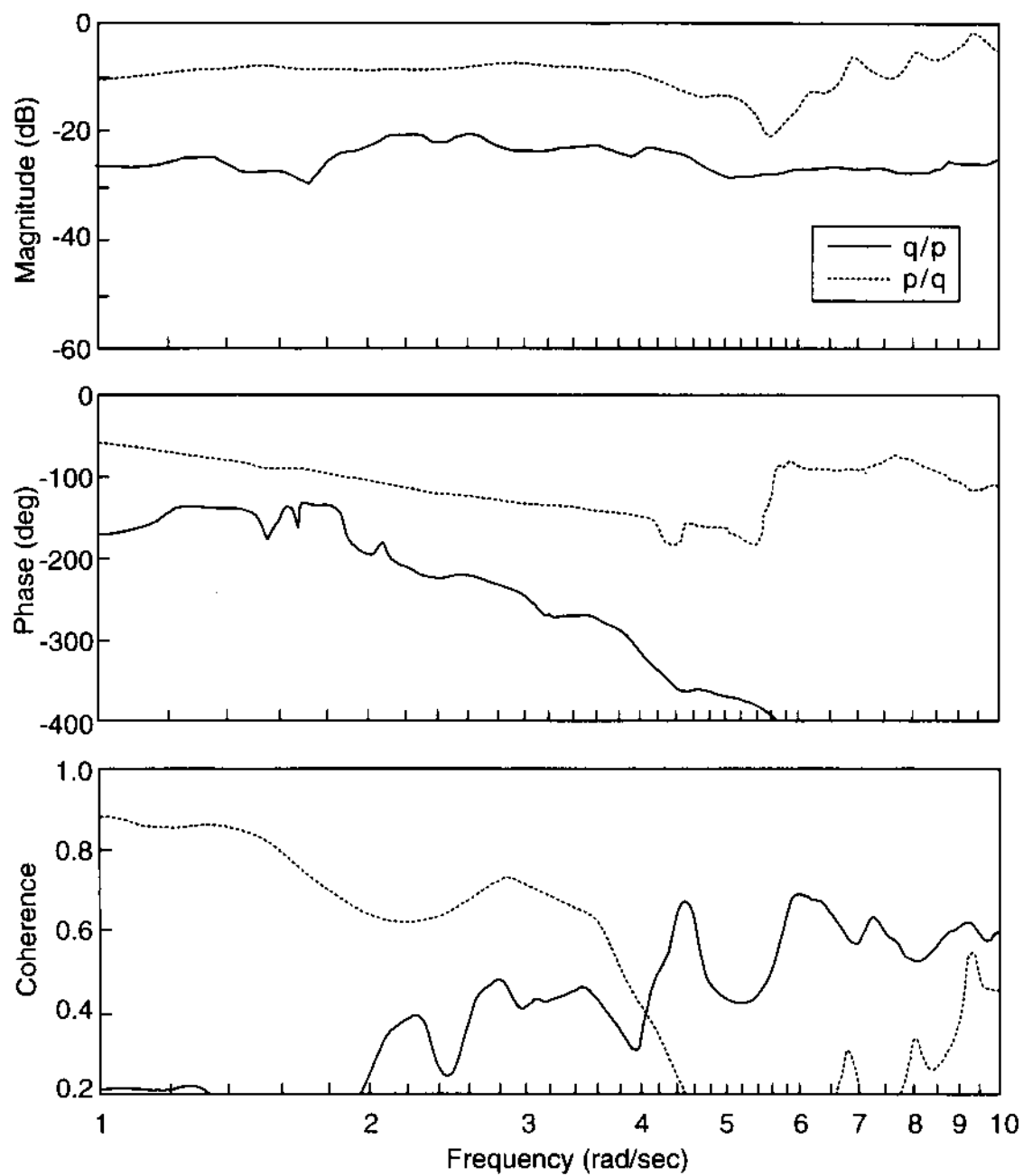


Figure 8.30. Bode plot of q/p (solid line) and p/q (dashed line) of an attack helicopter at 60 knots.

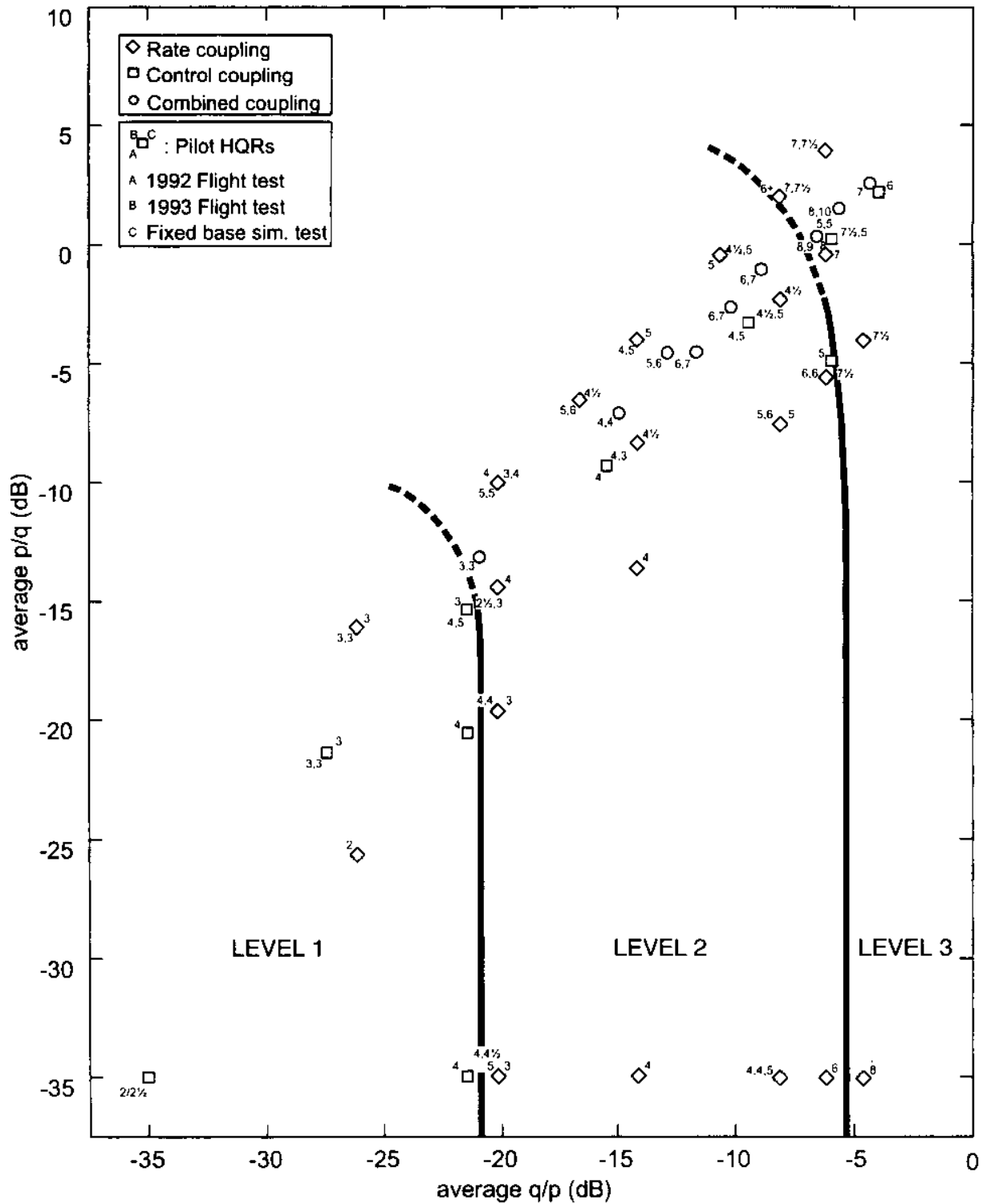


Figure 8.31. Individual pilot HQRs of all control, rate, and combined coupling cases in the frequency domain format using an averaged coupling parameter

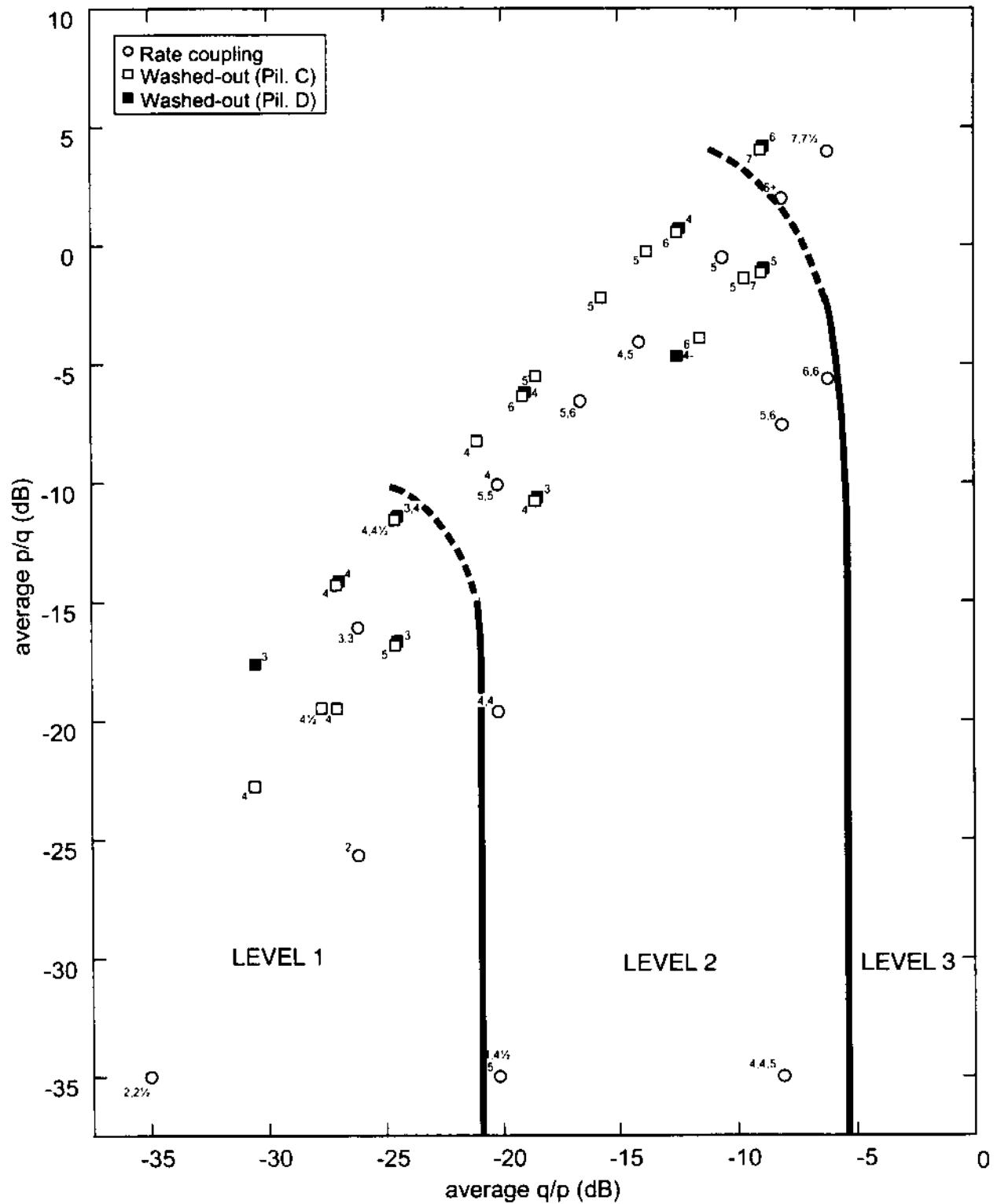


Figure 8.32. Individual pilot HQRs of all washed-out coupling cases and some selected rate coupling cases in the frequency domain format using an averaged coupling parameter.

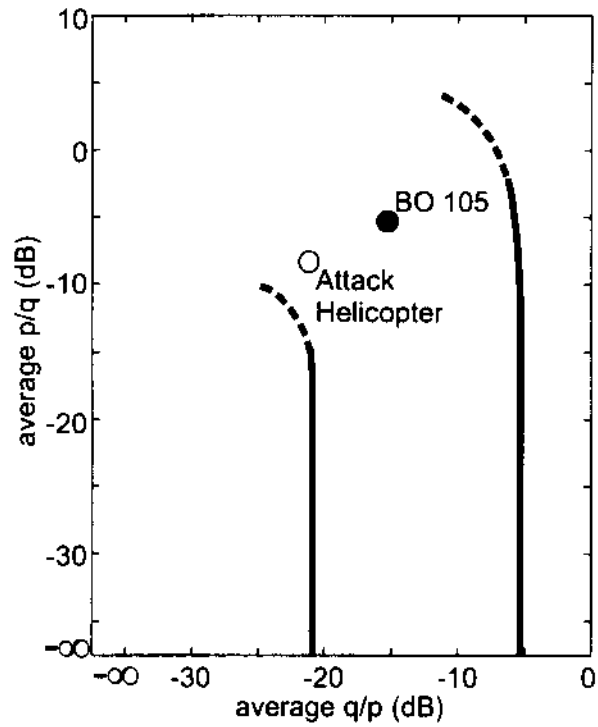


Figure 8.33. Suggested level boundaries of the pitch-roll coupling criterion using an averaged coupling parameter. Data points shown are for the BO 105 at 80 knots and an attack helicopter at 60 knots.

REPORT DOCUMENTATION PAGE			Form Approved OMB No. 0704-0188	
Public reporting burden for this collection of information is estimated to average 1 hour per response, including the time for reviewing instructions, searching existing data sources, gathering and maintaining the data needed, and completing and reviewing the collection of information. Send comments regarding this burden estimate or any other aspect of this collection of information, including suggestions for reducing this burden, to Washington Headquarters Services, Directorate for Information Operations and Reports, 1215 Jefferson Davis Highway, Suite 1204, Arlington, VA 22202-4302, and to the Office of Management and Budget, Paperwork Reduction Project (0704-0188), Washington, DC 20503.				
1. AGENCY USE ONLY (Leave blank)		2. REPORT DATE May 1995		3. REPORT TYPE AND DATES COVERED Technical Memorandum
4. TITLE AND SUBTITLE An Investigation of the Effects of Pitch-Roll (De)Coupling on Helicopter Handling Qualities			5. FUNDING NUMBERS 505-59-36	
6. AUTHOR(S) C. L. Blanken, H.-J. Pausder,* and C. J. Ockier*				
7. PERFORMING ORGANIZATION NAME(S) AND ADDRESS(ES) Aeroflightdynamics Directorate, U.S. Army Aviation and Troop Command, Ames Research Center, Moffett Field, CA 94035-1000			8. PERFORMING ORGANIZATION REPORT NUMBER A-950055	
9. SPONSORING/MONITORING AGENCY NAME(S) AND ADDRESS(ES) National Aeronautics and Space Administration Washington, DC 20546-0001 and U.S. Army Aviation and Troop Command, St. Louis, MO 63120-1798			10. SPONSORING/MONITORING AGENCY REPORT NUMBER NASA TM-110349 USAATCOM TR-95-A-003	
11. SUPPLEMENTARY NOTES Point of Contact: C. L. Blanken, Ames Research Center, MS 210-4, Moffett Field, CA 94035-1000; (415) 604-5836 *Deutsche Forschungsanstalt für Luft- und Raumfahrt, Forschungsbereich Flugmechanik/Flugführung, Institut für Flugmechanik, Abteilung Flugmechanik der Drehflügelflugzeuge, Lilienthalplatz 7, D-38108 Braunschweig				
12a. DISTRIBUTION/AVAILABILITY STATEMENT Unclassified—Unlimited Subject Category 08			12b. DISTRIBUTION CODE	
13. ABSTRACT (Maximum 200 words) An extensive investigation of the effects of pitch-roll coupling on helicopter handling qualities was performed by the U.S. Army and Deutsche Forschungsanstalt für Luft- und Raumfahrt (DLR), using a NASA ground-based and a DLR in-flight simulator. Over 90 different coupling configurations were evaluated using a high gain roll-axis tracking task. The results show that although the current ADS-33C coupling criterion discriminates against those types of coupling typical of conventionally controlled helicopters, it is not always suited for the prediction of handling qualities of helicopters with modern control systems. Based on the observation that high frequency inputs during tracking are used to alleviate coupling, a frequency domain pitch-roll coupling criterion that uses the average coupling ratio between the bandwidth and neutral stability frequency is formulated. This criterion provides a more comprehensive coverage with respect to the different types of coupling, shows excellent consistency, and has the additional benefit that compliance testing data are obtained from the bandwidth/phase delay tests, so that no additional flight testing is needed.				
14. SUBJECT TERMS Helicopter controllability, Coupling, Handling qualities			15. NUMBER OF PAGES 120	
			16. PRICE CODE A06	
17. SECURITY CLASSIFICATION OF REPORT Unclassified	18. SECURITY CLASSIFICATION OF THIS PAGE Unclassified	19. SECURITY CLASSIFICATION OF ABSTRACT	20. LIMITATION OF ABSTRACT	